

# **Einfluss der mechanischen Eigenschaften der Fruchthaut auf das Platzverhalten von Süßkirschen**

Von der Naturwissenschaftlichen Fakultät der  
Gottfried Wilhelm Leibniz Universität Hannover

zur Erlangung des Grades  
Doktor der Gartenbauwissenschaften (Dr. rer. hort.)

genehmigte Dissertation

von

M.Sc. Martin Brüggewirth  
geboren am 15.01.1988 in Bückeberg

Referent: Prof. Dr. agr. Moritz Knoche  
Korreferent: Prof. Dr. sc. Agr. Hartmut Stützel  
Tag der Promotion: 22.12.2016

## **Erklärung kumulative Dissertation**

aus:

Ordnung für die Promotion zur Doktorin der Gartenbauwissenschaften oder zum Doktor der Gartenbauwissenschaften (Dr. rer. Hort.) an der Gottfried Wilhelm Leibniz Universität Hannover (25.03.2013).

§ 8 Dissertation

**A: (3)**

<sup>1</sup>Besteht eine Dissertation aus mehreren wissenschaftlichen Publikationen (kumulative Dissertation), müssen die kumulierten Arbeiten unter einer gemeinsamen wissenschaftlichen Fragestellung entstanden sein. <sup>2</sup>Es ist eine ausführliche Darstellung voranzustellen, die eine kritische Einordnung der Forschungsthemen und wichtigsten Erkenntnisse aus den Publikationen in den Kontext der wissenschaftlichen Literatur zum Thema vornimmt ...

**Die voranzustellende ausführliche Darstellung ist in dieser Arbeit aufgeteilt in die Kapitel 3 und 9.**

**B: (3)**

... sowie die individuellen eigenen Beiträge und ggf. die Beiträge weiterer Autoren an den jeweiligen Publikationen darlegt.

**Die eigenen Beiträge und die Beiträge weiterer Autoren an den jeweiligen Publikationen sind im Folgenden aufgeführt.**

### **Publikation 1 (Kapitel 4)**

**Brüggenwirth, M., Fricke, H. und Knoche M.** (2014) Biaxial tensile tests identify epidermis and hypodermis as the main structural elements of sweet cherry skin. *Annals of Botany – Plants* doi: 10.1093/aobpla/plu019.

M. Knoche warb die Mittel zur Finanzierung des Vorhabens ein. H. Fricke etablierte das Testsystem in Voruntersuchungen. M. Brüggenwirth, H. Fricke und M. Knoche planten die Experimente. M. Brüggenwirth führte die Experimente aus. M. Brüggenwirth und M. Knoche analysierten die Daten und schrieben das Manuskript. M. Brüggenwirth, H. Fricke und M. Knoche überarbeiteten und editierten die Veröffentlichung.

### **Publikation 2 (Kapitel 5)**

**Brüggenwirth, M. und Knoche, M.** (2016a) Factors affecting mechanical properties of the skin of sweet cherry fruit. *Journal of the American Society for Horticultural Science* 141, 45-53.

M. Knoche warb die Mittel zur Finanzierung des Vorhabens ein. M. Brüggenwirth und M. Knoche planten die Experimente. M. Brüggenwirth führte die Experimente aus. M. Brüggenwirth und M. Knoche analysierten die Daten und schrieben das Manuskript. M. Brüggenwirth und M. Knoche überarbeiteten und editierten die Veröffentlichung.

### **Publikation 3 (Kapitel 6)**

**Brüggenwirth, M. und Knoche, M.** (2016b) Mechanical properties of skin of sweet cherry fruit of differing susceptibilities to cracking. *Journal of the American Society for Horticultural Science* 141, 162-168.

M. Knoche warb die Mittel zur Finanzierung des Vorhabens ein. M. Brüggenwirth und M. Knoche planten die Experimente. M. Brüggenwirth führte die Experimente aus. M. Brüggenwirth und M. Knoche analysierten die Daten

und schrieben das Manuskript. M. Brüggewirth und M. Knoche überarbeiteten und editierten die Veröffentlichung.

#### **Publikation 4 (Kapitel 7)**

**Brüggewirth, M. und Knoche, M.** (2016c) Time to fracture and fracture strain are negatively related in sweet cherry fruit skin. *Journal of the American Society for Horticultural Science* 141, 485-489.

M. Knoche warb die Mittel zur Finanzierung des Vorhabens ein. M. Brüggewirth und M. Knoche planten die Experimente. M. Brüggewirth führte die Experimente aus. M. Brüggewirth und M. Knoche analysierten die Daten und schrieben das Manuskript. M. Brüggewirth und M. Knoche überarbeiteten und editierten die Veröffentlichung.

#### **Publikation 5 (Kapitel 8)**

**Brüggewirth, M. und Knoche, M.** (2016d) Cell wall swelling, fracture mode, and the mechanical properties of cherry skins are closely related. *Planta* doi: 10.1007/s00425-016-2639-7.

M. Knoche warb die Mittel zur Finanzierung des Vorhabens ein. M. Brüggewirth und M. Knoche planten die Experimente. M. Brüggewirth führte die Experimente aus. M. Brüggewirth und M. Knoche analysierten die Daten und schrieben das Manuskript. M. Brüggewirth und M. Knoche überarbeiteten und editierten das Manuskript.

## Inhaltsverzeichnis

1. Zusammenfassung .....	1
2. Abstract .....	3
3. Allgemeine Einleitung .....	5
4. Biaxial tensile tests identify epidermis and hypodermis as the main structural elements of sweet cherry skin .....	10
5. Factors affecting mechanical properties of the skin of sweet cherry fruit.....	24
6. Mechanical properties of skin of sweet cherry fruit of differing susceptibilities to cracking .....	34
7. Time to fracture and fracture strain are negatively related in sweet cherry fruit skin .....	42
8. Cell wall swelling, fracture mode, and mechanical properties of the sweet cherry fruit skin are closely related .....	48
9. Generelle Diskussion.....	62
10. Literaturverzeichnis.....	68
11. Abkürzungsverzeichnis.....	72
Danksagungen .....	75
Publikationsliste .....	76
Lebenslauf.....	77

## 1. Zusammenfassung

Das Platzen von Süßkirschen (*Prunus avium* L.) nach Niederschlägen führt zu großen Ernteaussfällen weltweit. Der Mechanismus des Platzens ist trotz intensiver Forschungen immer noch unbekannt. Die meisten Informationen sind über die Wasseraufnahme vorhanden. Über die mechanischen Eigenschaften der Fruchthaut ist dagegen bisher wenig bekannt. Ziel war es, einen biaxialen Zugtest an Fruchthäuten zu etablieren und das mechanische Verhalten der Fruchthaut der Kirsche beim Platzen zu untersuchen.

Hierfür wurde ein Exokarpsegment (ES), bestehend aus Kutikula, Epidermis, Hypodermis und anhaftenden Mesokarpzellen von der Frucht geschnitten und im Elastometer (Druckkammer) montiert. Von der Innenseite des ES wurde anschließend ein Druck appliziert, durch den sich das ES nach außen wölbte. Der Druck [ $p$ : (kPa)] und die Auswölbung wurden gemessen und mithilfe der Auswölbung die biaxiale Dehnung [ $\epsilon$ : ( $\text{mm}^2 \text{mm}^{-2}$ )] berechnet. Aus  $p$  und  $\epsilon$  wurde das E-Modul [ $E$ : (MPa)] als Maß für die Steifigkeit bestimmt. Ein hohes  $E$  bedeutet eine hohe Steifigkeit. Eine kontinuierliche Druckerhöhung führte zum Versagen des ES und erlaubte die Bestimmung von Bruchdruck ( $p_{\text{fracture}}$ ) und Bruchdehnung ( $\epsilon_{\text{fracture}}$ ).

In einem normalen Prüftest ergab es eine lineare Beziehung zwischen  $p$  und  $\epsilon$  bis zum Bruch des ES. Der Abbau der Zellwände der Hypodermis und Epidermis mithilfe von Pektinasen führte zu niedrigerem  $p_{\text{fracture}}$  und  $\epsilon_{\text{fracture}}$ , während das Abschleifen der Kutikula nur  $\epsilon_{\text{fracture}}$  reduzierte. Wurde  $p$  konstant gehalten, nahm die Auswölbung der ES kontinuierlich weiter zu. Das E-Modul nahm mit zunehmender Transpiration ab, während  $p_{\text{fracture}}$  und  $\epsilon_{\text{fracture}}$  anstiegen. Eine Wasseraufnahme hatte keinen Effekt auf  $E$  und verringerte  $p_{\text{fracture}}$  und  $\epsilon_{\text{fracture}}$  nur leicht.

Die Fruchthaut der platzfesteren Sorte ‚Regina‘ zeigte ein höheres  $E$  und höhere  $p_{\text{fracture}}$  als bei der platzanfälligeren Sorte ‚Burlat‘. Diese Unterschiede von  $E$  und  $p_{\text{fracture}}$  zwischen ‚Regina‘ und ‚Burlat‘ blieben selbst nach der Zerstörung der Plasmamembran durch einen Frost/Auftau-Zyklus bestehen. Die Zellwandmasse pro Einheit Frischmasse war bei ‚Regina‘ höher als bei ‚Burlat‘.

Eine langsamere Erhöhung der Druckrate ( $p_{rate}$ ) im biaxialen Zugtest resultierte in einer längeren Zeit bis zum Bruch ( $t_{fracture}$ ), einer niedrigeren Dehnungsrate ( $\epsilon_{rate}$ ) und in einem höheren  $E$ . Dagegen nahmen  $p_{fracture}$  und  $\epsilon_{fracture}$  ab. Im Vergleich zum Platztest war die  $\epsilon_{fracture}$  jedoch fünffach höher als im biaxialen Zugtest.

Im biaxialen Zugtest rissen die antiklinale Zellwände der Epidermis vor allem *durch* die Zellwand und dies ohne eine Zunahme der Zellwandquellung. Im Gegensatz dazu rissen Früchte nach Inkubation in Wasser vor allem *entlang* der Zellwand, und zudem waren die Zellwände erheblich gequollen. Zellwandquellung konnte beobachtet werden, wenn die ES in Äpfelsäure, in hypertonen Glukoselösungen oder in Wasser inkubiert wurden. Verglichen zu den jeweiligen Kontrollen erhöhten diese Behandlungen immer die Anzahl der Risse entlang von Zellwänden, während sich  $p_{fracture}$  und  $E$  verringerten. Dagegen zeigten ES nach der Inkubation in  $CaCl_2$ -Lösung oder in hohen Ethanol-Konzentrationen dünne entquollene Zellwände sowie eine geringere Anzahl von Rissen entlang der Zellwände. Im Vergleich zur Kontrolle waren  $p_{fracture}$  und  $E$  erhöht.

Die Ergebnisse zeigen, dass (1) die Kirschfruchthaut sich elastisch und viskoelastisch verformt und in der tangentialen Ebene isotrop ist, (2) die mechanische Stabilität der Kirsche auf die Zellwände der Epidermis und Hypodermis nicht jedoch auf die Kutikula zurückzuführen ist, (3) die größere Platzanfälligkeit der Sorte ‚Burlat‘ im Gegensatz zu ‚Regina‘ auf physikalische und möglicherweise auch chemische Eigenschaften der Zellwand zurückzuführen ist, (4) die Wasseraufnahme offenbar weitere, über die Volumenzunahme der Frucht hinausgehende Einflüsse auf das Platzen hat und (5) Rissmodus, E-Modul und Bruchdruck ursächlich von der Zellwandquellung bestimmt werden. Viele Faktoren beeinflussen die mechanischen Eigenschaften der Fruchthaut nur indirekt über ihren Einfluss auf die Zellwandquellung. Damit ist die Zellwandquellung eine entscheidende Einflussgröße beim Platzen von Kirschen.

**Schlüsselwörter:** Biomechanik, Bruch, Mechanische Eigenschaften, Fruchthaut, Dehnung



## 2. Abstract

Rain cracking is a limitation of sweet cherry (*Prunus avium* L.) production worldwide. Despite of many studies in this topic the mechanistic basis of cracking is still poorly understood. Most information is available on water uptake. The mechanical properties of the sweet cherry fruit skin, however, received little attention. The objectives were to establish a standardized, biaxial tensile test of the skin and to use it to characterize and quantify mechanical properties of the sweet cherry fruit skin.

A segment of the exocarp (ES) comprising cuticle, epidermis, hypodermis and adhering flesh was excised from the fruit and mounted in the elastometer (pressure chamber). The ES was pressurized from its inner surface causing the ES to bulge. Pressure [ $p$ : (kPa)] and the extent of bulging were recorded and the biaxial strain [ $\epsilon$ : ( $\text{mm}^2 \text{mm}^{-2}$ )] due to bulging calculated. From the  $p$  and the  $\epsilon$  the modulus of elasticity [ $E$ : (MPa)] was determined which is a measure of stiffness. A high  $E$  indicates a high stiffness. Increasing  $p$  until failure allowed to quantify the pressure at fracture ( $p_{\text{fracture}}$ ) and the strain at fracture ( $\epsilon_{\text{fracture}}$ ).

In a typical test,  $\epsilon$  increased linearly with  $p$  until the skin fractured. Enzymatic digestion of the cell walls of epidermal and hypodermal cells decreased  $p_{\text{fracture}}$  and  $\epsilon_{\text{fracture}}$ , whereas abrading the cuticle decreased only  $\epsilon_{\text{fracture}}$ . When  $p$  was held constant, the ES continued to bulge ('creep') at a decreasing rate. Increasing transpiration decreased  $E$ , but increased  $p_{\text{fracture}}$  and  $\epsilon_{\text{fracture}}$ . Water uptake had little effect on  $E$ , whereas  $\epsilon_{\text{fracture}}$  and  $p_{\text{fracture}}$  somewhat decreased.

The skin of the less cracking susceptible cultivar 'Regina' was stiffer as indexed by a higher  $E$  and had a higher  $p_{\text{fracture}}$  than that of the more susceptible 'Burlat'. Differences in  $E$  and  $p_{\text{fracture}}$  between 'Regina' and 'Burlat' remained even after destroying their plasma membranes by a freeze/thaw cycle. Mass of cell walls per unit fresh mass was higher in 'Regina' than in 'Burlat'.

A longer time to fracture ( $t_{\text{fracture}}$ ) resulted in a lower  $p_{\text{fracture}}$  and a lower  $\epsilon_{\text{fracture}}$  indicating weaker skins. However, a five-fold difference in  $\epsilon_{\text{fracture}}$  remained between the biaxial tensile test of excised fruit skin and an immersion assay with intact fruit.

In the biaxial tensile tests the ES fractured predominantly *across* their anticlinal cell walls. There was no cell wall swelling. In contrast, fruit incubated in water fractured predominantly *along* the anticlinal epidermal cell walls and their epidermal cell walls were swollen. Swelling of cell walls also occurred when ES were incubated in malic acid, in hypertonic solutions of sucrose or in water. Compared to the un-treated controls, these treatments resulted in more frequent fractures *along* the cell walls, lower  $p_{\text{fracture}}$  and low  $E$ . Conversely, compared to the un-treated controls, incubating the ES in  $\text{CaCl}_2$  or in high concentrations of ethanol resulted in thinner cell walls, in less frequent fractures *along* the cell walls and in higher values of  $E$  and  $p_{\text{fracture}}$ .

The results demonstrate that (1) the sweet cherry skin is isotropic in the tangential plane and exhibits elastic and viscoelastic behavior, (2) the cell walls of epidermis and hypodermis, but not the cuticle, represent the structural 'backbone', (3) the greater cracking susceptibility of cultivar 'Burlat' in comparison to the less susceptible 'Regina' must be accounted for by cell wall physical and - possibly - also chemical properties, (4) the effect of water uptake on cracking extends beyond a mere increase in fruit skin strain resulting from fruit volume increase associated with water uptake, (5) fracture mode,  $E$ -modulus and pressure at fracture are primarily determined by cell wall swelling. The data demonstrate that many factors affecting mechanical properties exert their effects only indirectly by affecting cell wall swelling. The latter is a key factor in cracking.

**Keywords:** Biomechanics, fracture, mechanical properties, fruit skin, strain

### 3. Allgemeine Einleitung

Süßkirschen (*Prunus avium* L.) platzen oft nach Niederschlägen. Dies führt zu hohen Ernteaussfällen (Christensen, 1996). Geplatze Kirschen sind nicht marktfähig (Abb. 1D). Risse führen zu ungehinderte Wasseraufnahme bei Nässe und bilden Eintrittspforten für Pilzfäulen (Børve et al., 2000). Sie erhöhen die Transpiration bei Trockenheit und als Folge beginnen die Früchte zu schrumpeln. Diese Qualitätsverluste führen zur Unverkäuflichkeit der Kirschen. Ab 25% geplatzen Früchten am Baum ist eine Ernte nicht mehr wirtschaftlich, da der Aufwand des Pflückens am Baum und Aussortierens beim Verpacken zu groß wird (Looney, 1985). Aufgrund des Platzens wird der Kirschanbau weltweit eingeschränkt (Christensen, 1996). Auch andere weiche Früchte sind vom Platzen betroffen, wie Weinbeeren (Considine & Kriedemann, 1972; Becker et al., 2012), Tomaten (Lichter et al., 2002) Pflaumen (Mrozek & Burkhard, 1973) und *Ribes*-Beeren (Khanal et al., 2011). Trotz der hohen wirtschaftlichen Bedeutung und vielen Untersuchungen ist der Mechanismus des Platzens bei Kirschen wenig verstanden.

Die Fruchthaut der Kirsche ist ein komplexes Gewebe, das aus einer Kutikula und mehreren Zellschichten (Epidermis und Hypodermis) besteht (Abb. 1A). Die Kutikula ist ein lipophiler Polymerfilm hauptsächlich bestehend aus Cutin und Wachsen, der als äußerste Schicht auf den Epidermiszellen aufgelagert ist. Die Kutikula bei einer reifen Kirsche ist mit ca. 1  $\mu\text{m}$  sehr dünn (Peschel und Knoche, 2012). Die Epidermis ist eine einzellige Zellschicht bestehend aus kleinen isodiametrischen kollenchymatischen Zellen, die etwa 25  $\mu\text{m}$  dick ist. Die Epidermis besitzt keine Trichome und nur eine geringe Dichte von Stomata (0.0 - 1.7  $\text{mm}^{-2}$ ), die in der reifen Frucht funktionslos sind (Peschel et al., 2003). Unter der Epidermis liegt die Hypodermis, die aus zwei bis sieben Zellschichten besteht und ungefähr 50-100  $\mu\text{m}$  dick ist (Glenn & Poovaiah, 1989). Die Zellen der Hypodermis sind prosenchymatisch in periklinarer Richtung, kollenchymatisch und größer als die Epidermiszellen (Glenn & Poovaiah, 1989). Die Hypodermis bildet die Grenze der Fruchthaut (Exokarp) zu dem weichen Fruchtfleisch (Mesokarp). Die Mesokarpzellen sind großlumige isodiametrische

parenchymatische Zellen ( $227.4 \pm 2.9 \mu\text{m}$  Durchmesser), welche dünne Zellwände aufweisen (Yamaguchi et al., 2004).

Weiterhin ist die Fruchthaut der reifen Kirsche um 19-36% elastisch gedehnt und steht damit *in-vivo* unter einer Spannung (Grimm et al., 2012). Die Dehnung führt beim Einschneiden der Fruchthaut dazu, dass sich der Schnitt deutlich weitet, da sich die Fruchthaut entspannt (Abb. 1B). Die Kutikula der reifen Kirsche selbst weist sogar eine elastische Dehnung von etwa 80% auf (Knoche et al., 2004), wodurch es leicht zur Bildung von Rissen in der Kutikula kommt (Peschel & Knoche, 2005).

Bei den Rissen in der Kirschfruchthaut wird zwischen Mikrorissen und Makrorissen unterschieden. Mikrorisse sind mikroskopisch kleine Risse, die sich auf die Kutikula beschränken (Abb. 1C). Mikrorisse sind meist nicht mit dem bloßen Auge erkennbar und stellen direkt kein qualitätsminderndes Merkmal beim Verkauf von Früchten dar (Peschel & Knoche, 2005). Dennoch stellen Mikrorisse Eintrittspforten für Pilzfäulen dar und sind wahrscheinlich die Vorläufer von Makrorissen. Makrorisse sind mit bloßem Auge erkennbar und reichen durch die Kutikula über die Epidermis und Hypodermis bis in das Mesokarp hinein (Abb. 1D). Aufgrund der natürlichen Dehnung der Fruchthaut weiten sich die Makrorisse auf und treten vornehmlich in der Stielgrube und am Griffelansatz der Frucht auf (Christensen, 1996). Bisher ist der Rissmodus von Makrorissen bei Kirschen im Detail wenig untersucht (Glenn & Poovaiah, 1989; Weichert et al., 2004). Dabei kann die Untersuchung von Rissoberflächen wichtige Rückschlüsse liefern. Es ist bisher unbekannt, ob die Zellen der Fruchthaut entlang von antiklinalen Zellwänden (d.h. entlang der pektinhaltigen Mittelamelle) oder quer durch die Zellwände (d.h. durch Cellulosefibrillen) reißen.

Das Platzen von Kirschen hängt mit der Wasseraufnahme zusammen. Dennoch ist der exakte Mechanismus unbekannt. Das allgemeine Modell geht von einer Wasseraufnahme der Frucht aus. Die treibende Kraft für die Wasseraufnahme ist der osmotische Potentialgradient zwischen dem Wasser außen auf der Fruchthaut und dem kohlenhydrathaltigem Kirschsafte in der Frucht. Die Wasseraufnahme führt zu einer Volumenzunahme der Frucht, wodurch sich der Druck in der gesamten Kirsche erhöht (ähnlich eines Ballons, der mit Wasser

gefüllt wird). Die Fruchthaut wird dabei noch weiter gedehnt und die Spannung erhöht sich (Considine & Brown, 1981; Beyer & Knoche, 2003). Ist der Druck zu groß, so reißt die Fruchthaut und die Kirsche platzt. Daraus folgen zwei Ursachen, die zum Platzen der Kirsche führen. Zum einen eine hohe Wasseraufnahme der Frucht und zum anderen schwache mechanische Eigenschaften der Fruchthaut.

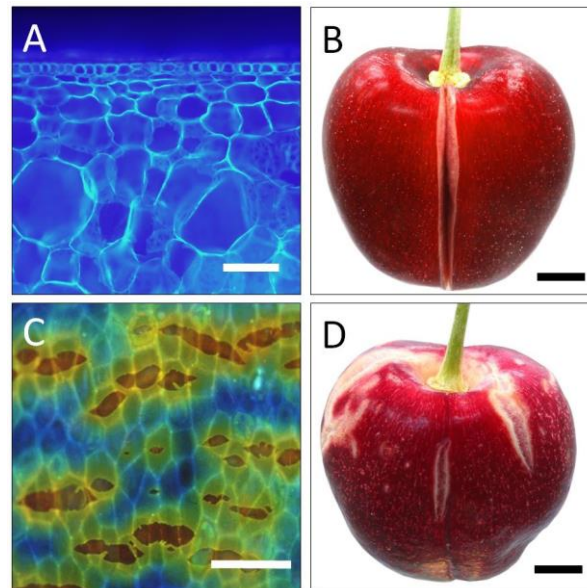


**Abbildung 1:** Morphologische Merkmale der Süßkirsche (A) Querschnitt einer Fruchthaut angefärbt mit Calcofluor-White im Fluoreszenzmikroskop. (B) Entspannung der Fruchthaut (Schnitt weitet sich) nach dem Einschneiden mit einer Rasierklinge. (C) Aufsicht auf eine Kutikula mit Mikrorissen angefärbt mit Acridin Orange im Fluoreszenzmikroskop (S. Peschel unveröffentlichte Daten). (D) Geplatzte Kirsche nach Inkubation in Wasser. Maßstab = 0.1 mm in A und C. Maßstab = 5 mm in B und D.

Die Wasseraufnahme in die Frucht ist in den letzten Jahren intensiv untersucht worden. Dabei kann die Wasseraufnahme über verschiedene parallele Eintrittswege erfolgen: (1) über polare Poren in der Kutikula (Weichert & Knoche, 2006), (2) über Mikrorisse in der Kutikula (Peschel & Knoche, 2005), (3) über die Stiel-Frucht-Verbindung (Beyer et al., 2002), und (4) über das Leitbündelsystem des Stiels (Meashem et al. 2014; Brüggewirth et al., 2016; Winkler et al., 2016). Eine Aufnahme über die funktionslosen Spaltöffnungen findet dagegen nicht statt (Peschel *et al.*, 2003; Peschel & Knoche, 2012).

Die mechanischen Eigenschaften der Fruchthaut sind dagegen bisher kaum untersucht. Mechanische Eigenschaften von Fruchthäuten oder der Kutikula können in einem uniaxialen oder biaxialen Zugtest bestimmt werden (Bargel et al., 2004; Matas et al., 2004; Knoche & Peschel, 2006). In einem uniaxialen Zugtest findet die Zugkraft nur in eine Richtung statt, während in einem biaxialen Zugtest auf den Prüfkörper zweidimensionale Zugkräfte wirken. Für die Untersuchung von Kirschfruchthäuten ist ein biaxialer Zugtest anzustreben. Zum einen treten bei der sphärischen Kirschform biaxiale Spannungen in der Fruchthaut auf, welche nur ein biaxialer Zugtest simuliert. Zum anderen zeigen erste Versuche in einem uniaxialen Zugtest, dass sich die Prüfkörper der Kirschfruchthaut bei Belastung senkrecht zur Zugrichtung einschnüren (E. Grimm unveröffentlichte Daten). Diese Einschnürung wird mit dem Poisson-Verhältnis beschrieben. Eine starke Einschnürung, d.h. ein hohes Poisson-Verhältnis, führt im uniaxialen Zugtest zu einer erheblichen Dehnung in Zugrichtung und damit zu einer Überschätzung der Dehnung und einer Unterschätzung des E-Moduls (vergleichbar mit einem Einkaufsnetz, das nur in eine Richtung auseinandergezogen wird). Bei einem uniaxialen Test mit der Kutikula treten diese Probleme nicht auf, da zelluläre Strukturen in der isotropen Kutikula fehlen. Allerdings ist eine isolierte Kirschkutikula so fragil, dass ein mechanischer Test äußerst schwierig durchzuführen ist (Knoche & Peschel, 2006).

Der erste und einzige biaxiale Zugtest von Fruchthäuten wurde von Bargel et al. (2004) beschrieben. In diesem Test wird ein Segment der Kirschfruchthaut in einer Druckkammer von innen ausgewölbt. Dabei werden Auswölbung und Druck bis zum Riss des Segments gemessen. Dieser biaxiale Zugtest hat allerdings zwei methodische Schwächen. Als Druckmedium wurde Wasser genutzt, was zu Interaktionen mit der Fruchthaut beispielsweise durch Wasseraufnahme und Platzen von Zellen führen kann (Simon, 1977). Zum anderen wird die *in-vivo* Spannung der Fruchthaut nicht erhalten (Grimm et al., 2012), was zu einer Überschätzung der maximalen Dehnung im biaxialen Zugtest führt. Aus diesen Gründen wurde dieses Testsystem modifiziert, indem als Druckmedium Silikonöl verwendet wird und die *in-vivo* Spannung der Fruchthaut durch das Aufkleben einer Unterlegescheibe erhalten bleibt (H. Fricke, unveröffentlichte Daten; M. Brüggewirth, unveröffentlichte Daten).

Die Etablierung eines geeigneten biaxialen Zugtests für die Kirschfruchthaut eröffnet die Möglichkeit eine Reihe von bisher unbekanntem mechanischen Eigenschaften der Kirschfruchthaut zu untersuchen.

(1) Bisher ist nicht bekannt, welche Bestandteile der Fruchthaut die tragende Schicht bilden. Ebenso ist unklar, ob die Fruchthaut ein isotropes Gewebe mit elastischen, viskoelastischen oder plastischen Verformungsverhalten ist.

(2) Faktoren, die das Platzen der Kirschen beeinflussen, sind bisher nicht im Zusammenhang mit den mechanischen Eigenschaften der Fruchthaut untersucht worden. Zu diesen Faktoren zählen Reifegrad, Temperatur, Wasseraufnahme und -abgabe sowie der Turgor der Früchte.

(3) Der Einfluss der mechanischen Eigenschaften der Fruchthäute auf das Platzverhalten von Sorten unterschiedlicher Platzfestigkeit ist bisher nicht bekannt.

(4) Das Platzen von Kirschen im Freiland braucht mehrere Stunden bis mehrere Tage. Es ist nicht bekannt, welche Auswirkung eine lange Bruchzeit und damit eine langsame Dehnungsrate der Fruchthaut auf die mechanischen Eigenschaften hat.

(5) Der Rissmodus ist bisher bei der Kirschfruchthaut nicht untersucht. Ebenso ist der Einfluss des Rissmodus auf die mechanischen Eigenschaften nicht bekannt.

Ziel der Untersuchung war es daher (1) die mechanischen Eigenschaften der Kirschfruchthaut zu charakterisieren, (2) den Einfluss von Faktoren, wie Reifegrad, Temperatur, Wasseraufnahme und -abgabe und der Turgor der Früchte auf die mechanischen Eigenschaften der Fruchthaut zu untersuchen, (3) Sorten unterschiedlicher Platzfestigkeit im biaxialen Zugtest zu vergleichen, (4) den Einfluss der Bruchzeit auf die mechanischen Eigenschaften von Fruchthäuten zu untersuchen und (5) den Rissmodus zu identifizieren und zu prüfen, ob ein Zusammenhang zwischen dem Rissmodus und den mechanischen Eigenschaften der Kirschfruchthaut existiert.

#### **4. Biaxial tensile tests identify epidermis and hypodermis as the main structural elements of sweet cherry skin**

Dieser Artikel wurde im Original 2014 in der Zeitschrift „Annals of Botany – Plants“ online veröffentlicht:

Brüggenwirth, M., Fricke, H. und Knoche, M. (2014) Biaxial tensile tests identify epidermis and hypodermis as the main structural elements of sweet cherry skin. *Annals of Botany – Plants* doi: 10.1093/aobpla/plu019.





## Research Article

# Biaxial tensile tests identify epidermis and hypodermis as the main structural elements of sweet cherry skin

Martin Brüggewirth, Heiko Fricke and Moritz Knoche\*

Institute for Horticultural Production Systems, Fruit Science Section, Leibniz University Hannover, Herrenhäuser Straße 2, 30419 Hannover, Germany

**Received:** 7 March 2014; **Accepted:** 1 April 2014; **Published:** 11 April 2014

**Associate Editor:** Michael B. Jackson

**Citation:** Brüggewirth M, Fricke H, Knoche M. 2014. Biaxial tensile tests identify epidermis and hypodermis as the main structural elements of sweet cherry skin. *AoB PLANTS* 6: plu019; doi:10.1093/aobpla/plu019

**Abstract.** The skin of developing soft and fleshy fruit is subjected to considerable growth stress, and failure of the skin is associated with impaired barrier properties in water transport and pathogen defence. The objectives were to establish a standardized, biaxial tensile test of the skin of soft and fleshy fruit and to use it to characterize and quantify mechanical properties of the sweet cherry (*Prunus avium*) fruit skin as a model. A segment of the exocarp (ES) comprising cuticle, epidermis, hypodermis and adhering flesh was mounted in the elastometer such that the *in vivo* strain was maintained. The ES was pressurized from the inner surface and the pressure and extent of associated bulging were recorded. Pressure : strain responses were almost linear up to the point of fracture, indicating that the modulus of elasticity was nearly constant. Abrading the cuticle decreased the fracture strain but had no effect on the fracture pressure. When pressure was held constant, bulging of the ES continued to increase. Strain relaxation upon releasing the pressure was complete and depended on time. Strains in longitudinal and latitudinal directions on the bulging ES did not differ significantly. Exocarp segments that released their *in vivo* strain before the test had higher fracture strains and lower moduli of elasticity. The results demonstrate that the cherry skin is isotropic in the tangential plane and exhibits elastic and viscoelastic behaviour. The epidermis and hypodermis, but not the cuticle, represent the structural 'backbone' in a cherry skin. This test is useful in quantifying the mechanical properties of soft and fleshy fruit of a range of species under standardized conditions.

**Keywords:** Biomechanics; fracture; mechanical properties; *Prunus avium*; rheology; skin; strain; stiffness.

## Introduction

A fruit's skin is a complex tissue comprising the polymeric cuticle, a layer of epidermal cells and, in most soft-fruit species, one or several layers of hypodermal cells. Fruit are unlike most other plant organs. Throughout their development, the skin is subjected to continuous strain due to growth (Skene 1980; Grimm *et al.* 2012).

Strain-induced skin failure severely compromises the skin's function as a barrier to the ingress of pathogens

and to the egress of water. For a soft, fleshy fruit, skin failure also limits its mechanical role as a structural 'shell' for the developing 'insides'. From the perspective of commercial horticulture, fruit skin failure is associated with greatly reduced crop quality and thus value. Prominent examples include the rain-cracking of many stone and berry fruit and the russetting of many pome fruit.

In the last two decades, a considerable number of studies have focused on the mechanical properties of fruit

\* Corresponding author's e-mail address: moritz.knoche@obst.uni-hannover.de

Published by Oxford University Press on behalf of the Annals of Botany Company.

This is an Open Access article distributed under the terms of the Creative Commons Attribution License (<http://creativecommons.org/licenses/by/3.0/>), which permits unrestricted reuse, distribution, and reproduction in any medium, provided the original work is properly cited.

skins. Many of these employed uniaxial tensile tests of isolated cuticles (for recent reviews, see [Dominguez \*et al.\* 2011a, b](#)), whereas only a few used entire skin composites ([Matas \*et al.\* 2004](#); [Khanal \*et al.\* 2013b](#)). In uniaxial tests, a specimen, usually a rectangular or dumbbell-shaped strip of cuticle or skin, is subjected to a defined force applied along the axis of extension and the force and extension are monitored. The force/extension (uniaxial strain) relationships so established are analysed.

The first, and only, biaxial test of fruit skin was published by [Bargel \*et al.\* \(2004\)](#) who reported a biaxial tensile test to compare the properties of cherry skin and polyethylene films. [Bargel \*et al.\* \(2004\)](#) pressurized circular skin samples from below and monitored the extent of bulging. In this biaxial test, the skin sample is subjected to force vectors oriented in radial directions—as the spokes of a wheel. Because the bulging of the skin is associated with an increase in area, a pressure/area extension (biaxial strain) relationship is established in a biaxial tensile test. This biaxial tensile test offers a number of important advantages over uniaxial testing. First, biaxial tests reflect the natural growth stresses occurring in roughly spherical organs such as fruits. Second, depending on the mechanical properties of the tissues and the geometry of the specimen, uniaxial tensile tests result in a considerable narrowing of the specimen during its extension. This can be easily visualized when stretching a piece of woven fabric. Extensions in the directions of the warp or weft are less than those ‘on the bias’ (i.e. at 45° to the thread directions). In the latter case, a uniaxial extension is accompanied by a significant narrowing. This narrowing yields a severe overestimation of strain and a severe underestimation of the modulus of elasticity ([Niklas 1992](#)). These arguments make the approach by [Bargel \*et al.\* \(2004\)](#) particularly interesting. However, two important findings have been reported since, which may affect the data and its interpretation. First, the skin of a cherry is markedly strained *in situ* and this strain is rapidly released upon excision ([Grimm \*et al.\* 2012](#)). The skin’s *in situ* strain is up to 36.0 % ([Grimm \*et al.\* 2012](#)). Maintaining this level of strain, *ex situ* (i.e. in an excised segment), requires special arrangements to be made. Second, exposing excised skin samples to water causes uncontrolled water uptake and bursting of cells ([Simon 1977](#)), which in turn is likely to affect the mechanical properties of the skin sample that it is desired to measure (assuming of course that the latter reside with the cellular components). The consequences of these findings for the reported rheological properties of the skin are unknown.

The objectives of our study therefore were (i) to compare the inferred mechanical properties of cherry skin using uniaxial and biaxial tensile tests, (ii) to establish a standardized test system and protocol for biaxial tensile testing

of fruit skin, and (iii) to characterize and quantify the rheological properties of cherry skin using this protocol.

## Methods

### Plant material

Mature sweet cherries ‘Adriana’, ‘Burlat’, ‘Merchant’, ‘NY242’, ‘Rainier’, ‘Regina’ and ‘Samba’ and sour cherries (*Prunus cerasus*) ‘Morellenfeuer’ and ‘Ungarische Traubige’ were obtained from glasshouse-grown or field-grown trees grafted on ‘Gisela 5’ rootstocks (*P. cerasus* × *P. canescens*) except for ‘Morellenfeuer’ (rootstock ‘Maxma Delbard’, *Prunus avium* × *P. mahaleb*). European plums (*Prunus* × *domestica*; ‘Hanita’, ‘Nancy’ and ‘Wangenheim’ grafted on ‘Wangenheimer’, ‘Jaspe Fereley’ and ‘St Julien’ rootstocks, respectively) were all field grown. Trees were cultivated at the experimental station of Leibniz University, Hannover (long. 9°49′E, lat. 52°14′N) or, in case of sweet cherry ‘NY242’, at the Esteburg research station, Jork (long. 9°40′E, lat. 53°31′N). Grapes (*Vitis vinifera*; ‘Fanny’, ‘Nero’) and cape gooseberries (*Physalis peruviana*) were purchased locally. For the latter species, cultivar and picking date were unknown. Fruit were selected for uniformity of maturity and size on the basis of colour and mass, and lack of visual defects. Almost all experiments were conducted using fruit picked on the same day. The only exception were the experiments on the effect of orifice diameter, thickness of the fruit skin samples and the effects of pectinase treatment, where fruit were placed in a cold room (2 °C, 95 % relative humidity) and examined within 36 h of harvest.

### Elastometer

A custom-made brass washer (12 mm inner diameter, 40 mm outer diameter, 3 mm thick) was mounted on the surface of a fruit in one of the two shoulder regions that border the cheek using a cyanacrylate adhesive (Loctite 406; Henkel AG & Co. KGaA/Loctite Deutschland GmbH, Munich, Germany). The fruit, with the washer attached, was placed in a sealed box above water (100 % relative humidity) and held for 10 min to accelerate curing of the adhesive. The ES was excised by cutting tangentially beneath the washer with a sharp razor blade. Because a cherry skin is naturally stressed *in vivo*, without the washer, this stress would normally be released very rapidly upon excision ([Grimm \*et al.\* 2012](#)). The washer procedure ensures that the *in vivo* stress is preserved in the excised ES ([Knoche and Peschel 2006](#)). The ES so obtained has the approximate shape of a ‘cap’ of a sphere with a maximum thickness in the middle of  $\sim 2.4 \pm 0.02$  mm of an average fruit of  $10.4 \pm 0.1$  g. The ES comprises cuticle, epidermis, hypodermis and adhering flesh tissue ([Glenn and Poovaiah 1989](#)). A washer with the ES

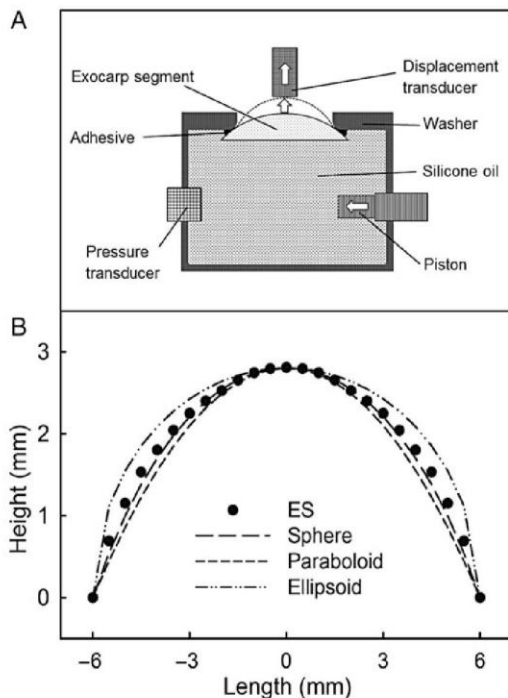


**Figure 1.** (A) Schematic drawing of the elastometer used for biaxial tensile testing. A hydrostatic pressure is generated by displacing silicone oil using a piston. An increase in pressure causes the ESs of sweet cherries to bulge outwards. The system pressure and height of bulging are measured using electronic pressure and displacement transducers, respectively. (B) The contour of the bulged ES was determined from a cross-section of an imprint and digitized. A range of geometrical models (spheroid, paraboloid and ellipsoid) were fitted to the contour.

attached was then mounted in the elastometer such that the cut surface (flesh) of the ES was oriented towards the silicone oil held in the body of the elastometer (Fig. 1A).

The elastometer consists of a chamber filled with silicone oil (Wacker AK10; Wacker Chemie AG, Munich, Germany). A motorized piston could be driven into the chamber, displacing the oil at a rate of  $153 \mu\text{l min}^{-1}$ . The displacement of the oil resulted in (i) an increase in pressure that was monitored with a pressure transducer (Typ 40PC100G; Honeywell International, Morristown, NY, USA) and (ii) the bulging of the 12-mm-diameter portion of the ES within the washer. The amount of bulging was quantified using a displacement transducer (KAP-S/5N; AST Angewandte System Technik GmbH, Wolnzach, Germany) of a material testing machine (BXC-FR2.5TN; Zwick GmbH & Co. KG, Ulm, Germany). The transducer probe (circular, flat, diameter 3 mm) was placed in contact with the skin surface at the centre of the ES and imposed a downward force on the skin of 0.05 N. The material testing machine was programmed to quantify the upward displacement (mm) caused by the bulging

of the ES during the test. Unless otherwise stated, the pressure was increased continuously until the ES fractured. The recorded oil pressure in the elastometer at failure is referred to as the fracture pressure ( $p_{\text{fracture}}$ , kPa), and the corresponding biaxial strain at failure is referred to as the fracture strain ( $\varepsilon_{\text{fracture}}$   $\text{mm}^2 \text{mm}^{-2}$ ). The static pressure in the system due to gravity was negligibly small. All experiments were performed under standard conditions at  $22^\circ\text{C}$ .

$\varepsilon$  and  $\varepsilon_{\text{fracture}}$  were calculated from the height of the bulging ES. A preliminary experiment was conducted to identify the geometry of the bulging ES. Castings (female) of several bulging ESs were prepared using a silicone casting material (Provil<sup>®</sup> novo light regular; Heraeus Kulzer GmbH, Hanau, Germany). Subsequently, castings (male) were prepared from these, using hot-melt glue. The (male) castings were cross-sectioned and their contours were digitized using a binocular microscope system with image analysis (MZ10 F; Leica Microsystems GmbH, Wetzlar, Germany; Olympus DP71; Olympus Europa GmbH, Hamburg, Germany; software Cell-P; Olympus Soft Imaging Solution GmbH, Münster, Germany). Different geometrical models (e.g. spheroid, paraboloid and ellipsoid) were tested (Fig. 1B). The shape of the bulging ES was best described by the spheroid model as indexed by minimum deviance (M. Brüggewirth, unpubl. res.). Therefore, all geometrical calculations were performed using this model. The surface area ( $A$ ) of the bulging ES was calculated from the height ( $h$ ) of the bulge and the inner radius of the washer ( $R$ ) according to

$$A = (R^2 + h^2) \times \pi$$

The biaxial strain ( $\varepsilon$ ) was then calculated as the increase in  $A$  ( $\Delta A$ ) as the ES bulged, relative to its initial surface area ( $A_0$ ):

$$\varepsilon = \frac{\Delta A}{A_0}$$

The modulus of elasticity ( $E$ ) is a measure of the sample stiffness—a high  $E$  value implies a stiff ES requiring a high pressure for a small relative increase in area. Conversely, a low  $E$  is characteristic of an extensible ES where a low pressure causes a large increase in relative area. The  $E$  value was calculated from

$$E = \frac{p \times R^2 \times (R^2 + h^2)}{h^3 \times t \times 2}$$

where  $p$  is the pressure in the elastometer,  $t$  the thickness of the load-bearing skin layer (0.1 mm),  $R$  the radius of the orifice of the washer and  $h$  the height of the bulging ES. It is important to recognize that the strain in the bulging

ES is not uniform but instead increases concentrically towards the centre (Chanliaud *et al.* 2002). Thus, the  $E$  calculated from the above equation is the apparent modulus averaged over the entire ES.

### Experiments

To compare data obtained in biaxial and uniaxial tensile tests of cherry skin and to quantify Poisson's ratio, both tests were conducted on the ES obtained from the same batch of 'Regina' fruit under standard conditions. Because it is technically impossible to maintain the *in vivo* strain of the skin when preparing skin segments for uniaxial tensile tests, we quantified the relaxation of the ES on excision by applying a  $3 \times 3$  mm square pattern of four tiny white blobs of silicone adhesive (744 Silicone Adhesive/Sealant; Dow Corning®, Midland, MI, USA) before excising the ES. The dot pattern was photographed for image analysis. A dumbbell-shaped, biconcave specimen was then excised using a custom-made punch, such that the dot pattern was positioned in the waist region of the sample. The waist width of the ES was 4.25 mm, the maximum width 10 mm and the length 30 mm. Thickness averaged 2 mm. Preliminary experiments established that dumbbell-shaped ESs were needed to avoid failure of the ES at the clamps. The ESs were then mounted in a universal material testing machine (Z 0.5; Zwick/Roell, clamping distance  $l_0 = 18$  mm) equipped with a 10 N force transducer (KAP-Z; Zwick/Roell). The strain rate was  $3 \text{ mm min}^{-1}$ . Calibrated digital photographs of the dot pattern were taken every 15 s (Canon EOS 550D, lens EFS 60 mm, f/2.8 Macro USM; Canon Deutschland GmbH, Krefeld, Germany). The distances between the dots in axial and transverse directions were quantified using image analysis (software Cell-P). The strains ( $\varepsilon_{\text{uniaxial}}^{\text{axial}}$  and  $\varepsilon_{\text{uniaxial}}^{\text{transverse}}$ ) were calculated from the increase in length ( $\Delta l$ ) relative to initial length ( $l_0$ ) according to

$$\varepsilon_{\text{uniaxial}} = \frac{\Delta l}{l_0}$$

Poisson's ratio ( $\nu$ ) of cherry skin was calculated from

$$\nu = -\frac{\varepsilon_{\text{uniaxial}}^{\text{axial}}}{\varepsilon_{\text{uniaxial}}^{\text{transverse}}}$$

Frequency distributions of  $E$ ,  $p_{\text{fracture}}$  and  $\varepsilon_{\text{fracture}}$  were established by pooling control treatments of all experiments performed on the ES excised from mature field-grown 'Regina' fruit under standard conditions (22 °C).

To determine whether the elastometer can also be used for skins of other fruit crops, ESs from sour cherry, plum, grape and cape gooseberry were tested and their  $E$ ,  $p_{\text{fracture}}$  and  $\varepsilon_{\text{fracture}}$  were determined as described above.

Potential relationships between the mechanical properties of ESs excised from the same fruit were studied in 'Regina'. Two washers per fruit were mounted on the two shoulders of the fruit, and the ESs were then excised and tested as described above.

The consequence of releasing the *in vivo* strain of the skin when mounting the ES in the elastometer was investigated by comparing the  $E$ ,  $p_{\text{fracture}}$  and  $\varepsilon_{\text{fracture}}$  of ESs ('Samba') that released or maintained their *in vivo* strain. For release of the *in vivo* strain, the ESs were excised (undercut) from the fruit using a razor blade and left on the fruit *in situ* to relax for 1 h to minimize drying. Because the half-time for strain relaxation is only 2.7 min (Grimm *et al.* 2012), the *in vivo* strain was considered to have been released by the end of the 1-h rest period. Thereafter, the brass washer was mounted on the relaxed ES and then transferred to the elastometer. These ESs were compared with those from the same batch of fruit in which the strain was maintained by mounting the washer prior to excision of the ES as described above. The amount of strain released from the relaxing ES was quantified in a separate experiment using the procedure described earlier (Grimm *et al.* 2012). Briefly, a square dot pattern of silicone sealant blobs (744 Silicone Adhesive/Sealant) was applied to the shoulder of the fruit. Digital photographs (Canon EOS 550D, lens EFS 60 mm, f/2.8 Macro USM) were taken before and immediately after excision of the ES, and thereafter at regular time intervals up to 48 h after excision. The areas enclosed by the dots were quantified (software Cell-P).

To identify potential anisotropy, the orientation of the 'Regina' ES in the washer was labelled. A square dot pattern ( $3 \times 3$  mm) of silicone sealant (744 Silicone Adhesive/Sealant) was applied to the centre of the ES. The ESs were then mounted in the elastometer. The pressure inside the chamber was increased stepwise and digital photographs of the dot pattern on the bulging ES were taken at each pressure step (Canon EOS 550D, lens EFS 60 mm, f/2.8 Macro USM). The distances between the dots in the longitudinal (parallel to the styler scar, pedicel axis) and latitudinal directions (perpendicular to the styler scar, pedicel axis) were quantified using image analysis (software Cell-P), corrected for curvature of the bulging segment, and the strains in the longitudinal and latitudinal directions were calculated according to

$$c = \frac{4h^2 + D^2}{8h}$$

$$b = 2 \times c \times \arcsin\left(\frac{k}{2c}\right)$$

In these equations,  $h$  represents the height of the bulging ES,  $D$  the diameter of the orifice equivalent to the inner

diameter of the washer,  $c$  the radius of the hypothetical sphere of which the ES bulging through the washer is a portion,  $k$  the distance between the dots and  $b$  the length of the arc.

From the longitudinal strain ( $\varepsilon_{\text{longitudinal}}$ ) and the latitudinal strain ( $\varepsilon_{\text{latitudinal}}$ ), the biaxial strain ( $\varepsilon_{\text{biaxial}}^{\text{calculated}}$ ) was calculated according to

$$\varepsilon_{\text{biaxial}}^{\text{calculated}} = (\varepsilon_{\text{longitudinal}} + 1) \times (\varepsilon_{\text{latitudinal}} + 1) - 1$$

$\varepsilon_{\text{biaxial}}^{\text{calculated}}$  was then compared with the biaxial strain obtained from the height of the bulging ES as described above.

The effect of orifice diameter was investigated by mounting the ES excised from 'Regina' cherries in stainless steel washers of inner diameters of 6.4, 8.4, 10.5, 12 and 13 mm.

The effect of ES thickness was studied in field-grown 'NY242' fruit. Exocarp segments were cut to different thicknesses using spacers between the washer and the razor blade. Exocarp segments thinner than 1 mm were prepared by gently scraping away the flesh tissue using a sharpened scoop.

The roles of the cuticle, of the epidermal cell walls and of the hypodermal cell walls on the mechanical properties of the ES were examined in mature 'Regina' cherries. The cuticle was ground using fine sandpaper (K800; EMIL LUX GmbH & Co. KG, Wermelskirchen, Germany) and the treatment effect was documented by fluorescence microscopy (MZ10 F; Leica Microsystems GmbH, GFP plus filter module with 480/40 nm excitation wavelength, emission wavelength  $\geq 510$  nm) following infiltration of the ES using a 0.1% acridine orange solution for 10 min. To address the role of cell walls of the tissue underlying the cuticle and to mimic the process of fruit softening, ESs mounted in washers were incubated in a 10% v/v solution containing pectinase (Panzym Super E; Novozymes A/S, Bagsvaerd, Denmark). The pH of the non-buffered solution was pH 5.1 at the beginning and pH 5.0 at the end of the 3-h incubation period at 22 °C. Thereafter, the ESs were removed from the enzyme solution and tested in the elastometer as described above.

The total strain of a bulging ES ('Merchant') was partitioned into elastic, viscoelastic and plastic strains. The ESs were mounted as described above and subjected to a creep-relaxation test, comprising 'loading', 'holding' and 'unloading' phases. First, during the loading phase, the pressure was increased to 10 kPa. Next, in the holding phase, the pressure was held constant for 10 min allowing the ES to creep. Last, in the unloading phase, the pressure was suddenly decreased to 0 kPa, allowing the ES to relax. The instantaneous strain during the loading phase is referred to as the elastic strain. The total strain at the

end of the holding phase is equal to the sum of the viscoelastic and the plastic strains (in the literature it is sometimes referred to as the 'creep strain'). The strain that remains after the relaxation phase is the plastic strain.

## Data analysis and presentation

Data analysis was limited to those ESs that did not fracture at the edge of the orifice. Fracture at the edge of the ESs may have resulted from a mounting artefact or a skin flaw that was not noticed in a visual inspection. The majority of ESs failed in the centre. The fraction that failed at the edge amounted to ~20% of the population of ESs investigated. These results were excluded from the analysis. Unless otherwise stated, the ES data presented are the means  $\pm$  standard errors of the means (SEM). Following analysis of variance, mean comparisons were performed using Tukey's studentized range test ( $P \leq 0.05$ , packet multcomp 1.2–12, procedure glht, R 2.13.1; R Foundation for Statistical Computing, Wien, Austria) and the  $t$ -test ( $P \leq 0.05$ , R 2.13.1). The significance of coefficients of correlation ( $r$ ) and determination ( $r^2$ ) for probabilities ( $P$ ) of 0.05, 0.01 and 0.001 are indicated by \*, \*\*, and \*\*\*, respectively.

## Results

Performing uniaxial tensile tests using dumbbell-shaped, biconcave ES specimens resulted in linear increases in force and axial strain vs. testing time, to the point of fracture (Fig. 2A). The corresponding force vs. (axial) strain diagrams were also linear ( $r^2 = 0.99^{***}$ ; Fig. 2B). As the ES extended in the axial direction, considerable narrowing was observed, perpendicular to the applied force. Calculating the corresponding  $\varepsilon_{\text{uniaxial}}^{\text{transverse}}$  revealed that this  $\varepsilon_{\text{uniaxial}}^{\text{transverse}}$  was linearly and negatively related to the axial force ( $r^2 = 0.99^{***}$ ; Fig. 2B). The Poisson's ratio calculated from the slopes of the force vs.  $\varepsilon_{\text{uniaxial}}^{\text{axial}}$  and force vs.  $\varepsilon_{\text{uniaxial}}^{\text{transverse}}$  relationships was  $0.74 \pm 0.03$ .

When displacing silicone oil by driving the piston into the chamber of the elastometer,  $p$  increased linearly with time, causing the ES to bulge as indicated by an essentially linear increase in height (Fig. 3A and B). The  $\varepsilon$  value calculated therefrom also increased with time. The modulus  $E$  increased rapidly to a maximum of 18 MPa at ~25 s after initiation of the test and was then approximately constant until failure (Fig. 3C). When the ES failed,  $p$ ,  $\varepsilon$ , and  $E$  decreased instantaneously. The pressure-strain diagrams were essentially linear up to the point of fracture ( $r^2 = 0.98^{***}$ ; see Fig. 3D for a representative ES).

Frequency distributions of  $E$ ,  $p_{\text{fracture}}$  and  $\varepsilon_{\text{fracture}}$  were approximately symmetrical and the corresponding normal probability plots were linear, indicating that  $E$ ,  $p_{\text{fracture}}$

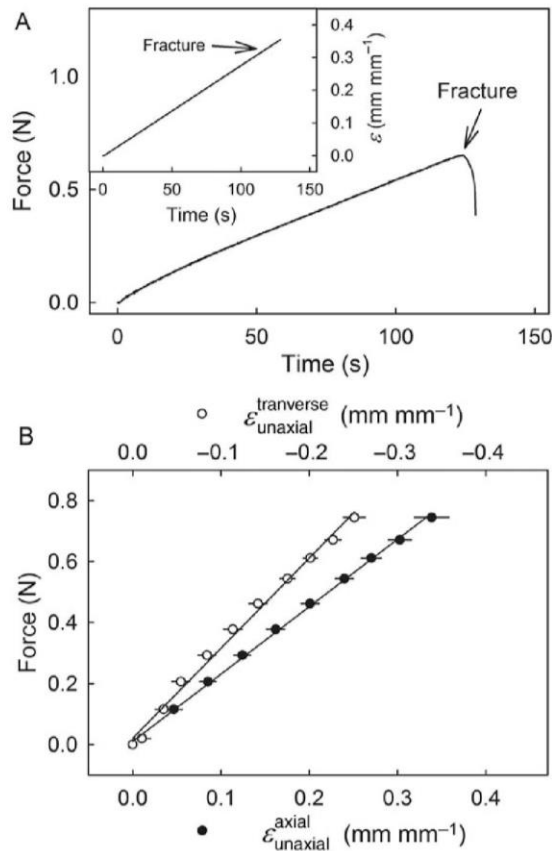


**Figure 2.** Uniaxial tensile test of a biconcave, dumbbell-shaped, exocarp strip carved from sweet cherry skin. (A) Representative time course of force and strain ( $\epsilon$ ; inset) until fracture. (B) Relationship between force and the strains in the directions of the applied force (axial strain;  $\epsilon_{\text{unaxial}}^{\text{axial}}$ ) and perpendicular to the applied force (transverse strain;  $\epsilon_{\text{unaxial}}^{\text{transverse}}$ ). Note that the negative  $\epsilon_{\text{unaxial}}^{\text{transverse}}$  results from the marked narrowing of the strip when subjected to a uniaxial load. Data represent means  $\pm$  SEM ( $n = 10$ ).

and  $\epsilon_{\text{fracture}}$  followed a normal distribution (Fig. 4). There was little difference between the means and medians of  $E$ ,  $p_{\text{fracture}}$  and  $\epsilon_{\text{fracture}}$  for the ES of fruit from the 2012 and 2013 seasons. However, the variability was somewhat larger in 2013 as indicated by the lower slope of the normal probability plots and the larger standard errors, coefficients of variations and ranges (Table 1).

Qualitatively similar data as in sweet cherry were obtained for sour cherries, plums, grapes and cape gooseberries, but the range in mechanical properties was somewhat larger (Table 2). The lowest  $E$  was measured for the sour cherry cultivar ‘Ungarische Traubige’, and the highest for the ‘Hanita’ plum. The maximum  $p_{\text{fracture}}$  was measured in the ‘Fanny’ grape berry, and the highest  $\epsilon_{\text{fracture}}$  in the sour cherry cultivar ‘Ungarische Traubige’ (Table 2).

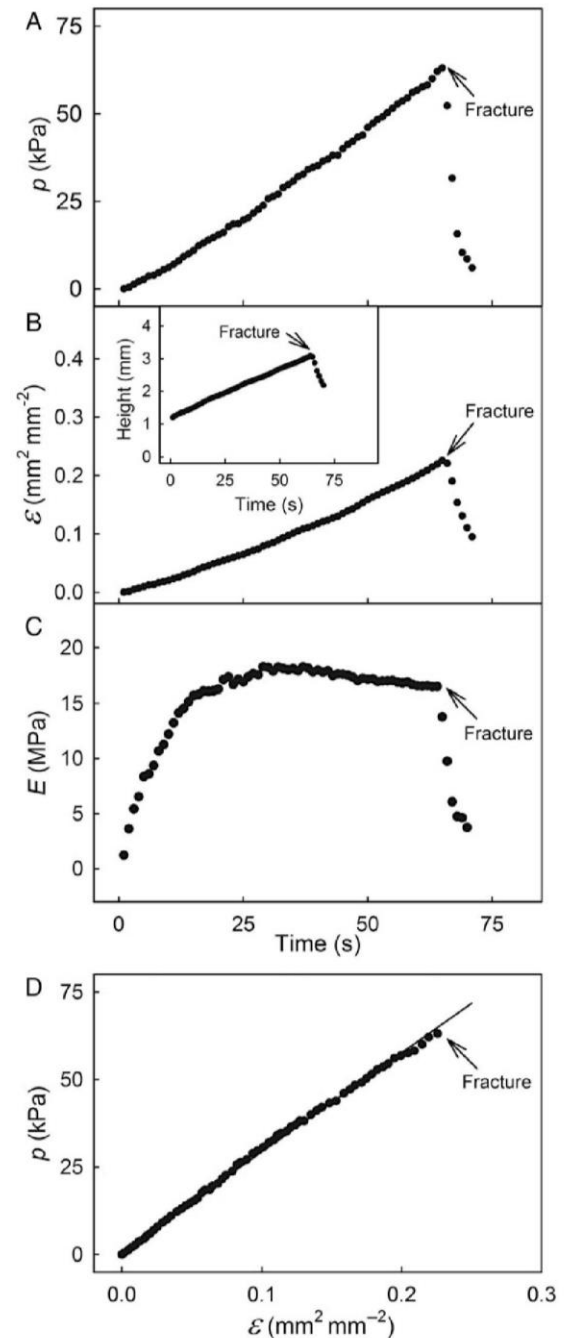


**Figure 3.** Representative time courses of the change in pressure ( $p$ ; A), in strain ( $\epsilon$ ; B), in height of the bulging ES of sweet cherry fruit (B, inset), and in the modulus of elasticity ( $E$ ; C) during a biaxial tensile test. The last six data points represent points recorded after fracture. (D) Pressure/strain diagram of a representative ES until fracture.

The  $E$ ,  $p_{\text{fracture}}$  and  $\epsilon_{\text{fracture}}$  of pairs of ESs excised from opposite sides of the same fruit were significantly correlated, with coefficients of correlation of  $r = 0.73^{***}$ ,  $0.74^{***}$  and  $0.54^{**}$ , respectively (Fig. 5).

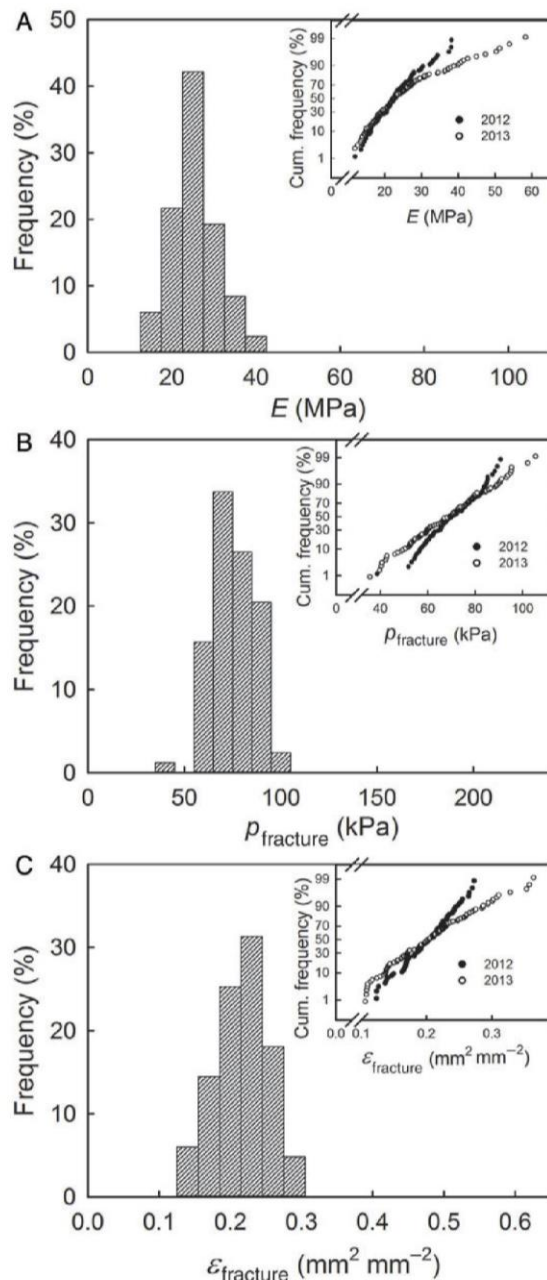


**Figure 4.** Frequency distributions of the modulus of elasticity ( $E$ ; A), the pressure at fracture ( $p_{\text{fracture}}$ ; B) and the strain at fracture ( $\varepsilon_{\text{fracture}}$ ; C) of ESs of sweet cherry fruit in 2012. Insets: probability plots of cumulative frequency distributions of  $E$ ,  $p_{\text{fracture}}$  and  $\varepsilon_{\text{fracture}}$  of the same cultivar in 2012 ( $n = 84$ ) and 2013 ( $n = 115$ ).

Upon excision, the ES relaxed and decreased in surface area, indicating the presence of significant strain *in vivo*. For the batch of fruit used in this experiment, the *in vivo* strains averaged  $15.5 \pm 1.4\%$ , which is somewhat lower than the strains reported by Grimm et al. (2012; range

18.7–36.0%). The presence of *in vivo* strain significantly affected the mechanical properties of the ES (Table 3). Exocarp segments that released the *in vivo* strain and relaxed before the biaxial tensile test had higher  $\varepsilon_{\text{fracture}}$  and lower  $E$  than those ESs where the *in vivo* strain was maintained (Table 3). There were no significant differences in  $p_{\text{fracture}}$  between ESs with and without *in vivo* strain (Table 3).

The  $\varepsilon_{\text{latitudinal}}$  and  $\varepsilon_{\text{longitudinal}}$  on the bulging ES were essentially identical, indicating that the cherry skin was isotropic in the tangential plane (Fig. 6). The  $\varepsilon_{\text{biaxial}}^{\text{calculated}}$  measured from the dot pattern applied to the centre of the ES increased linearly as the pressure increased (data not shown) and was linearly related to the biaxial strain obtained from the height of the bulging ES ( $r^2 = 0.97^{***}$ ). It should be noted that the biaxial strain derived from the dot pattern in the centre of the ES was always larger by a factor of  $2.16 \pm 0.06$  ( $r^2 = 0.99^{***}$ ) than the mean strain obtained from the height of the bulging ES (Fig. 6, inset).

The value of  $E$  increased linearly as the orifice diameter increased, suggesting that ESs were stiffer when mounted in a larger orifice (Fig. 7). However,  $p_{\text{fracture}}$  and  $\varepsilon_{\text{fracture}}$  decreased as the orifice diameter increased (Fig. 7).

The mechanical properties of ESs also depended on their thickness. Increasing thickness also caused the values of  $E$  and  $p_{\text{fracture}}$  to increase but that of  $\varepsilon_{\text{fracture}}$  decreased (Fig. 8).

Enzyme digestion of the cell walls of epidermal and hypodermal cells decreased  $p_{\text{fracture}}$  and  $\varepsilon_{\text{fracture}}$ , whereas abrading the cuticle decreased only  $\varepsilon_{\text{fracture}}$  (Table 4). Neither treatment had any effect on  $E$ .

Increasing  $p$  during the loading phase of the creep-relaxation test caused an increase in instantaneous elastic strain (Fig. 9A). When  $p$  was held constant during the subsequent holding phase, the ES extended (crept) due to viscoelastic strain. Upon unloading, the ES relaxed, indicating a release of elastic and viscoelastic strains. No irreversible, plastic strain was detected. Plotting viscoelastic strain during the holding period vs. log-transformed time yielded a linear relationship ( $r^2 = 0.98^{***}$ ; Fig. 9B).

## Discussion

Our data demonstrate that (1) the elastometer allows a reproducible *in vitro* test of cherry skin; (2) the cherry skin is isotropic in the tangential plane and shows both elastic and viscoelastic strain; (3) the epidermis and hypodermis represent the structural ‘backbone’ of cherry skin. The contribution of the cuticle to the skin’s mechanical properties is minimal. These findings are discussed in detail below.

**Table 1.** Means, medians, standard errors of means (SEM), coefficients of variation (CV) and ranges of modulus of elasticity ( $E$ ), fracture pressure ( $p_{\text{fracture}}$ ) and fracture strain ( $\varepsilon_{\text{fracture}}$ ) in ESs excised from sweet cherries and subjected to a biaxial tensile test. Exocarp segments were prepared from the cheek of mature fruit in the 2012 ( $n = 84$ ) and 2013 ( $n = 115$ ) growing seasons.

	Year	Mean	Median	SEM	CV	Range	
						Min.	Max.
$E$ (MPa)	2012	23.2	22.2	0.66	0.25	12.0	41.2
	2013	25.2	22.7	0.94	0.40	10.5	60.3
$p_{\text{fracture}}$ (kPa)	2012	70.8	70.0	1.2	0.15	38.6	92.6
	2013	69.0	69.6	1.4	0.22	35.6	107.6
$\varepsilon_{\text{fracture}}$ ( $\text{mm}^2 \text{mm}^{-2}$ )	2012	0.20	0.20	0.01	0.18	0.12	0.34
	2013	0.21	0.20	0.01	0.29	0.11	0.38

**Table 2.** Modulus of elasticity ( $E$ ), fracture pressure ( $p_{\text{fracture}}$ ) and fracture strain ( $\varepsilon_{\text{fracture}}$ ) of ESs excised from the equatorial region of mature fruit of sour cherry, European plum, grape and cape gooseberry. Data are means and standard errors of means of 25 replications per species.

Species	Cultivar	$E \pm \text{SE}$ (MPa)	$p_{\text{fracture}} \pm \text{SE}$ (kPa)	$\varepsilon_{\text{fracture}} \pm \text{SE}$ ( $\text{mm}^2 \text{mm}^{-2}$ )
Sour cherry	Morellenfeuer	$5.9 \pm 0.2$	$27.8 \pm 0.8$	$0.30 \pm 0.01$
	Ungarische Traubige	$3.5 \pm 0.2$	$36.2 \pm 1.1$	$0.53 \pm 0.01$
European plum	Hanita	$35.9 \pm 3.2$	$53.1 \pm 4.2$	$0.15 \pm 0.01$
	Wangenheim	$25.4 \pm 7.8$	$65.8 \pm 3.4$	$0.18 \pm 0.01$
	Nancy	$27.3 \pm 1.9$	$56.8 \pm 3.0$	$0.18 \pm 0.01$
Grape berry	Fanny	$21.5 \pm 1.6$	$78.9 \pm 2.5$	$0.23 \pm 0.02$
	Nero	$20.8 \pm 1.7$	$75.0 \pm 2.8$	$0.19 \pm 0.01$
Cape gooseberry	Unknown	$20.5 \pm 0.8$	$94.7 \pm 3.9$	$0.25 \pm 0.01$

An *in vitro* test system simulating growth stresses must meet the following conditions. (i) Skin samples must maintain their key mechanical properties when excised and mounted in the testing device. (ii) The test strains imposed on the ES *in vitro* must operate in the same directions as the ‘natural’ ones *in vivo*. (iii) All strains must be applied in a defined manner. The elastometer used in our study met all three requirements.

First, the *in vivo* strain was maintained in our tests by attaching a washer to the ES area of the fruit before excision. This procedure essentially fixes and maintains the *in vivo* strain in the excised ES (Knoche and Peschel 2006). Indeed, if strain were not fixed, and the ES had relaxed upon excision, then  $\varepsilon_{\text{fracture}}$  would increase and  $E$  would decrease, whereas  $p_{\text{fracture}}$  would not be affected (Table 3). Also, silicone oil was used to pressurize the elastometer, not water. Compared with water, silicone oil is much less likely to modify tissue water potential (water uptake, cell bursting etc.). If water were to be used, osmotic buffering probably would be required to avoid modifying tissue water relations.

Second, both the biaxial tensile test by Bargel et al. (2004) and our elastometer subject skin samples to biaxial tangential strains, thereby simulating the distribution of growth strains in spherical fruit *in vivo*. Because the orifice of the washer is circular, the force vectors are expected to be uniform at least in the centre of the bulging ES where most ESs failed. It may be argued that biaxial  $\varepsilon_{\text{fracture}}$  can also be calculated from  $\varepsilon_{\text{fracture}}$  determined in uniaxial tests. However, performing the calculations clearly demonstrates that this would result in a four-fold overestimation of  $\varepsilon_{\text{fracture}}$  ( $79 \pm 3.9\%$  vs.  $20 \pm 0.6\%$  for the calculated biaxial vs. the true  $\varepsilon_{\text{fracture}}$ ; Table 1).

Third, the elastometer allowed the ES to be stressed in a defined manner, i.e. using a pressurized fluid to strain the ES at a constant and defined rate up to some preset level or by performing creep-relaxation tests with and without cyclic application of pressure (M. Brüggewirth, unpubl. res.). It is important to recognize that the application of uniform pressure does not result in uniform strain across the ES. In a bulging, circular specimen, a strain gradient



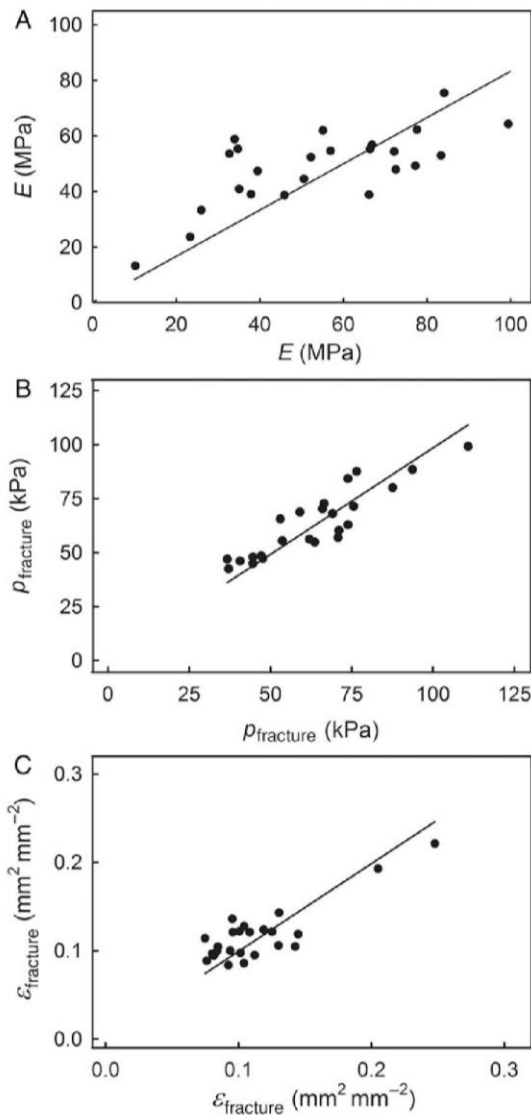


**Figure 5.** Relationship between the modulus of elasticity ( $E$ ; A), the pressures at fracture ( $p_{\text{fracture}}$ ; B) and the strain at fracture ( $\varepsilon_{\text{fracture}}$ ; C) of pairs of ESs excised from opposite shoulders of the same sweet cherry fruit. Data represent means  $\pm$  SEM ( $n = 24$ ).

**Table 3.** Effect of maintaining or releasing the *in vivo* strain and stress of ESs excised from mature sweet cherries on the modulus of elasticity ( $E$ ), fracture pressure ( $p_{\text{fracture}}$ ) and fracture strain ( $\varepsilon_{\text{fracture}}$ ). \*Means within columns followed by the same letter are not significantly different, *t*-test.  $P < 0.05$ . Values are means and standard errors of means of 10 replicates.

<i>In vivo</i> strain	$E$ (MPa)	$p_{\text{fracture}}$ (kPa)	$\varepsilon_{\text{fracture}}$ ( $\text{mm}^2 \text{mm}^{-2}$ )
Maintained	$16.6 \pm 1.2\text{a}^*$	$51.0 \pm 1.6\text{a}$	$0.21 \pm 0.01\text{a}$
Released	$11.4 \pm 1.0\text{b}$	$50.6 \pm 1.6\text{a}$	$0.29 \pm 0.01\text{b}$

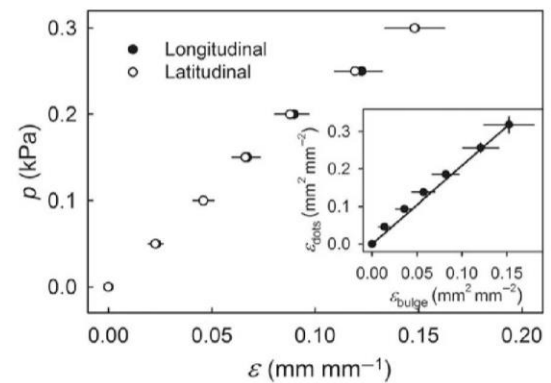


**Figure 6.** Relationship between pressure ( $p$ ) and longitudinal or latitudinal strains ( $\varepsilon$ ) of ESs excised from sweet cherry. The longitudinal strain is that in the direction of the stylar scar/pedicle axis, and the latitudinal strain is perpendicular to it. The two strains were measured using a square pattern of dots applied to the ES. Inset: relationship between the biaxial strain calculated from the height of the bulging ES and the biaxial strain measured using the dot pattern. The regression line has a slope of  $2.16 \pm 0.06$  ( $r^2 = 0.99^{***}$ ). Data represent means  $\pm$  SEM ( $n = 10$ ).

exists from a high value in the centre to a lower one at the edge (Chanliaud et al. 2002). Further, the strain at the edge is uniaxial. A strain gradient was also present in our ES, where the strain calculated from the dot pattern in the centre was twice the mean strain calculated from the height of the bulging ES (Fig. 6, inset). The decrease of  $p_{\text{fracture}}$  and  $\varepsilon_{\text{fracture}}$  observed when the washer orifice diameter was increased is also accounted for by a gradient in strain. The probability of failure increases because strains in the centre of the bulging ES of larger diameter would be greater.

The elastometer allows reproducible testing of the ES of fleshy fruit such as cherries under defined conditions. Reproducibility is indicated by the significant correlation of evaluations of  $E$ ,  $p_{\text{fracture}}$  and  $\varepsilon_{\text{fracture}}$  in pairwise comparisons where these mechanical properties were tested on pairs of ESs excised from the two shoulders of the same fruit (Fig. 5). Also, frequency distributions of the mechanical properties were very similar for fruit from the 2012 and 2013 seasons. The normal probability plots were largely linear, indicating symmetrical distributions with coefficients of variation ranging from 0.15 to 0.40. These values are not unusual for biological materials that are well known to be highly variable compared with non-biological ones (Table 1). Thus, the elastometer proved to be a useful tool for standardized testing of fruit skins.

In cherries, preferential orientation of epidermal cells has been reported for the cheek and neighbouring shoulder region (Peschel and Knoche 2005). This, however, had no effect on isotropy, for the skin of the shoulder regions

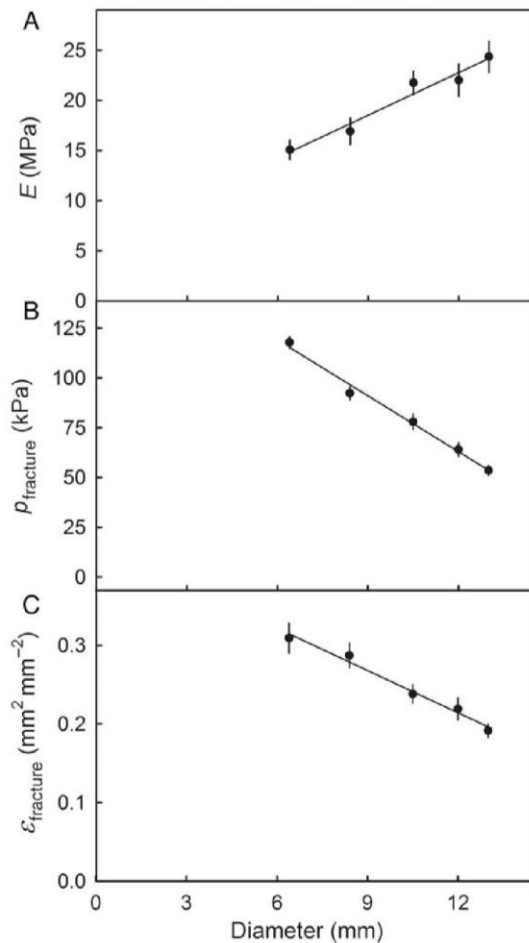


**Figure 7.** Effect of diameter of ESs excised from sweet cherry fruit on the modulus of elasticity ( $E$ ; A), pressure at fracture ( $p_{\text{fracture}}$ ; B) and the strain at fracture ( $\epsilon_{\text{fracture}}$ ; C). Data represent means  $\pm$  SEM ( $n = 20$ ).

was found to be isotropic in the tangential plane, with  $\epsilon_{\text{longitudinal}}$  and  $\epsilon_{\text{latitudinal}}$  being indistinguishable (Fig. 6).

Based on the following observations, cherry skin behaves like a viscoelastic composite. (i) During the holding phase of the creep-relaxation experiments, strain increased continuously. This ‘creep’ strain during the holding phase must have been primarily viscoelastic because there was essentially no irreversible (i.e. ‘plastic’) strain detectable during the unloading phase (Fig. 9). (ii) Plotting the strain increase during the holding phase vs. a logarithmic timescale yields a linear relationship: a characteristic of viscoelastic materials (Cosgrove 1993). Viscoelasticity of cherry skin is also reported in Grimm et al. (2012) and is typical of the skins of other soft-fruit species such as grape (Hankinson et al. 1977) and tomato (Petracek and Bukovac 1995; Matas et al. 2004). Moreover, it is a characteristic of cell walls in general (Cosgrove 1993)

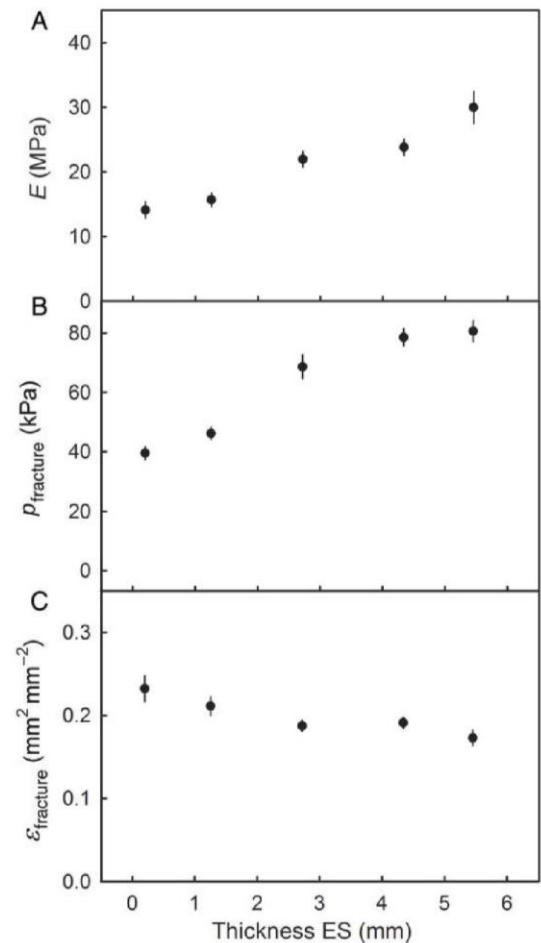


**Figure 8.** Effect of thickness of ESs excised from sweet cherry skin on the modulus of elasticity ( $E$ ; A), the pressure at fracture ( $p_{\text{fracture}}$ ; B) and the strain at fracture ( $\epsilon_{\text{fracture}}$ ; C). Data represent means  $\pm$  SEM ( $n = 20$ ).

being primarily related to hemicelluloses (Chanliaud et al. 2002) and is typical for the deformation of turgid cells (Niklas and Spatz 2012).

The elastic strain component, which makes up an even larger contribution to total strain than does viscoelastic strain, also originates from the cell walls (Jackman et al. 1992) and particularly from the cellulosic fraction (Chanliaud et al. 2002). At the loads applied in our experiments, a plastic strain was not detectable (Fig. 9). In this respect, cherry skins may differ from tomato and grape skins where irreversible, plastic components of deformation have been identified (Lang and Düring 1990; Petracek and Bukovac 1995; Matas et al. 2004).

The pressure/strain diagrams obtained in our experiments were essentially linear, which contrasts with Bargel et al. (2004) who report rising slopes in their pressure/displacement diagrams (e.g. see Fig. 5 in Bargel et al.

**Table 4.** Effect of abrading the cuticle and of digesting cell walls of epidermal and hypodermal cells of ESs excised from the cheek of mature sweet cherries on the modulus of elasticity ( $E$ ), fracture pressure ( $p_{\text{fracture}}$ ) and fracture strain ( $\varepsilon_{\text{fracture}}$ ). The cuticle was abraded using sandpaper. In a further treatment, the support of the cuticle by epidermal and hypodermal cell layers was weakened by digesting the cell walls of the epidermal and hypodermal cell layers using pectinase. Untreated ES served as control. For details see the Methods section. \*Means separation by Tukey's studentized range test,  $P < 0.05$ . Values are means and standard errors of means.

Treatment	N	$E$ (MPa)	$p_{\text{fracture}}$ (kPa)	$\varepsilon_{\text{fracture}}$ ( $\text{mm}^2 \text{mm}^{-2}$ )
Control	18	$13.6 \pm 1.0\text{a}^*$	$44 \pm 2.3\text{a}$	$0.20 \pm 0.01\text{a}$
Abraded cuticle	19	$16.8 \pm 1.5\text{a}$	$41 \pm 2.4\text{a}$	$0.17 \pm 0.01\text{b}$
Digested epidermis and hypodermis	22	$14.1 \pm 1.1\text{a}$	$26 \pm 2.0\text{b}$	$0.16 \pm 0.01\text{b}$

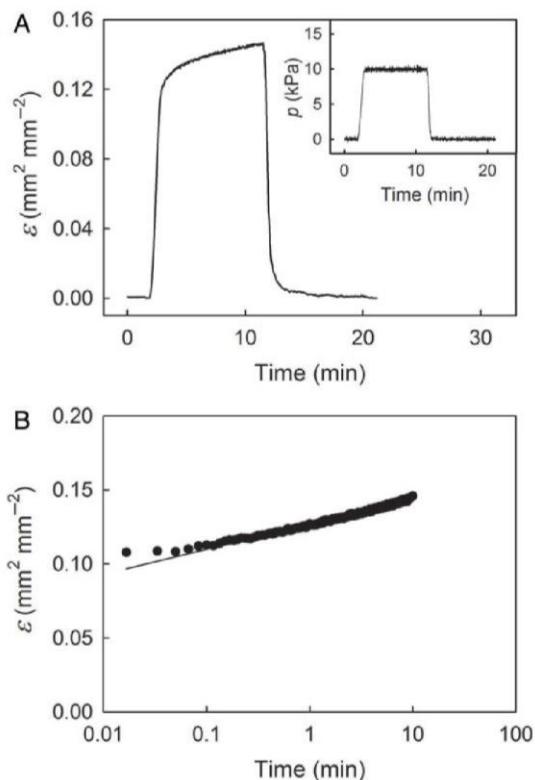


**Figure 9.** Representative time course of strain ( $\varepsilon$ ; A) and pressure ( $p$ ; A, inset) of an ES excised from sweet cherry skin during a biaxial, creep-relaxation test. The pressure was increased during the initial loading phase, held constant during the holding phase and decreased during the subsequent unloading phase. (B) Strain during the holding phase is redrawn on a log-transformed timescale.

2004). This observation is interpreted as a 'strain hardening' of the fruit skin (Bargel et al. 2004). However, an alternative explanation is that those samples released their *in vivo* strain immediately following excision and that the subsequent increases in the slope of their pressure/displacement diagrams were the result of a re-establishment of the *in vivo* strain that had been present prior to excision. Grimm et al. (2012) demonstrated that cherry skin is significantly strained (18.7–36 % depending on cultivar)

and that this *in vivo* strain is released very rapidly upon excision (half-time = 2.7 min). This interpretation would also account in part for the markedly higher  $\varepsilon_{\text{fracture}}$  of 90 % that was observed by Bargel et al. (2004; recalculated from their Fig. 6). However, when simulating the release of strain in our elastometer, the difference in  $\varepsilon_{\text{fracture}}$  between ESs that maintained or released their *in vivo* strain was smaller, indicating that other factors may also be involved. The release of strain had no effect on  $p_{\text{fracture}}$ . The range of  $p_{\text{fracture}}$  in our study (35–107 kPa; Table 1) is similar to that in Bargel et al. (2004; range 40–110 kPa). No differences in  $p_{\text{fracture}}$  were observed either with or without *in vivo* strain (Table 3).

We suggest that the mechanical properties of the ES are dominated by those of the epidermis and hypodermis and not by those of the cuticle. This hypothesis is supported by the following observations.

(i) Fruit softening, simulated by incubation in pectinase, reduced both  $E$  and  $\varepsilon_{\text{fracture}}$  by ~30 % (Table 4). Consistent with this is the earlier observation that complete skin failure occurred in ESs that had their *in vivo* strain fixed (using a washer) and that were incubated with the washer attached in cellulase and pectinase (Knoche and Peschel 2006). During incubation, the enzymes weakened the cellular support of the cuticular membrane (CM). The subsequently occurring failure of the CM indicates that the CM is quite unable to sustain the degree of strain existing *in vivo* without the mechanical support offered by the underlying cell layers (Knoche and Peschel 2006).

(ii) Abrasion of the cuticle had only a small effect on the mechanical behaviour of the ES (Table 4). The slight decrease in strain observed here may have resulted from minor damage to some of the epidermal cell walls during abrasion. Also, Knoche and Peschel (2006) and Grimm et al. (2012) further demonstrate that the mechanical contribution of the cuticle in strain release is small and negligible. These observations are not surprising considering the delicate nature of the c. 1- $\mu\text{m}$ -thick cuticle (Knoche and Peschel 2006) relative to the c. 85- $\mu\text{m}$ -thick cellular component of the skin composite (i.e. the epidermis + hypodermis; Glenn and Poovaiah 1989).

Also, considering the common presence of CM micro-cracks (Peschel and Knoche 2005) vs. the obvious, load-bearing properties of the collenchymatous (thickened) epidermal and hypodermal cells. Moreover, in apple, pear and tomato that have even thicker CM (c. 28.2, 17.3 and 15.5 g m<sup>-2</sup> equivalent to a calculated mean thickness of 23.3, 14.3 and 12.8 µm for apple, pear and tomato, respectively; Khanal *et al.* 2013a, b) it is the cell layers of the skin that seem to support its mechanical stability (Matas *et al.* 2004; Khanal *et al.* 2013a; Khanal and Knoche 2014).

(iii) We observed little effect of varying the thickness of the ES (from 0.2 to 5.5 mm) on its mechanical properties. Noting that our technique varies only the depth of the adhering flesh cells, we can infer that these cells contribute very little to the skin's mechanical properties (Fig. 8). We reasonably conclude that the mechanical properties of the skin reside in the c. 85-µm-thick epidermal and hypodermal cell layers and are not significantly affected by either the CM or the flesh cells. Incidentally, we note that the cells in these layers have much smaller lumina and thicker walls than the flesh cells (Glenn and Pooaiah 1989).

## Conclusions

Our experiments demonstrate that the elastometer is a useful instrument that allows strained skin samples to be tested *in vitro* under conditions that simulate those likely to be found *in vivo*. Using this system it is now possible to quantify and establish the basis of the fundamental mechanical properties of fruit skins. The data presented here indicate that the cherry skin is isotropic in the tangential plane and exhibits both elastic and viscoelastic behaviour. It has further been established that the epidermis and hypodermis (but not the cuticle or flesh) represent the structural 'backbone' of cherry skin. These findings have important consequences, including a new understanding of the mechanism of skin failure *in vivo*. Viscoelastic deformation decreases skin stress (i.e. limits stress buildup with growth) and also prevents the development of significant tissue pressure inside the fruit. Based on current theories for cracking, this will decrease the likelihood of skin failure.

## Sources of Funding

This study was supported in part by a grant from the Deutsche Forschungsgemeinschaft (KN402/8-1).

## Contributions by the Authors

M.K. obtained the funds to support the study. H.F. conducted preliminary experiments to establish the test

system. M.K., H.F. and M.B. designed the experiments. M.B. conducted the experiments. M.K. and M.B. analysed the data and wrote the manuscript. M.K., H.F. and M.B. revised and edited the paper.

## Conflicts of Interest Statement

None declared.

## Acknowledgements

We thank D. Reese and C. Knake for building and programming the elastometer, Dr E. Grimm for helpful discussions, and Drs S. Lang and H.-C. Spatz for very useful comments on an earlier version of this manuscript and for suggesting the equation for quantifying the modulus of elasticity.

## Literature Cited

- Bargel H, Spatz HC, Speck T, Neinhuis C. 2004. Two-dimensional tension test in plant biomechanics—sweet cherry fruit skin as a model system. *Plant Biology* **6**:432–439.
- Chanliaud E, Burrows KM, Jeronimidis G, Gidley MJ. 2002. Mechanical properties of primary plant cell wall analogues. *Planta* **215**: 989–996.
- Cosgrove DJ. 1993. Wall extensibility—its nature, measurement and relationship to plant-cell growth. *New Phytologist* **124**:1–23.
- Dominguez E, Heredia-Guerrero JA, Heredia A. 2011a. The biophysical design of plant cuticles: an overview. *New Phytologist* **189**: 938–949.
- Dominguez E, Cuartero J, Heredia A. 2011b. An overview on plant cuticle biomechanics. *Plant Science* **181**:77–84.
- Glenn GM, Pooaiah BM. 1989. Cuticular properties and postharvest calcium applications influence cracking of sweet cherries. *Journal of the American Society for Horticultural Science* **114**:781–788.
- Grimm E, Peschel S, Becker T, Knoche M. 2012. Stress and strain in the sweet cherry skin. *Journal of the American Society for Horticultural Science* **137**:383–390.
- Hankinson B, Rao VNM, Smit CJB. 1977. Viscoelastic and histological properties of grape skins. *Journal of Food Science* **42**:632–635.
- Jackman RL, Marangoni AG, Stanley DW. 1992. The effect of turgor pressure on puncture and viscoelastic properties of tomato tissue. *Journal of Texture Studies* **23**:491–505.
- Khanal BP, Knoche M. 2014. Mechanical properties of apple skin are determined by epidermis and hypodermis. *Journal of the American Society for Horticultural Science* **139**:139–148.
- Khanal BP, Grimm E, Knoche M. 2013a. Russeting in apple and pear: a plastic periderm replaces a stiff cuticle. *AoB PLANTS* **5**: pls048; doi:10.1093/aobpla/pls048.
- Khanal BP, Grimm E, Finger S, Blume A, Knoche M. 2013b. Intracuticular wax fixes and restricts strain in leaf and fruit cuticles. *New Phytologist* **200**:134–143.
- Knoche M, Peschel S. 2006. Water on surface aggravates microscopic cracking of the sweet cherry fruit cuticle. *Journal of the American Society for Horticultural Science* **131**:192–200.
- Lang A, Düring H. 1990. Grape berry splitting and some mechanical properties of the skin. *Vitis* **29**:61–70.

- Matas AJ, Cobb ED, Bartsch JA, Paolillo DJ, Niklas KJ. 2004. Biomechanics and anatomy of *Lycopersicon esculentum* fruit peels and enzyme-treated samples. *American Journal of Botany* **91**: 352–360.
- Niklas KJ. 1992. *Plant biomechanics—an engineering approach to plant form and function*. Chicago, IL, USA: The University of Chicago Press.
- Niklas KJ, Spatz H-C. 2012. *Plant physics*. Chicago, IL, USA: The University of Chicago Press.
- Peschel S, Knoche M. 2005. Characterization of microcracks in the cuticle of developing sweet cherry fruit. *Journal of the American Society for Horticultural Science* **130**:487–495.
- Petracek PD, Bukovac MJ. 1995. Rheological properties of enzymatically isolated tomato fruit cuticle. *Plant Physiology* **109**:675–679.
- Simon EW. 1977. Leakage from fruit cells in water. *Journal of Experimental Botany* **28**:1147–1152.
- Skene DS. 1980. Growth stresses during fruit-development in Cox Orange Pippin apples. *Journal of Horticultural Science* **55**:27–32.

## **5. Factors affecting mechanical properties of the skin of sweet cherry fruit**

Dieser Artikel wurde im Original 2016 in der Zeitschrift „Journal of the American Society for Horticultural Science“ veröffentlicht:

Brüggenwirth, M. und Knoche, M. (2016a) Factors affecting mechanical properties of the skin of sweet cherry fruit. *Journal of the American Society for Horticultural Science* 141, 45-53.

J. AMER. SOC. HORT. SCI. 141(1):45–53. 2016.

## Factors Affecting Mechanical Properties of the Skin of Sweet Cherry Fruit

Martin Brüggewirth and Moritz Knoche<sup>1</sup>

*Institute for Horticultural Production Systems, Leibniz-University Hannover, Herrenhäuser Straße 2, 30419 Hannover, Germany*

ADDITIONAL INDEX WORDS. *Prunus avium*, biaxial strain, cracking, fracture, tensile test, turgor

**ABSTRACT.** The skins of all fruit types are subject to sustained biaxial strain during the entire period of their growth. In sweet cherry (*Prunus avium* L.), failure of the skin greatly affects fruit quality. Mechanical properties were determined using a biaxial bulging test. The factors considered were the following: ripening, fruit water relations (including turgor, transpiration, and water uptake), and temperature. Excised discs of fruit skin were mounted in a custom elastometer and pressurized from their anatomically inner surfaces. This caused the skin disc to bulge outwards, stretching it biaxially, and increasing its surface area. Pressure ( $p$ ) and biaxial strain ( $\varepsilon$ ) due to bulging were quantified and the modulus of elasticity [ $E$  (synonyms elastic modulus, Young's modulus)] was calculated. In a typical test,  $\varepsilon$  increased linearly with  $p$  until the skin fractured at  $p_{\text{fracture}}$  and  $\varepsilon_{\text{fracture}}$ . Stiffness of the skin decreased in ripening late stage III fruit as indicated by a decrease in  $E$ . The value of  $p_{\text{fracture}}$  also decreased, whereas that of  $\varepsilon_{\text{fracture}}$  remained about constant. Destroying cell turgor decreased  $E$  and  $p_{\text{fracture}}$  relative to the turgescence control. The  $E$  value also decreased with increasing transpiration, while  $p_{\text{fracture}}$  and (especially)  $\varepsilon_{\text{fracture}}$  increased. Water uptake had little effect on  $E$ , whereas  $\varepsilon_{\text{fracture}}$  and  $p_{\text{fracture}}$  decreased slightly. Increasing temperature decreased  $E$  and  $p_{\text{fracture}}$ , but had no effect on  $\varepsilon_{\text{fracture}}$ . Only the instantaneous elastic strain and the creep strain increased significantly at the highest temperatures. A decrease in  $E$  indicates decreasing skin stiffness that is probably the result of enzymatic softening of the cell walls of the skin in the ripening fruit, of relaxation of the cell walls on eliminating or decreasing turgor by transpiration and, possibly, of a decreasing viscosity of the pectin middle lamellae at higher temperatures. The effects are consistent with the conclusion that the epidermal and hypodermal cell layers represent the structural “backbone” of the sweet cherry fruit skin.

Rain cracking is a limitation in sweet cherry production almost wherever this high-value crop is grown (Christensen, 1996). Fruit cracking in many species, including grape (*Vitis vinifera* L.) and sweet cherry, is thought to be related to water uptake by the fruit. Thus, any net water uptake necessarily increases fruit volume and subjects the skin to additional strain (Considine and Brown, 1981). If the limit of extensibility of the fruit skin is exceeded, the fruit cracks. On the basis of this concept, the following two categories of factors will affect cracking susceptibility: 1) the fruit's water uptake/loss characteristics—these determine the rate and total amount of water accumulated by the fruit, and 2) the fruit's mechanical characteristics, particularly those of the principle load-bearing layer of the fruit—its skin (Brüggewirth et al., 2014). Water uptake by sweet cherries has been investigated in some detail, including that through the fruit surface (Beyer et al., 2002, 2005; Beyer and Knoche, 2002; Weichert and Knoche, 2006) and that through the pedicel vasculature (Hovland and Sekse, 2004; Measham et al., 2010). In contrast, there have been only a few studies that have addressed the mechanical properties of the sweet cherry skin (Bargel et al., 2004; Brüggewirth et al., 2014; Knoche and Peschel, 2006).

Investigating the mechanical properties of the fruit skin is challenging. First, the sweet cherry is about spherical and

hence, any strain of its skin during growth and water uptake is biaxial. Thus, a biaxial laboratory test is essential, if the in vivo strain in the skin is to be mimicked with any degree of accuracy. Second, uniaxial tests of skin strips result in marked narrowing of the sample as tension is applied. This is indexed by a high Poisson ratio and a gross overestimation of fracture strain and extensibility, and a gross underestimation of the  $E$  (Brüggewirth et al., 2014). Third, the sweet cherry skin is already markedly strained in vivo and these elastic and viscoelastic strains are reversible (Grimm et al., 2012). Thus, on excision the skin relaxes almost instantaneously and special care has to be taken to prevent this relaxation (Brüggewirth et al., 2014).

The first biaxial tensile test for sweet cherry fruit skin was described by Bargel et al. (2004). Excised fruit skin segments were pressurized from the inner side and the extent of bulging for each pressure increment was quantified. Brüggewirth et al. (2014) modified the test to prevent relaxation of the fruit skin after excision, thereby maintaining the in vivo strain in the fruit surface. Furthermore, the skin segments were pressurized using silicone oil rather than water thereby eliminating any uncontrolled water uptake and bursting of cells on the inner side (Simon, 1977). This test protocol offers a standardized test for identifying mechanical properties of sweet cherry fruit skins. Among the factors known to affect mechanical properties of fruit is the degree of ripening, especially during the later stages of development (Brummell, 2006; Christensen, 1996). Also, the fruit's turgescence is expected to be affected by the balance between transpiration and water uptake (Considine and Brown, 1981). Furthermore, many fleshy fruits, including sweet cherries, are soft to the touch when warm, but firmer at low temperatures (M. Brüggewirth and M. Knoche, unpublished

Received for publication 17 Sept. 2015. Accepted for publication 27 Oct. 2015. This research was funded in part by a grant from the Deutsche Forschungsgemeinschaft. We thank Dieter Reese and Christoph Knake for constructing, engineering, and programming the elastometer, Friederike Schroeder and Simon Sitzenstock for technical support, Bishnu P. Khanal and Sandy Lang for helpful discussion and useful comments on an earlier version of this manuscript.

<sup>1</sup>Corresponding author. E-mail: moritz.knoche@obst.uni-hannover.de.

data). Also, increasing temperature markedly increased cracking (for review, see Christensen, 1996). As with all materials, one would expect the mechanical properties of a fruit skin to be affected by temperature.

The objectives of this study were to quantify the effects of 1) ripeness stage; 2) turgor, transpiration, and water uptake; and 3) temperature on the mechanical properties of sweet cherry fruit skin using a biaxial tensile test.

### Materials and Methods

**PLANT MATERIAL.** Fruit of sweet cherry cultivars Adriana, Kordia, Sam, and Sweetheart were harvested at commercial maturity from field-grown or glasshouse-grown trees at the Horticultural Research Station of the Leibniz University in Ruthe, Germany (lat. 52°14' N, long. 9°49' E) in the 2012, 2013, and 2015 growing seasons. Trees were grafted on 'Gisela 5' rootstocks (*Prunus cerasus* L. × *Prunus canescens* Bois). Fruit were selected for freedom from visual defects and for uniformity of development based on size and color. In a preliminary experiment, the effect of storing sweet cherry at 2 °C and at water vapor concentrations close to saturation for up to 30 d on mechanical properties of the fruit skin was investigated. During the first 4 d of storage, stiffness of the skin increased as indexed by a 81% increase in the  $E$ . The pressure at fracture slightly increased (+10%) and the strain at fracture decreased [−26% (M. Brüggewirth, unpublished data)]. There was no further change in mechanical properties between 4 and 30 d of storage. To avoid potential artifacts resulting from storage, all fruit were harvested in the mornings, covered by a damp paper towel, brought to the laboratory, and used in experiments within 2 h.

**GENERAL EXPERIMENTAL PROCEDURE.** Biaxial tensile tests were performed using the elastometer described in detail by Brüggewirth et al. (2014). Briefly, a brass washer (12 mm i.d.) was mounted on one of the two shoulders of a sweet cherry fruit using cyanoacrylate adhesive (Loctite 406; Henkel/Loctite Deutschland, Munich, Germany). Next, an exocarp segment [ES (synonym fruit skin segment)] comprising the exocarp and some adhering mesocarp [thickness (mean ± SE) 2.5 ± 0.0 mm] was excised by cutting horizontally beneath the washer using a razor blade. This procedure preserved the *in vivo* strain of the skin after excision (Brüggewirth et al., 2014; Grimm et al., 2012; Knoche and Peschel, 2006). The brass washer with the ES was mounted in the elastometer, whose chamber was then filled with silicone oil (AK10; Wacker Chemie, Munich, Germany) and any visible air bubbles were carefully removed.

The chamber was pressurized by driving a motorized piston into the oil. This displaced the oil, reduced the chamber volume, and caused the ES to bulge outward. Pressure in the chamber was recorded using a pressure transducer (Typ 40PC100G; Honeywell International, Morristown, NJ) and the deflection of the bulging ES was recorded by the displacement transducer (KAP-S/5N; AST Angewandte System Technik, Wolnzach, Germany) of a universal material testing machine (BXC-FR2.5TN; Zwick Roell, Ulm, Germany). Unless specified otherwise, pressure was increased continually until the ES fractured. The pressure at the moment of failure is referred to as the fracture pressure [ $p_{\text{fracture}}$  (kilopascals)] and the area (i.e., biaxial) strain at failure as the fracture strain [ $\epsilon_{\text{fracture}}$  (square millimeters per square millimeter)]. The strain ( $\epsilon$ ) was calculated as the fractional increase in surface area; i.e., the increase in area [ $\Delta A$  (square millimeters)] due to the bulging of the ES,

relative to the initial area [ $A_0$  (square millimeters)] before bulging:

$$\epsilon = \frac{\Delta A}{A_0}$$

Surface areas of the ES were calculated from (changing) deflection height and the (fixed) diameter of the washer, and assumed a spherical shape (Brüggewirth et al., 2014). Stiffness of the bulging ES was described by the  $E$  using the equation described by Brüggewirth et al. (2014), where  $r$  (millimeters) is the radius of the washer orifice,  $p$  (megapascals) the pressure,  $h$  (millimeters) the height of the bulging ES, and  $t$  the thickness of the load-bearing layer ( $t = 0.1$  mm):

$$E = \frac{p \times r^2 \times (r^2 + h^2)}{h^3 \times t \times 2}$$

Unless otherwise stated, experiments were conducted at 22 °C.

**EXPERIMENTS.** Relationships between ripening during late stage III development and the mechanical properties of the fruit skin were investigated in 'Sweetheart' fruit. Fruit was sampled at 90, 98, 103, and 110 d after full bloom for maximum difference in ripeness, the mass determined and fruit color quantified on the Commission Internationale de l'Éclairage (CIE) 1976 ( $L^*$ ,  $a^*$ ,  $b^*$ ) scale as defined by the CIE (McGuire, 1992) using a chromameter (CR-200; Minolta, Osaka, Japan). To describe the change in color of the developing fruit, the hue angle was calculated as described by McGuire (1992). Three readings were taken per fruit that were averaged. Color is a good indicator of ripening in stage III sweet cherry (Hansen, 2011) and closely related to sugar content, whereas mass changes are usually quite small and fruit size is rather variable. For a representative batch (range in hue angle from 2.8° to 30.0°) of 'Sweetheart' fruit, the regression equation describing the relationship between osmolarity and hue angle was: osmolarity (millimoles per kilogram) =  $[0.86 \times \text{hue angle (degrees)}^2] - [53.9 \times \text{hue angle (degrees)}] + 1742.7$ ;  $r^2 = 0.86^{***}$ . There was no significant relationship between fruit mass and hue angle or mass and osmolarity (M. Brüggewirth, unpublished data). Hence, the mechanical properties reported are expressed as a function of hue angle.

The effect of turgor on the mechanical properties of 'Adriana' ES was investigated by destroying membrane integrity of excised ES by a single freeze/thaw cycle (−18 °C for 30 min, followed by thawing for 30 min at 22 °C) or by solubilizing plasma membranes by incubating ES in a surfactant solution (1% Triton X-100 for 12 h; Union Carbide, Antwerp, Belgium). Untreated ES served as controls. For technical reasons, the washer was mounted on the fruit before the freeze–thaw cycle and before the surfactant treatment and hence, the original strain of the turgescient fruit was preserved. There was no relaxation of the fruit skin during the treatment.

Potential relationships between the amount of water transpired and the mechanical properties of the skin were investigated in intact fruit of 'Sweetheart' sweet cherry. Fruit, with pedicel detached, were incubated in a sealed chamber for 0, 24, 48, and 96 h above dry silica gel [0% relative humidity (Geyer and Schönherr, 1988)]. To avoid confounding mass loss with storage duration, control fruit were stored in a sealed chamber above water (100% relative humidity) for the same time periods. Weight loss due to transpiration was determined



gravimetrically ( $n = 20$ ). Thereafter, ES were prepared, mounted in the elastometer and tested as described above.

The effect of the reverse process of osmotic water uptake on the mechanical properties of fruit skin was studied in a two-step experiment in ‘Sweetheart’. First, the time course of water uptake and cracking was established. Water uptake was determined gravimetrically by incubating fruit in deionized water and subsequent weighing at 0, 0.75, and 1.5 h ( $n = 15$ ). Cracking was monitored using a modified cracking assay as described by Verner and Blodgett (1931) and Christensen (1996). Fruit were inspected at 0, 2, 4, 6, 10, and 24 h for macroscopically visible cracks. Because uptake and cracking were quantified on the same batch of fruit, the time to 50% and 100% cracking and the amount of water uptake at 50% and 100% cracking could be calculated. In the second part of the experiment, mechanical properties of the skin of fruit incubated in deionized water until 50% and 100% cracking was determined using the elastometer and the procedure described above. Fruit from the 50% sampling was first partitioned into two populations—cracked and noncracked. Nonincubated (intact) fruit served as controls. The ES of cracked fruit was taken from the remaining intact shoulder of the fruit so that there was no confounding with position on the fruit. This procedure allowed comparison of mechanical properties of the skin of fruit that had cracked with those of fruit that under the same conditions had not cracked.

The effect of temperature on the mechanical properties of fruit skin of ‘Sam’ was investigated by carrying out a creep test at 5, 15, 25, and 35 °C. In this assay, the ES were pressurized during the loading phase (I) by increasing pressure to 20 kPa at a constant rate. During the subsequent hold, phase (II) pressure was held constant at 20 kPa for 5 min. Thereafter, pressure was increased until the skin segment fractured (III). This protocol allowed quantification of the following: elastic strain (I), creep strain (II), and fracture strain (III). The elastic component corresponded to deformation of the ES during the loading phase (I), the creep strain (the sum of viscoelastic strain and plastic strain) to that during the hold phase (II), and the fracture strain to that at fracture during phase (III) (Brüggenwirth et al., 2014). It should be noted that the sweet cherry skin on the fruit surface is already significantly strained (elastic, viscoelastic, and plastic) due to the deformation that occurred as a result of fruit growth (Grimm et al., 2012; Knoche et al., 2004). For estimates of a “total” strain that includes the fruit growth, these strains would have to be added to those determined in our biaxial tensile tests.

**DATA ANALYSIS.** Data analyses were limited to those fruit skin segments that fractured in the center of the orifice of the elastometer. ES that fractured at the edge were excluded from analysis because this could have resulted from a mounting artifact (Brüggenwirth et al., 2014). Data are presented as values of individual fruit (Figs. 1, 2B–D, 3B–D, and 5A and B) or as means  $\pm$  SE (Figs. 2A, 3A, 4, and 5C and D). Mean comparisons were conducted using Tukey’s Studentized range test ( $P < 0.05$ ; packet multcomp 1.2–12, procedure glht, R 2.13.1; R Foundation for Statistical Computing, Vienna, Austria). Significance of coefficients of correlation ( $r$ ) and determination ( $r^2$ ) at the 0.05, 0.01, and 0.001  $P$  levels is indicated by \*, \*\*, and \*\*\*, respectively.

## Results

Pressure and biaxial strain increased linearly with time until the skin segment fractured (Fig. 1A). The  $E$  calculated from

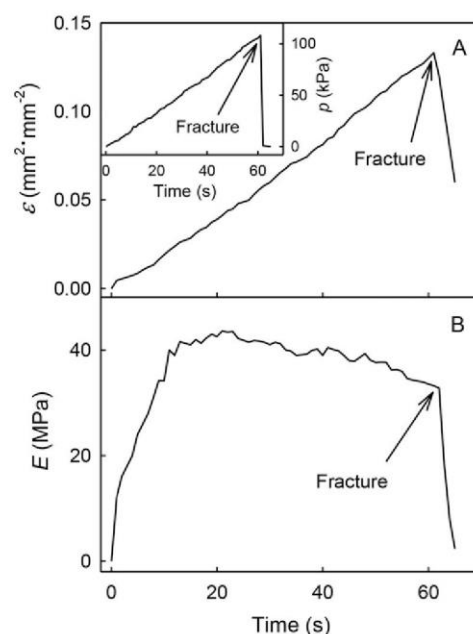


Fig. 1. Time course of increase in (inset A) pressure ( $p$ ), (A) strain ( $\epsilon$ ), and (B) modulus of elasticity ( $E$ ) of a bulging skin segment of a mature sweet cherry fruit mounted in the elastometer (a typical result).

paired data for pressure and strain, increased to a maximum  $\approx 20$  s after test initiation and then declined slightly before the segment fractured (Fig. 1B).

During ripening in late stage III fruit, fruit mass increased and at the same time hue angle decreased, implying that the fruit darkened (Fig. 2A). The progress of ripening was more consistently represented when expressed as a color change, than as a mass change. The decrease in hue angle associated with increasing ripening was accompanied by a decreased  $E$  ( $r^2 = 0.68^{***}$ ) and  $p_{\text{fracture}}$  ( $r^2 = 0.80^{***}$ ), but had no effect on  $\epsilon_{\text{fracture}}$  ( $r^2 = 0.19$ ) (Fig. 2B–D).

Compared with the turgescence control, destroying membrane integrity by a single freeze–thaw cycle or by incubating skin segments in a surfactant solution decreased  $E$  and  $p_{\text{fracture}}$ , but had no effect on  $\epsilon_{\text{fracture}}$  (Table 1).

The amount of water transpired increased linearly with time above dry silica, but there was no change in mass over the same time period at 100% relative humidity [Fig. 3A (inset)]. Mechanical properties were variable and depended on the mass of water transpired. The value of  $E$  decreased with increasing transpiration, whereas that of  $p_{\text{fracture}}$  and, especially, of  $\epsilon_{\text{fracture}}$  increased significantly with transpiration. Slopes of linear regressions and coefficients of determination for these relationships were:  $E$ ,  $a = -8.5 \pm 1.2 \text{ MPa}\cdot\text{g}^{-1}$ ,  $r^2 = 0.51^{***}$ ;  $p_{\text{fracture}}$ ,  $a = 6.0 \pm 1.3 \text{ kPa}\cdot\text{g}^{-1}$ ,  $r^2 = 0.36^{***}$ ;  $\epsilon_{\text{fracture}}$ ,  $a = 0.05 \pm 0.003 \text{ mm}^2\cdot\text{mm}^{-2}\cdot\text{g}^{-1}$ ,  $r^2 = 0.77^{***}$ , respectively (Fig. 3A–C). Quantitatively similar data were obtained in ‘Kordia’ (M. Brüggenwirth, data not shown).

Cumulative water uptake increased linearly with time up to 1.5 h [Fig. 4 (inset)], whereas the percentage of cracked fruit increased sigmoidally with time and cumulative water uptake (Fig. 4). From these relationships, the time required to achieve 0%, 50%, and 100% of cracked fruit was calculated. Fruit incubated for a period equal to the 50% cracking threshold were

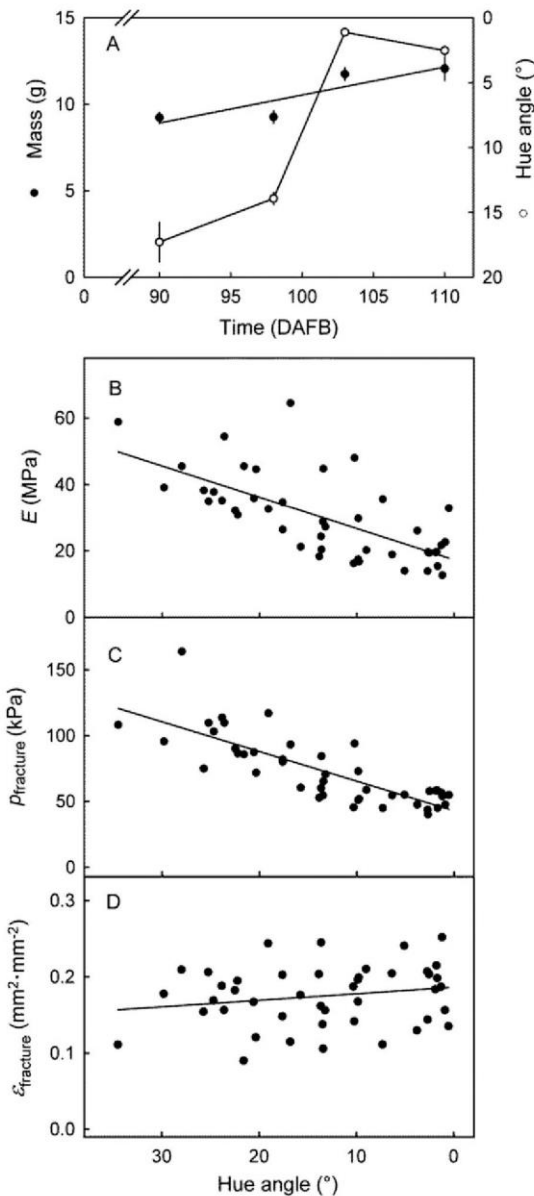


Fig. 2. Relationship between late stage III development of sweet cherry fruit and the mechanical properties of the skin. (A) Time course of change in fruit mass and color as indexed by the hue angle. (B–D) Relationships between the hue angle of the fruit skin and the mechanical properties of the skin as indexed by (B) its modulus of elasticity ( $E$ ), (C) pressure at fracture ( $p_{fracture}$ ), and (D) strain at fracture ( $\epsilon_{fracture}$ ). High hue angles imply less mature, pale fruit, low hue angles imply more mature, darker fruit. X-axis scale in (A) in days after full bloom (DAFB). Values in (A) represent means  $\pm$  SE ( $n = 5\text{--}30$ ), those in B–D individual fruit.

subdivided in two, roughly equal, populations—cracked and noncracked. Biaxial tensile tests revealed no effect of water uptake and/or cracking status on  $E$ , whereas  $p_{fracture}$  and or  $\epsilon_{fracture}$  slightly decreased in cracked fruit (Table 2).

Increasing pressure during the loading phase (I) increased the instantaneous elastic strain at all temperatures (Fig. 5A). In the subsequent holding phase (II) at constant pressure, the skin stretched due to creep strain, comprising both viscoelastic and plastic strain components. In the final phase (III), an increase in

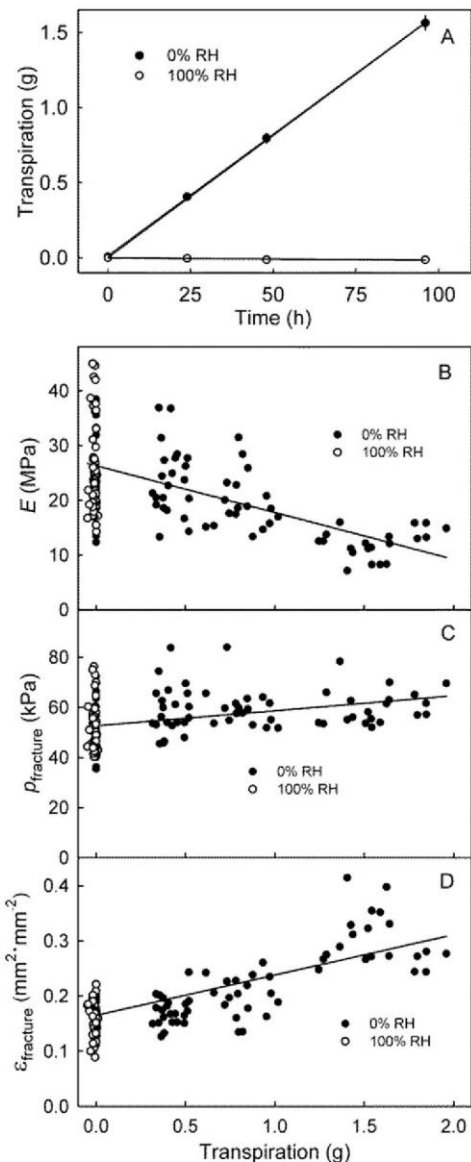


Fig. 3. Effect of transpiration of sweet cherry fruit on the mechanical properties of the excised skin. (A) Time course of transpiration. Mechanical properties were indexed by the (B) modulus of elasticity ( $E$ ), (C) pressure at fracture ( $p_{fracture}$ ), and (D) strain at fracture ( $\epsilon_{fracture}$ ). Values in (A) represent means  $\pm$  SE ( $n = 20$ ), those in B–D individual fruit. Fruit held at 100% relative humidity (RH) for the same period of time served as control.

pressure resulted in failure of the skin at all temperatures. Increasing temperature decreased the values of  $E$  and  $p_{fracture}$  (Fig. 5C), but had no effect on that of  $\epsilon_{fracture}$  ( $\epsilon_{fracture}$  (square millimeters per square millimeter) =  $[0.159 (\pm 0.01) \times \text{temperature } (^{\circ}\text{C})] + 0.0004 (\pm 0.0005)$ ,  $r^2 = 0.52^*$ ). Only the instantaneous elastic strain and creep strain increased significantly at the highest temperature (Fig. 5D).

### Discussion

The mechanical properties of the skin of a sweet cherry fruit are primarily determined by the epidermal and the hypodermal

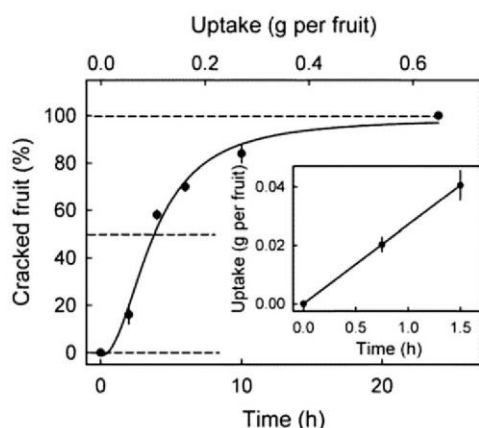


Fig. 4. Time courses of cracking (main graph) and of water uptake (inset) in sweet cherry fruit incubated in deionized water. Dashed lines indicate times and cracking levels when fruit were sampled for determining the mechanical properties of excised skin samples. For details of mechanical tests, see Table 2.

layers (Brüggenwirth et al., 2014; Grimm et al., 2012). Thus, any effects of the factors investigated here must be accounted for within these two tissues. Mechanically relevant properties of soft tissues include the amount of applied stress, the properties of cell walls, and of the middle lamellae. Also involved are cell turgor, the permeability of the plasma membrane, and the sizes and shapes of the cells (Niklas, 1992; Vincent, 1990a).

#### Effect of ripening

Fruit ripening is characterized by softening due to the activity of cell wall-degrading enzymes, particularly pectinases (Andrews and Li, 1995; Barrett and Gonzalez, 1994; Brummell, 2006). In ‘Satoshnik’ sweet cherry, the cleavage of neutral sugar side chains from pectins is causal in fruit softening (Kondo and Danjo, 2001). Also, when incubating fruit in water, soluble pectin increased in solution (Glenn and Poovaiah, 1989). The role of cellulase in cell wall degradation and softening of cherry is not clear. There was no evidence of cellulase activity during ripening in ‘Royal Anne’ and ‘Bada’ (Barrett and Gonzalez, 1994), whereas cellulase activity increased in ‘Bing’ (Andrews and Li, 1995). The changes in the skin’s mechanical properties during ripening are consistent with enzymatic cell wall degradation. The progressive reduction in  $E$  is indicative of decreased stiffness and increased softening. Furthermore, the reduction in  $p_{\text{fracture}}$  is consistent with a continuing softening primarily caused by increased pectinase activity.

The  $E$  values measured in the sweet cherry skin are of similar order of magnitude as those from other biaxial tests of skins of apple [*Malus × domestica* Borkh.,  $76.1 \pm 8.7$  MPa (M. Brüggewirth, unpublished data)], tomato [*Solanum lycopersicum* L.,  $55.9 \pm 9.6$  MPa (M. Brüggewirth, unpublished data)], sour cherry (*Prunus cerasus*; range  $3.5 \pm 0.2$  to  $5.9 \pm 0.2$  MPa), cape gooseberry (*Physalis peruviana* L.,  $20.5 \pm 0.8$  MPa), european plum (*Prunus × domestica* L.,  $25.4 \pm 7.8$  to  $35.9 \pm 3.2$  MPa), and grapes ( $20.8 \pm 1.7$  to  $21.5 \pm 1.6$  MPa) (Brüggenwirth et al., 2014) or from uniaxial tests of skins of tomato [ $43.5 \pm 4.8$  and  $27.1 \pm 1.9$  MPa for ‘Inbred 10’ and ‘Sweet 100’, respectively (Matas et al., 2004)], or apple [ $16.6 \pm 1.2$  MPa (B.P. Khanal, unpublished data)].

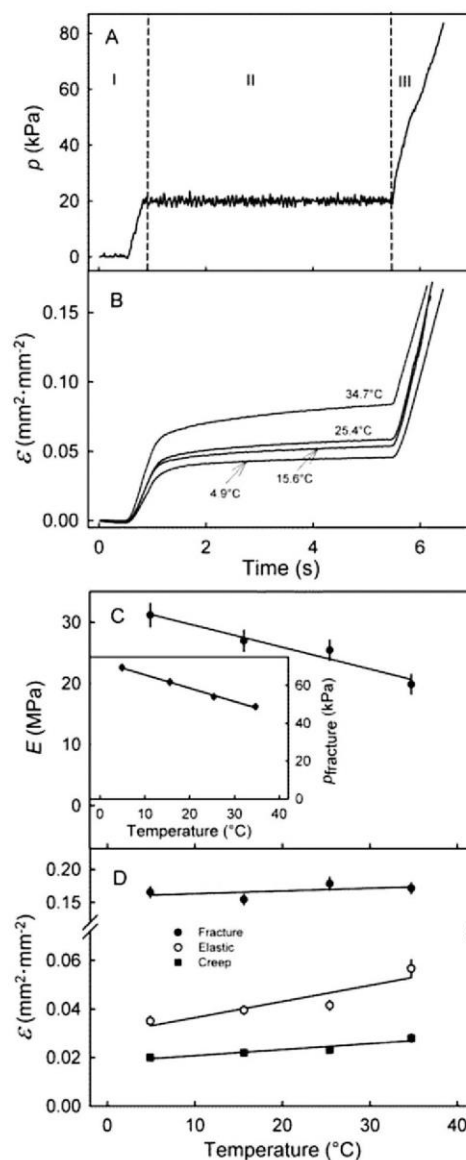


Fig. 5. Effect of temperature on the mechanical properties of the skin of sweet cherry fruit as determined in a biaxial creep test. (A) Representative time course of pressure ( $p$ ) applied to the skin. The pressure was increased during the initial loading phase (I), held constant during the holding phase (II), and increased until skin fracture (III). (B) Representative time courses of strains ( $\epsilon$ ). (C and D) Effect of temperature on the (C) modulus of elasticity ( $E$ ) and (inset C) pressure at fracture ( $p_{\text{fracture}}$ ), and (D) the elastic and the creep strain ( $\epsilon$ ). The elastic component corresponds to instantaneous deformation of the skin during phase (I). The creep strain (sum of viscoelastic strain plus plastic strain) refers to the deformation of the exocarp segment during phase (II). Values in C and D represent means  $\pm$  SE ( $n = 21$ ).

#### Effect of turgor, transpiration, and water uptake

The effects of water loss and water uptake on the mechanical properties of the skin are accounted for primarily by changes in the physical properties of the cell walls caused by the manipulation of factors affecting turgor. If turgor is eliminated by destroying the membranes, water moves more freely and the cell walls relax. This releases reversible strain (Grimm et al., 2012) and results in decreased stiffness as indexed by a lowering

of  $E$  and  $p_{\text{fracture}}$ . These data are consistent with those reported by Oey et al. (2007) in which relationships between tissue turgor and mechanical properties in apples were investigated. The only difference between the findings by Oey et al. (2007) in apple and our observations for sweet cherry skin is the apparent lack of an effect of eliminating turgor on  $\epsilon_{\text{fracture}}$ . Oey et al. (2007) reported an increase in  $\epsilon_{\text{fracture}}$  in apple. This discrepancy is probably related to differences in experimental procedure. In our tensile tests, the skin was mounted in a washer that prevented relaxation associated with turgor elimination (Knoche and Peschel, 2006). If it were technically possible to mount a relaxed cherry fruit in the elastometer washer [which it is not (M. Brüggewirrh, unpublished data)], we would expect  $\epsilon_{\text{fracture}}$  to increase after eliminating turgor.

It is important to point out that the low turgor in sweet cherry fruit relative to the  $\psi_s$  (Knoche et al., 2014; Schumann et al., 2014) is not necessarily contradictory to a role of turgor in tensile properties of the tissue. The water in the symplast is not compressible and so, regardless of cell turgor, will oppose any sudden change in skin cell shape, such as a decrease in the diameter:thickness ratio that is inevitably associated with biaxial stretching. Mechanically, turgor is maintained by elastic strain in the cell wall (Niklas, 1992; Vincent, 1990a). De Belie et al. (2000) argued that the effect of turgor on the tensile properties of flesh samples of european pear (*Pyrus communis* L.) and asian pear [*Pyrus pyrifolia* (Burm. f.) Nakai] was related to their mode of failure. Turgor had no effect on the measured tissue failure properties, when failure occurred along cell walls between cells as opposed to across cell walls by cell wall fracture (De Belie et al., 2000). In addition, an abrupt decrease in the force at failure of apple flesh subjected to tensile tests was interpreted as evidence of cell rupture (Oey et al., 2007). If these conclusions for apple are also applicable to the skin of sweet cherries, then the effect of turgor in our study would be indicative of failure across cell walls. Unfortunately, definitive evidence is lacking. As far as we are aware, the mode of failure of the skin in sweet cherry fruit cracking has not yet been critically investigated.

Transpiration causes fruit shrinkage, and thus results in decreasing biaxial strain and stress in the skin and a relaxation of their cell walls (Grimm et al., 2012). This explanation accounts for the effect of transpiration on the mechanical properties of the fruit skin observed in our study. Fruit mass decreased by  $\approx 1.56 \pm 0.05$  g during transpiration. For a 10 g fruit of spherical shape, a 1.6 g mass loss translates to a 10.7% decrease in skin surface area. This estimate corresponds well with the measured increase in  $\epsilon_{\text{fracture}}$  of 14.6% (Fig. 3). This explanation also holds for the loss of stiffness as indexed by the decrease in  $E$ . The slight increase in  $p_{\text{fracture}}$  with increasing transpirational water loss may be accounted for by the decreasing volume of the shrinking and relaxing cells and the corresponding increase in the amount of cell wall material per unit area of the fruit surface.

For the opposite process, water uptake, we expect similar changes to those for transpiration but in the opposite direction. However, water uptake had only small, essentially negligible, effects on the mechanical properties of the skin. The most likely explanation for this apparent contradiction is that the scale of the mass change caused by water uptake was much smaller ( $0.65 \pm 0.12$  g) than that caused by transpiration ( $-1.56 \pm 0.05$  g). Consequently, the increase in strain associated with water uptake was surprisingly small and unexpected, particularly in the light of 100% cracking at the longest exposure. Several factors must be considered:

1) The biaxial tensile test focuses on the fruit skin. Any effects of the flesh are largely eliminated by its substantial removal from the sample. Flesh effects in vivo (before excision) will include exposure to juice resulting from compartmentation loss (particularly around the pit) or heterogeneity arising from localized cell death. Both these effects have been demonstrated for grape berries that have similar mechanical architecture to sweet cherry (Considine and Brown, 1981; Lang and Düring, 1991; Tilbrook and Tyerman, 2008) and malic acid, a major constituent of sweet cherry fruit juice, markedly increases sweet cherry cracking (Winkler et al., 2015). Also, in

Table 1. Effect of turgor on mechanical properties of the sweet cherry fruit skin as indexed by the modulus of elasticity ( $E$ ), pressure at fracture ( $p_{\text{fracture}}$ ), and strain at fracture ( $\epsilon_{\text{fracture}}$ ). Turgor was destroyed by subjecting excised fruit skin to a freeze–thaw cycle or by incubating it in 1% Triton X-100 surfactant (Union Carbide, Antwerp, Belgium) for 12 h. Before eliminating turgor, fruit skin segments were mounted in a washer to prevent relaxation on excision.

Treatment	n	$E$	$p_{\text{fracture}}$	$\epsilon_{\text{fracture}}$
		[mean $\pm$ SE (MPa)]	[mean $\pm$ SE (kPa)]	[mean $\pm$ SE (mm <sup>2</sup> ·mm <sup>-2</sup> )]
Control	15	14.3 $\pm$ 0.9 a <sup>z</sup>	29 $\pm$ 1.7 a	0.17 $\pm$ 0.01 a
Freeze/thaw	15	7.9 $\pm$ 0.9 b	14 $\pm$ 1.0 b	0.17 $\pm$ 0.01 a
Surfactant	18	8.6 $\pm$ 0.6 b	19 $\pm$ 1.0 b	0.19 $\pm$ 0.01 a

<sup>z</sup>Mean separation within columns by Tukey’s Studentized range test at  $P < 0.05$ .

Table 2. Effect of incubation of sweet cherry fruit in deionized water on cracking and on the mechanical characteristics of the fruit skin. The characteristics quantified in the biaxial tensile test were the modulus of elasticity ( $E$ ), the pressure at fracture ( $p_{\text{fracture}}$ ), and the strain at fracture ( $\epsilon_{\text{fracture}}$ ) (n = 10).

Incubation time (h)	Fruit cracking (%)	Tested fruit	$E$	$p_{\text{fracture}}$	$\epsilon_{\text{fracture}}$
			[mean $\pm$ SE (MPa)]	[mean $\pm$ SE (kPa)]	[mean $\pm$ SE (mm <sup>2</sup> ·mm <sup>-2</sup> )]
0	0	Intact	19.8 $\pm$ 1.8 a <sup>z</sup>	58.6 $\pm$ 3.8 a	0.22 $\pm$ 0.01 a
3	50	Intact	32.2 $\pm$ 7.9 a	50.9 $\pm$ 2.1 ab	0.16 $\pm$ 0.02 ab
3	50	Cracked	29.3 $\pm$ 7.3 a	42.0 $\pm$ 5.0 b	0.13 $\pm$ 0.02 ab
24	100	Cracked	32.9 $\pm$ 5.2 a	41.2 $\pm$ 2.2 b	0.12 $\pm$ 0.01 b

<sup>z</sup>Mean separation within columns by Tukey’s Studentized range test at  $P < 0.05$ .

our earlier study, we observed a slight decrease in  $\epsilon_{\text{fracture}}$  when thickness of the ES increased (Brüggenwirth et al., 2014). Structural heterogeneity could also arise from the presence of vascular bundles. In cherry, these lie just beneath the epidermal and hypodermal cell layers,  $\approx 2.1 \pm 0.1$  mm below the fruit surface (M. Brüggenwirth unpublished data). Because the thickness of the experimental skin segments averaged  $2.4 \pm 0.0$  mm (Brüggenwirth et al., 2014), vascular bundles would likely have been present in all segments. If these should give rise to structural heterogeneity in the excised skin or in the intact fruit, the distribution of stress and strain could be nonuniform and this could cause failure (Brown and Considine, 1982). The strength of the weakest link would then determine the strength of the entire skin. At this stage, we have found no evidence that this is a significant factor.

2) The fruit skins selected for biaxial strain testing were free of visible blemishes. This was necessary because fruit having visible skin cracks cannot be mounted in the elastometer. It may be argued that this selection may have eliminated susceptible, predamaged fruit. However, a bias is unlikely to have occurred because the fruit used in the cracking assay were from the same batch and subjected to the same selection procedure.

3) Biaxial testing is best performed on skin segments from regions of the fruit that have uniform curvature of maximum radius of curvature. Skin from the stem cavity region is concave and, therefore, impossible to investigate. That from the stylar scar region is convex but has asymmetric curvature. The shoulder, cheek, and suture regions are best having more uniform curvatures. It may be argued that cracking occurs most frequently in the stylar scar and stem cavity regions (Knoche and Peschel, 2006; Yamaguchi et al., 2002) where microscopic cracks are also more frequent (Peschel and Knoche, 2005). Because of likely microcracking, the shoulder region would have been less satisfactory for quantifying cracking-relevant properties of the skin on this account too. Nevertheless, preliminary tests showed that some of these factors are of little account anyway because when results were compared for skin segments from cheek, shoulder, suture, and stylar scar regions, only slight differences in  $E$  (range  $16.7 \pm 0.9$  to  $21.7 \pm 1.2$  MPa),  $p_{\text{fracture}}$  (range  $62 \pm 3$  to  $73 \pm 2$  kPa), and  $\epsilon_{\text{fracture}}$  (range  $0.18 \pm 0.01$  to  $0.27 \pm 0.01$  mm<sup>2</sup>·mm<sup>-2</sup>) were obtained (M. Brüggenwirth, unpublished data).

#### Effect of temperature

Our results establish that skin stiffness decreases with rising temperature. This property fits with the norm for most materials, not just with biological ones (Niklas, 1992). It is also consistent with our earlier observations for rising temperatures of a more rapid and greater relaxation of ES (Grimm et al., 2012) and increased creep strain (Niklas, 1992). It is also in line with earlier observations that cracking is more severe under warmer conditions (Christensen, 1996). Likewise in grape, Lang and Düring (1990) reported a decrease in stiffness and strength as temperature increased. Vincent (1990b) hypothesized that the effect of temperature on mechanics of plant tissues may be related to the viscoelastic properties of the middle lamellae. At higher temperatures, stiffness will decrease because the viscosity of pectins is known to decrease (Kar and Arslan, 1999), making the “glue” between adjacent cells less stiff. However, direct evidence for many of these mechanisms is still lacking. Some of these features could even account for

the effects of temperature on fruit texture—they feel firmer when cool, softer when warm.

**PRACTICAL IMPLICATIONS.** The changes in mechanical properties observed here in response to ripening, water uptake, and increasing temperature, are broadly in line with reports of increased cracking susceptibility in more mature fruit and at higher temperatures (for review, see Christensen, 1996). Also, based on the critical turgor pressure concept, increased turgor should result in increased cracking susceptibility (Measham et al., 2009; Sekse et al., 2005) but direct experimental evidence for this view, seems to be lacking. Actually, the turgor recorded in cells of the outer mesocarp is very low, relative to their  $\psi_s$ , hence, increased turgor as the cause of fruit cracking becomes very unlikely (Knoche et al., 2014; Schumann et al., 2014).

It is interesting that for excised skin, the applied pressure at fracture in the elastometer is of similar magnitude to measurements of both fruit turgor and of cell turgor in still-attached skin. This contrasts with measurements of the strain at fracture in the elastometer, which are markedly greater than the strains at fracture, measured for still-attached skins under water (Brüggenwirth et al., 2014; Schumann et al., 2014). The amount of water taken up at 50% cracking ( $WU_{50}$ ) typically ranges from 24 to 234 mg/fruit (Weichert et al., 2004; Winkler et al., 2015). Assuming a spherical, 10 g fruit, having a density of 1 kg·dm<sup>-3</sup> and a surface area of 22.4 cm<sup>2</sup>, this would be equivalent to an  $\epsilon_{\text{fracture}}$  value of 0.0016 to 0.016 mm<sup>2</sup>·mm<sup>-2</sup>. Making the same calculation for cracking thresholds of 0.44% (Christensen, 1996), up to a 13% water uptake (Kertesz and Nebel, 1935) yields an  $\epsilon_{\text{fracture}}$  value between 0.0029 and 0.085 mm<sup>2</sup>·mm<sup>-2</sup>. These  $\epsilon_{\text{fracture}}$  are markedly lower than those measured for excised skin in the elastometer. The reasons for this difference are unknown but may be related to one or more of the following: first, the surface area of a complete fruit is very much greater than that of a skin segment in the elastometer. The ratio of surface area of fruit to that of the ES ( $\approx 20:1$ ) will increase the probability (20-fold) that a skin defect might initiate a crack. Indeed, in our earlier study, we observed decreased pressures at fracture and decreased strains at fracture as segment areas in the elastometer increased. This is consistent with a “defect” hypothesis (Brüggenwirth et al., 2014). Second, the rates of strain in the elastometer ( $\approx 0.20$  mm<sup>2</sup>·mm<sup>-2</sup>·min<sup>-1</sup>) greatly exceed those associated with water uptake in intact fruit ( $\approx 0.03$  mm<sup>2</sup>·mm<sup>-2</sup>·min<sup>-1</sup>). The effect of strain rate on the mechanical characteristics of sweet cherry skin has not yet been studied. Nevertheless, for viscoelastic materials in general, one expects a low strain rate to yield a higher value for strain at fracture, and a lower pressure at fracture (vice versa for a high strain rate). This suggests that the strain rate difference is an unlikely explanation for what we observe. Third, the skin of a submerged fruit is wet, whereas the skin sample in the elastometer is dry. We know, surface wetness induces microcracks in the sweet cherry cuticle (Knoche and Peschel, 2006). However, wetness had no effect on the mechanical properties of the skin in a head-to-head comparison of dry skin ( $\epsilon_{\text{fracture}}$   $0.21 \pm 0.01$  mm<sup>2</sup>·mm<sup>-2</sup>) vs. wet skin ( $\epsilon_{\text{fracture}}$   $0.22 \pm 0.01$  mm<sup>2</sup>·mm<sup>-2</sup>; M. Brüggenwirth, unpublished data). Also, microcracks in the cuticle have no direct effects on the skin’s mechanical properties (Brüggenwirth et al., 2014). Fourth, differential responses among cultivars can be excluded as a potential explanation since, in our cultivar comparisons, the range in  $\epsilon_{\text{fracture}}$  (range  $0.17 \pm 0.01$  to  $0.22 \pm 0.01$  mm<sup>2</sup>·mm<sup>-2</sup>; M. Brüggenwirth, unpublished data) was very much smaller

than the difference between the  $\epsilon_{\text{fracture}}$  value determined using the elastometer and that calculated from the volume of water uptake at cracking. The former were an order of magnitude greater.

Our use of a range of cultivars in the different experiments deserves some comment. For each cultivar, and from each location, top-quality fruit is available for only a few days each season. Hence, for research involving time-consuming, sequential, experimentation, the use of a range of cultivars grown under a range of conditions (sites, seasons, etc.) is undesirable, but unavoidable. However, looking on the positive side, this can be considered to expand the generality of our conclusions compared with a hypothetical situation where it was possible to obtain more uniform samples (single cultivar, single source) over an extended period. It should also be recognized that our experiments were structured such that this diversity of cultivar and source does not introduce logical problems of interpretation. First, our comparisons were limited to head-to-head comparisons of treatments within each experiment and using appropriate controls. Second, there is no published evidence (nor is it very likely) that the mechanism of skin failure on a fruit's shoulder will differ much among cultivars. Third, the experiments focus on individual factors affecting the mechanical properties of the fruit skin and there is no published or intrinsic evidence for any interaction among these factors and cultivar. Clearly, quantitative responses will likely differ among cultivars and sources (and seasons etc.), but qualitatively they seem to remain much the same.

### Conclusions

Our experiments indicate skin stiffness decreases with ripening, decreasing turgor (increased transpiration), elimination of turgor (freeze/thaw), and increasing temperature. These responses could well find their explanations in a series of changes including the following: enzymatic softening of the cell wall during ripening, relaxation of the cell wall on artificially decreasing or eliminating turgor, and a potential decrease in viscosity of the pectin middle lamellae at higher temperatures (as hypothesized by Vincent, 1990b). These conclusions are also consistent with earlier studies that have identified the epidermal and hypodermal cell layers (and "not" the cuticle) as the structural "backbone" of a sweet cherry skin (Brüggenwirth et al., 2014; Grimm et al., 2012).

It is interesting that the fruit pressure at fracture is of similar magnitude to normal fruit turgor (the average turgor of a population of healthy fruit on the tree), as previously reported (Knoche et al., 2014; Schumann et al., 2014). However, the strain at fracture (here and previously, Brüggenwirth et al., 2014) is significantly greater in biaxial tensile skin tests than in estimates based on the water uptake of submerged fruit. The mechanistic basis of this observation is unclear, with detailed studies being required to elucidate it. Such studies might usefully include a modification of the elastometer to allow variations to be made in strain rate for kinetic studies.

### Literature Cited

Andrews, P.K. and S. Li. 1995. Cell wall hydrolytic enzyme activity during development of nonclimacteric sweet cherry (*Prunus avium* L.) fruit. *J. Hort. Sci.* 70:561–567.

- Bargel, H., H.C. Spatz, T. Speck, and C. Neinhuis. 2004. Two-dimensional tension test in plant biomechanics—Sweet cherry fruit skin as a model system. *Plant Biol.* 6:432–439.
- Barrett, D.M. and C. Gonzalez. 1994. Activity of softening enzymes during cherry maturation. *J. Food Sci.* 59:574–577.
- Beyer, M. and M. Knoche. 2002. Studies on water transport through the sweet cherry fruit surface: V. Conductance for water uptake. *J. Amer. Soc. Hort. Sci.* 127:325–332.
- Beyer, M., S. Peschel, M. Knoche, and M. Knörger. 2002. Studies on water transport through the sweet cherry fruit surface: IV. Regions of preferential uptake. *HortScience* 37:637–641.
- Beyer, M., S. Lau, and M. Knoche. 2005. Studies on water transport through the sweet cherry fruit surface: IX. Comparing permeability in water uptake and transpiration. *Planta* 220:474–485.
- Brown, K. and J. Considine. 1982. Physical aspects of fruit growth: Stress distribution around lenticels. *Plant Physiol.* 69:585–590.
- Brummell, D.A. 2006. Cell wall disassembly in ripening fruit. *Funct. Plant Biol.* 33:103–119.
- Brüggenwirth, M., H. Fricke, and M. Knoche. 2014. Biaxial tensile tests identify epidermis and hypodermis as the main structural elements of sweet cherry skin. *Ann. Bot. Plants* 6:plu019.
- Christensen, J.V. 1996. Rain-induced cracking of sweet cherries: Its causes and prevention, p. 297–327. In: A.D. Webster and N.E. Looney (eds.). *Cherries: Crop physiology, production and uses*. CAB Intl., Wallingford, UK.
- Considine, J. and K. Brown. 1981. Physical aspects of fruit growth: Theoretical analysis of distribution of surface growth forces in fruit in relation to cracking and splitting. *Plant Physiol.* 68:371–376.
- De Belie, N., I.C. Hallett, F.R. Harker, and J. De Baerdemaeker. 2000. Influence of ripening and turgor on the tensile properties of pears: A microscopic study of cellular and tissue changes. *J. Amer. Soc. Hort. Sci.* 125:350–356.
- Geyer, U. and J. Schönherr. 1988. In vitro test for effects of surfactants and formulations on permeability of plant cuticles, p. 21–33. In: B. Cross and H.B. Scher (eds.). *Pesticide formulations: Innovations and developments*. Amer. Chem. Soc., Washington, DC.
- Glenn, G.M. and B.M. Poovaiah. 1989. Cuticular properties and postharvest calcium applications influence cracking of sweet cherries. *J. Amer. Soc. Hort. Sci.* 114:781–788.
- Grimm, E., S. Peschel, T. Becker, and M. Knoche. 2012. Stress and strain in the sweet cherry skin. *J. Amer. Soc. Hort. Sci.* 137:383–390.
- Hansen, M. 2011. When is the best time to pick? 15 Mar. 2011. <<http://www.goodfruit.com/when-is-the-best-time-to-pick/>>.
- Hovland, K.L. and L. Sekse. 2004. Water uptake through sweet cherry (*Prunus avium* L.) fruit pedicels: Influence of fruit surface water status and intact fruit skin. *Acta Agr. Scandinavica Section B Soil Plant Sci. J.* 54:91–96.
- Kar, F. and N. Arslan. 1999. Effect of temperature and concentration on viscosity of orange peel pectin solutions and intrinsic viscosity-molecular weight relationship. *Carbohydr. Polym.* 40:277–284.
- Kertesz, Z.I. and B.R. Nebel. 1935. Observations on the cracking of cherries. *Plant Physiol.* 10:763–772.
- Knoche, M., M. Beyer, S. Peschel, B. Oparlakov, and M.J. Bukovac. 2004. Changes in strain and deposition of cuticle in developing sweet cherry fruit. *Physiol. Plant.* 120:667–677.
- Knoche, M. and S. Peschel. 2006. Water on the surface aggravates microscopic cracking of the sweet cherry fruit cuticle. *J. Amer. Soc. Hort. Sci.* 131:192–200.
- Knoche, M., E. Grimm, and H.J. Schlegel. 2014. Mature sweet cherries have low turgor. *J. Amer. Soc. Hort. Sci.* 139:3–12.
- Kondo, S. and C. Danjo. 2001. Cell wall polysaccharide metabolism during fruit development in sweet cherry 'Satohishiki' as affected by gibberellic acid. *J. Jpn. Soc. Hort. Sci.* 70:178–184.
- Lang, A. and H. Düring. 1990. Grape berry splitting and some mechanical properties of the skin. *Vitis* 29:61–70.
- Lang, A. and H. Düring. 1991. Partitioning control by water potential gradient: Evidence for compartmentation breakdown in grape berries. *J. Expt. Bot.* 42:1117–1122.

- Matas, A.J., E.D. Cobb, J.A. Bartsch, D.J. Paolillo, and K.J. Niklas. 2004. Biomechanics and anatomy of *Lycopersicon esculentum* fruit peels and enzyme-treated samples. *Amer. J. Bot.* 91:352–360.
- McGuire, R.G. 1992. Reporting of objective color measurements. *HortScience* 27:1254–1255.
- Measham, P.F., S.A. Bound, A.J. Gracie, and S.J. Wilson. 2009. Incidence and type of cracking in sweet cherry (*Prunus avium* L.) are affected by genotype and season. *Crop Pasture Sci.* 60:1002–1008.
- Measham, P.F., S.A. Bound, A.J. Gracie, and S.J. Wilson. 2010. Vascular flow of water induces side cracking in sweet cherry (*Prunus avium* L.). *Adv. Hort. Sci.* 24:243–248.
- Niklas, K.J. 1992. *Plant biomechanics: An engineering approach to plant form and function.* Univ. Chicago Press, Chicago, IL.
- Oey, M.L., E. Vanstreels, J. De Baerdemaeker, E. Tijskens, H. Ramon, M.L.A.T.M. Hertog, and B. Nicolai. 2007. Effect of turgor on micromechanical and structural properties of apple tissue: A quantitative analysis. *Postharvest Biol. Technol.* 44:240–247.
- Peschel, S. and M. Knoche. 2005. Characterization of microcracks in the cuticle of developing sweet cherry fruit. *J. Amer. Soc. Hort. Sci.* 130:487–495.
- Schumann, C., H.J. Schlegel, E. Grimm, M. Knoche, and A. Lang. 2014. Water potential and its components in developing sweet cherry. *J. Amer. Soc. Hort. Sci.* 139:349–355.
- Sekse, L., K.L. Bjerke, and E. Vangdal. 2005. Fruit cracking in sweet cherries: An integrated approach. *Acta Hort.* 667:471–474.
- Simon, E.W. 1977. Leakage from fruit cells in water. *J. Expt. Bot.* 28:1147–1152.
- Tilbrook, J. and S.D. Tyerman. 2008. Cell death in grape berries: Varietal differences linked to xylem pressure and berry weight loss. *Funct. Plant Biol.* 35:173–184.
- Verner, L. and E.C. Blodgett. 1931. *Physiological studies of the cracking of sweet cherries.* Univ. Idaho Agr. Expt. Sta. Bul. 184.
- Vincent, J.F.V. 1990a. *Structural biomaterials,* revised ed. Princeton Univ. Press, Princeton, NJ.
- Vincent, J.F.V. 1990b. Fracture properties of plants. *Adv. Bot. Res.* 17:235–287.
- Weichert, H. and M. Knoche. 2006. Studies on water transport through the sweet cherry fruit surface. 10. Evidence for polar pathways across the exocarp. *J. Agr. Food Chem.* 54:3951–3958.
- Weichert, H., C.V. Jagemann, S. Peschel, M. Knoche, D. Neumann, and W. Erfurth. 2004. Studies on water transport through the sweet cherry fruit surface: VIII. Effect of selected cations on water uptake and fruit cracking. *J. Amer. Soc. Hort. Sci.* 129:781–788.
- Winkler, A., M. Ossenbrink, and M. Knoche. 2015. Malic acid promotes cracking of sweet cherry fruit. *J. Amer. Soc. Hort. Sci.* 140:280–287.
- Yamaguchi, M., I. Sato, and M. Ishiguro. 2002. Influences of epidermal cell sizes and flesh firmness on cracking susceptibility in sweet cherry (*Prunus avium* L.) cultivars and selections. *J. Jpn. Soc. Hort. Sci.* 71:738–746.

## **6. Mechanical properties of skin of sweet cherry fruit of differing susceptibilities to cracking**

Dieser Artikel wurde im Original 2016 in der Zeitschrift „Journal of the American Society for Horticultural Science“ veröffentlicht:

Brüggenwirth, M. und Knoche, M. (2016b) Mechanical properties of skin of sweet cherry fruit of differing susceptibilities to cracking. *Journal of the American Society for Horticultural Science* 141, 162-168.



J. AMER. SOC. HORT. SCI. 141(2):162–168. 2016.

## Mechanical Properties of Skins of Sweet Cherry Fruit of Differing Susceptibilities to Cracking

Martin Brüggewirth and Moritz Knoche<sup>1</sup>

Fruit Science Section, Institute for Biological Production Systems, Leibniz University Hannover, Herrenhäuser Straße 2, 30419 Hannover, Germany

ADDITIONAL INDEX WORDS. *Prunus avium*, epidermis, hypodermis, modulus of elasticity, strain, tensile test

**ABSTRACT.** Rain cracking of sweet cherry fruit (*Prunus avium* L.) may be the result of excessive water uptake and/or of mechanically weak skins. The objectives were to compare mechanical properties of the skins of two cultivars of contrasting cracking susceptibility using biaxial tensile tests. We chose ‘Regina’ as the less-susceptible and ‘Burlat’ as the more-susceptible cultivar. Cracking assays confirmed that cracking was less rapid and occurred at higher water uptake in ‘Regina’ than in ‘Burlat’. Biaxial tensile tests revealed that ‘Regina’ skin was stiffer as indexed by a higher modulus of elasticity ( $E$ ) and had a higher pressure at fracture ( $p_{\text{fracture}}$ ) than ‘Burlat’. There was little difference in their fracture strains. Repeated loading, holding, and unloading cycles of the fruit skin resulted in corresponding changes in strains. Plotting total strains against the pressure applied for ascending, constant, and descending pressures yielded essentially linear relationships between strain and pressure. Again, ‘Regina’ skin was stiffer than ‘Burlat’ skin. Partitioning total strain into elastic strain and creep strain demonstrated that in both cultivars most strain was accounted for by the elastic component and the remaining small portion by creep strain. Differences in  $E$  and  $p_{\text{fracture}}$  between ‘Regina’ and ‘Burlat’ remained even after destroying their plasma membranes by a freeze/thaw cycle. This indicates that differences in skin mechanical properties must be accounted for by differences in the cell walls, not by properties related to cell turgor. Microscopy of skin cross-sections revealed no differences in cell size between ‘Regina’ and ‘Burlat’ skins. However, mass of cell walls per unit fresh weight was higher in ‘Regina’ than in ‘Burlat’. Also, the ratio of tangential/radial diameters of epidermal cells was lower in ‘Regina’ ( $1.86 \pm 0.12$ ) than in ‘Burlat’ ( $2.59 \pm 0.15$ ). The results suggest that cell wall physical (and possibly also chemical) properties account for the cultivar differences in skin mechanical properties, and hence in cracking susceptibility.

Wherever sweet cherries are grown, rain-induced fruit cracking imposes a major limitation to production (Christensen, 1996). Susceptibility to rain cracking differs among cultivars (Christensen, 1995, 1999, 2000; Measham et al., 2009), but the mechanistic basis of differential cracking susceptibility among cultivars is not clear. From the coincidence of rainfall and fruit cracking, it is inferred that cracking is related to water uptake into the fruit. Water uptake, in turn, leads to an increase in volume, causing the fruit surface area to increase. When the limits of extensibility are exceeded, the fruit is expected to crack.

Based on the above logic, differential cracking susceptibility among cultivars could result from either (or both) of two, mechanistically unrelated, factors. First, the net import of water into the fruit will affect cracking by causing fruit volume to increase, thereby straining the skin beyond some defined upper limit. Second, mechanical properties of the fruit skin will affect the fracture limits. Recent investigations (Brüggewirth et al., 2014) have established that it is the epidermal and hypodermal cell layers (not the cuticle) that represent the structural “backbone” of the skins of sweet cherry fruit. Thus, differences in cracking susceptibility among sweet cherry cultivars could be the result of different water-uptake characteristics and/or of

the mechanical properties of the epidermal and hypodermal cell layers.

Water uptake across the fruit surface has been studied in detail in the last decade. The pathways and mechanisms of transfer have been identified (Beyer et al., 2005; Knoche et al., 2000; Weichert and Knoche, 2006). However, among 29 cultivars, there was no close relationship between variation in cracking susceptibility and variation in the major characteristics of the fruit surface: water permeance, strain, mass of cuticle per unit area, stomatal density, etc. (Peschel and Knoche, 2012). Some information is available on vascular transport, but to our knowledge differences among cultivars have not been identified (Brüggewirth and Knoche, 2015; Hovland and Sekse, 2004a, 2004b; Measham et al., 2009, 2010, 2014).

Little information is available on the mechanical properties of the sweet cherry fruit skin (Bargel et al., 2004). Recently, Brüggewirth et al. (2014) modified the biaxial bulging test to quantify the mechanical properties of excised fruit skins under standardized laboratory conditions. Modifications included dimensional fixation of a skin segment in a washer before excision, to prevent any release of elastic strain [built up in the skin due to growth (Grimm et al., 2012)]. Silicone oil was used to give a hydrostatic pressure to the skin segment from the physiological inside to prevent uncontrolled water uptake from that side—this could have confounded the test results (Simon, 1977). In contrast to the more common, uniaxial tensile tests of engineering, biaxial tensile tests better mimic the growth stresses and strains occurring in vivo. In a spherical organ of nearly isotropic growth, stresses and strains are of course fairly uniformly biaxial, not uniaxial. Also, sweet cherry skin exhibits high Poisson ratio properties, so a uniaxial tensile test using

Received for publication 18 Nov. 2015. Accepted for publication 23 Dec. 2015. This research was funded in part by grants from the Deutsche Forschungsgemeinschaft.

We thank Dieter Reese and Christoph Knake for constructing, engineering, and programming the elastometer; Friederike Schroeder and Simon Sitzenstock for technical support; Bishnu P. Khanal and Sandy Lang for helpful discussion and useful comments on an earlier version of this manuscript.

<sup>1</sup>Corresponding author. E-mail: moritz.knoche@obst.uni-hannover.de.

a skin strip is associated with severe narrowing, and hence a gross overestimation of skin extensibility (Brüggenwirth et al., 2014).

The purpose of this study was to 1) quantify the key mechanical properties of two sweet cherry cultivars of contrasting cracking susceptibility, using a biaxial tensile test and 2) investigate the mechanistic basis of any differences between the two cultivars. Because many fruit may vary diurnally in diameter, and hence surface area (Lang, 1990; Measham et al., 2014; Montanaro et al., 2012; Ohta et al., 1997) and because this may cause the skin to fatigue, we also investigated the effects of repeated loading and unloading cycles on the mechanical properties of the fruit skin of the two cultivars.

### Materials and Methods

**PLANT MATERIAL.** Fruit of sweet cherry ‘Adriana’, ‘Burlat’, ‘Hedelfinger’, ‘Merchant’, ‘Regina’, ‘Sam’, and ‘Samba’ grafted on ‘Gisela5’ (*Prunus cerasus* L. × *Prunus canescens* Bois) were collected from greenhouse-grown trees in the 2013 and 2014 seasons. All fruit were obtained from the experimental station of the Leibniz University, Hannover, Germany (lat. 52°14’N, long. 9°49’E). Water was supplied via drip irrigation. The drip irrigation was operated for 2-h intervals (corresponding to ≈15 mm of precipitation) as needed based on visual inspection of the moisture of the top soil (<20 cm). Fruit were harvested at maturity and selected for uniformity (based on color and size) and were free of visual defects. All fruit for mechanical testing were processed within 12 h of harvest. When held for more than 2 h, fruit was placed in a cold room at 5 °C, for shorter periods of time fruit was held at ambient temperature and covered with a damp paper towel. The ‘Regina’ and ‘Burlat’ fruit used for microscopy of the cross-sections of the fruit surface were fixed in Karnovsky solution (Karnovsky, 1965).

**THE ELASTOMETER.** For a detailed description of the elastometer, the reader is referred to Brüggenwirth et al. (2014). Briefly, an excised exocarp segment [ES (synonym fruit skin segment)] is mounted on a polymethylmethacrylate (Lucite®; Mitsubishi Rayon Lucite Group, Southampton, UK) chamber filled with silicone oil (AK10; Wacker Chemie, Munich, Germany). The chamber is pressurized by driving a motorized piston into it, causing the volume of the chamber to decrease at a rate of ≈153 μL·min<sup>-1</sup>. The volume displacement causes the chamber pressure to increase and the ES to bulge outward. The pressure inside the chamber and the extent of bulging are monitored using a pressure transducer (Typ 40PC100G; Honeywell, Morristown, NJ) and a displacement transducer (KAP-S/5N; AST Angewandte System Technik, Wolnzach, Germany) from a material testing machine (BXC-FR2.5TN; Zwick Roell, Ulm, Germany). To preserve the in vivo strain of the fruit skin following excision, a brass washer (aperture diameter 12 mm) was glued to the shoulder of an intact sweet cherry fruit using cyanoacrylate adhesive (Loctite 406; Henkel/Loctite Deutschland, Munich, Germany) (Knoche and Peschel, 2006). By cutting underneath the washer with a razor blade, an ES was excised having an average thickness of ≈2.4 ± 0.02 mm. The ES remained fixed to the washer after excision, which prevented relaxation, thereby maintaining the in vivo strain that existed before excision (Brüggenwirth et al., 2014; Knoche and Peschel, 2006). The ES so-obtained comprise

cuticle, epidermis, hypodermis, and some adhering mesocarp tissue.

The surface area ( $A$ ) of the bulging ES is calculated from Eq. [1], where  $r$  is the radius of the washer aperture and  $h$  is the height of the bulge ES (Brüggenwirth et al., 2014).

$$A = (r^2 + h^2) \times \pi \quad [1]$$

An estimate of the total strain ( $\varepsilon$ ) is obtained from the change in surface area ( $\Delta A$ ) relative to the initial surface area ( $A_0$ ) of the bulging ES and is given in Eq. [2].

$$\varepsilon = \frac{\Delta A}{A_0} \quad [2]$$

In some experiments, the modulus of elasticity ( $E$ ) was estimated from the height ( $h$ ) of the bulging ES, the radius ( $r$ ) of the aperture, the pressure ( $p$ ), and the thickness ( $t$ ) of the bearing layer ( $t = 0.1$  mm) using Eq. [3] (Brüggenwirth et al., 2014).

$$E = \frac{p \times r^2 \times (r^2 + h^2)}{h^3 \times t \times 2} \quad [3]$$

All mechanical tests were performed at 22 °C.

**EXPERIMENTS.** The modulus of elasticity [ $E$  (megapascals)], the pressure at fracture [ $p_{\text{fracture}}$  (kilopascals)], and strain at fracture [ $\varepsilon_{\text{fracture}}$  (square millimeters per square millimeter)] was quantified for a range of cultivars. Biaxial tensile tests were carried out as described above.

Total, elastic, and creep strains and the effects of repeated loading, holding, and unloading cycles were measured for ‘Regina’ and ‘Burlat’. These cultivars were selected because of their contrasting cracking susceptibilities (Christensen, 1999). ES were excised and mounted as described above. Experiments were initiated by increasing the pressure during the loading phase. During the subsequent holding phase, pressure was maintained constant and then decreased in the unloading phase. The time period for a complete loading/holding/unloading cycle was ≈5 minutes. Preliminary experiments established that the test protocol had to be adapted to the cultivar tested because fracture limits differed between ‘Regina’ and ‘Burlat’. First, the pressure applied to ‘Burlat’ skin was about half of that in ‘Regina’. Second, the number of loading and unloading cycles was reduced by half for ‘Burlat’ skin, compared with that for ‘Regina’. Higher numbers of cycles resulted in fracture of the skins (M. Brüggenwirth, unpublished data). Three types of experiments were conducted. In the first experiment, the effect of increasing loading was studied by increasing the pressure stepwise in 5-kPa increments (0 to 40 kPa for ‘Regina’ and 0 to 20 kPa for ‘Burlat’). In the second experiment, pressure was held constant during each cycle (25 kPa for ‘Regina’ and 10 kPa for ‘Burlat’). The last experiment comprised pressures that decreased stepwise by 5-kPa increments (40 to 0 kPa for ‘Regina’ and 20 to 0 kPa for ‘Burlat’). Data were analyzed by partitioning the strain during each cycle into a total strain, an elastic strain, and a creep strain. The elastic strain was defined as the strain during the loading phase, and the creep strain was defined as the deformation occurring during the holding phase. Total strain represented the sum of the elastic strain and the creep strain.

The effect of eliminating cell turgor by destroying plasma membrane integrity was investigated in ‘Regina’ and ‘Burlat’.

To do this, the ES were frozen for 30 minutes at  $-18\text{ }^{\circ}\text{C}$ , then thawed for 30 minutes at  $22\text{ }^{\circ}\text{C}$ , and then tested in the elastometer.

**CRACKING AND WATER UPTAKE.** Cracking and water uptake relationships were established for ‘Regina’ and ‘Burlat’ sweet cherry fruit by incubation in deionized water at  $22\text{ }^{\circ}\text{C}$ . Water uptake was restricted to the fruit surface by previously sealing the stem cavity with silicone rubber (SE9186 Coating; Dow Corning, Midland, MI). Cracking was quantified in two batches of 25 fruit each, by visual inspection of fruit at 2, 4, 6, 8, 10, and 24 h for macroscopically visible cracks. The time to 50% fruit cracking ( $T_{50}$ ) was calculated using a four-parameter sigmoidal regression model, fitted to a plot of the percentage of fruit cracking vs. time (Winkler et al., 2015). Fruit that had cracked was removed from the solution, and noncracked fruit was returned for further incubation. Water uptake was quantified gravimetrically after 0.75 and 1.5 h ( $n = 15$ ). The water uptake required for 50% fruit cracking ( $WU_{50}$ ) was calculated by multiplying the  $T_{50}$  by the rate of water uptake.

**MICROSCOPY.** Dimensions of epidermal and hypodermal and parenchyma cells were quantified in fruit of ‘Regina’ and ‘Burlat’ fixed in Karnovsky solution (Karnovsky, 1965). Fruit were removed from the fixation solution and thoroughly washed in deionized water. Cross-sections were prepared from the shoulder region of the fruit, using parallel razor blades (spacing 3 mm), and the sections were incubated for 7 min in 0.1% (w/w) calcofluor white (fluorescent brightener 28; Sigma-Aldrich Chemie, Munich, Germany). Thereafter, cross-sections were rinsed with deionized water, positioned on a microscope slide, transferred to the stage of a fluorescence microscope (model BX-60; Olympus Europa, Hamburg, Germany), and viewed under ultraviolet light at  $\times 400$  (model BX-60, filter U-MWB 330–385 nm excitation wavelength,  $\geq 420$  nm emission wavelength; Olympus Europa). Calibrated micrographs were taken using a digital camera (DP71, Olympus Europa), and the digital images were analyzed (software Cell’P, Olympus Europa). For the cells of the epidermis, hypodermis, and outer mesocarp, the cell sizes were measured (one radial and two tangential diameters) and the distances of the cell centers from the cuticle were quantified along a line drawn perpendicular to the fruit surface.

**MASS OF CELL WALLS.** Tissue cylinders (8 mm diameter) were punched using a biopsy punch (Kai Europe, Solingen, Germany) and cut to discs of 2.5 mm height using parallel razor blades. The discs comprised cuticle, epidermis and hypodermis, and the outer mesocarp. Discs were frozen in liquid  $\text{N}_2$  and held at  $-20\text{ }^{\circ}\text{C}$ . For analysis, discs were transferred into 3 mL of 80% ethanol, homogenized for 2 minutes, and thereafter heated to  $80\text{ }^{\circ}\text{C}$  for 15 minutes. Samples were then transferred into Eppendorf tubes and centrifuged at  $20,800\text{ g}_n$ . The supernatant was removed, the pellet washed with 2 mL of 80% ethanol, and centrifuged again. This procedure was repeated twice using pure acetone. Thereafter, the pellet was dried at  $70\text{ }^{\circ}\text{C}$  and weighed. Dry mass of cell walls per unit fresh weight was

Table 1. Modulus of elasticity ( $E$ ), pressure fracture ( $p_{\text{fracture}}$ ), and strain fracture ( $\epsilon_{\text{fracture}}$ ) of exocarp segments (ES) excised from cheeks of selected, greenhouse-grown, sweet cherry fruit at maturity ( $n = 25$ ).

Cultivar	$E$	$p_{\text{fracture}}$	$\epsilon_{\text{fracture}}$
	[mean $\pm$ SE (MPa)]	[mean $\pm$ SE (kPa)]	[mean $\pm$ SE ( $\text{mm}^2 \cdot \text{mm}^{-2}$ )]
Adriana	$17.7 \pm 1.4^z$ bc	$40.3 \pm 1.3^z$ de	$0.17 \pm 0.01^z$ b
Burlat	$8.7 \pm 0.5$ e	$24.9 \pm 1.2$ f	$0.20 \pm 0.01$ ab
Hedelfinger	$25.3 \pm 1.1$ a	$67.8 \pm 1.9$ a	$0.20 \pm 0.01$ ab
Merchant	$15.2 \pm 0.8$ cd	$38.8 \pm 1.3$ e	$0.18 \pm 0.01$ b
Regina	$18.9 \pm 1.0$ bc	$59.1 \pm 2.0$ b	$0.22 \pm 0.01$ a
Sam	$14.9 \pm 0.7$ d	$48.1 \pm 1.5$ c	$0.22 \pm 0.01$ a
Samba	$19.2 \pm 1.0$ b	$46.0 \pm 1.3$ cd	$0.17 \pm 0.01$ b

<sup>z</sup>Mean separation by Tukey’s studentized range test at  $P < 0.05$ .

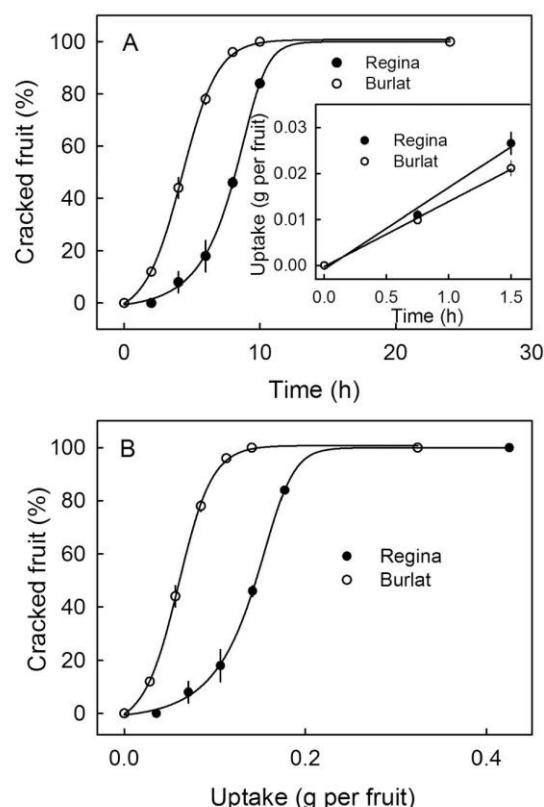


Fig. 1. (A) Time course of cracking and of water uptake (inset) of ‘Regina’ and ‘Burlat’ sweet cherry fruit incubated in deionized water. (B) Relationship between cracked fruit and water uptake. For further details, see Table 2.

calculated. The experiment was conducted with seven replicates comprising 10 discs per replicate.

**DATA ANALYSIS.** Data analysis was limited to segments that fractured in the center of the washer aperture. Segments fracturing at the edge of the aperture were excluded because artifacts resulting from the mounting procedure could not be excluded. Data are presented as means  $\pm$  SEs of means. Mean comparisons were made using Tukey’s studentized range test at  $P < 0.05$  (packet multcomp 1.2–12, procedure glht, R 2.13.1; R Foundation for Statistical Computing, Vienna, Austria). Significance of coefficients of correlation ( $r$ ) and of determination

( $r^2$ ) at the probability levels 0.05, 0.01, and 0.001 are indicated by \*, \*\*, and \*\*\*, respectively.

### Results

The mechanical properties of the fruit skins differed significantly among cultivars (Table 1). ‘Hedelfinger’ and ‘Regina’ had the stiffest fruit skins as indexed by high values for  $E$  and  $p_{fracture}$ , whereas ‘Burlat’ had the lowest values for  $E$  and  $p_{fracture}$ . There was little difference among the various cultivars for the value of  $\varepsilon_{fracture}$ , which ranged from 0.17 to 0.22 (Table 1).

Incubating fruit in deionized water resulted in cracking of both ‘Regina’ and ‘Burlat’ (Fig. 1). Cracking was markedly more rapid in ‘Burlat’ than in ‘Regina’ as indexed by a lower  $T_{50}$  (Table 2). Cumulative water uptake increased linearly with time (i.e., a constant uptake rate) in ‘Regina’ and ‘Burlat’ and occurred at similar rates in the two cultivars. Calculating cumulative water uptake at 50% cracking revealed that ‘Regina’ fruit required, on average, about three times more water to crack than ‘Burlat’ fruit (Table 2).

Repeated loading, holding, and unloading of the fruit skin imposed cyclic changes in the skin strains in both cultivars (Fig. 2). The maximum number of strain cycles sustained by ‘Regina’ segments was markedly higher than that by ‘Burlat’ segments (M. Brüggewirth, unpublished data). Increasing pressure during any one loading cycle resulted in an instantaneous and proportional increase in strain. During the holding phase, the strain of the skins of both cultivars continued to increase. Upon release of the pressure, the skins of both cultivars returned to their initial dimensions, i.e., before the application of pressure.

Plotting total strains during any one cycle against the pressure applied for ascending, constant, or descending pressures yielded the relationships depicted in Fig. 3. In both cultivars, strains were essentially linearly related to the applied pressure with little difference between the ascending and descending paths [i.e., minimal hysteresis (Fig. 3)]. However, the slopes of the strain/pressure

relationships were markedly higher for the skins of ‘Burlat’ than for those of ‘Regina’ (Table 3). Thus, a given pressure caused markedly higher strain in the less stiff ‘Burlat’ skin than in the stiffer ‘Regina’ skin. Partitioning total strain into its elastic and creep components demonstrated that 1) most of the total strain in both cultivars was accounted for by the elastic component, with the creep strain being relatively small and 2) the slopes of both the elastic strain vs. pressure and of the creep strain vs. pressure relationships

Table 2. Water uptake and cracking in ‘Burlat’ and ‘Regina’ sweet cherry. Cracking was indexed by the amount of water uptake for 50% of fruit to crack ( $WU_{50}$ ) or by time to 50% fruit cracking ( $T_{50}$ ).

Cultivar	Rate of water uptake [mean $\pm$ SE (mg·h <sup>-1</sup> )]	Cracking	
		$WU_{50}$ [mean $\pm$ SE (mg)]	$T_{50}$ [mean $\pm$ SE (h)]
Burlat	14.1 $\pm$ 1.1 <sup>a</sup>	50.5 $\pm$ 2.3	3.6 $\pm$ 0.2
Regina	17.7 $\pm$ 1.6 a	145.8 $\pm$ 0.7	8.2 $\pm$ 0.4

<sup>a</sup>Mean separation by  $t$  test at  $P < 0.05$ .

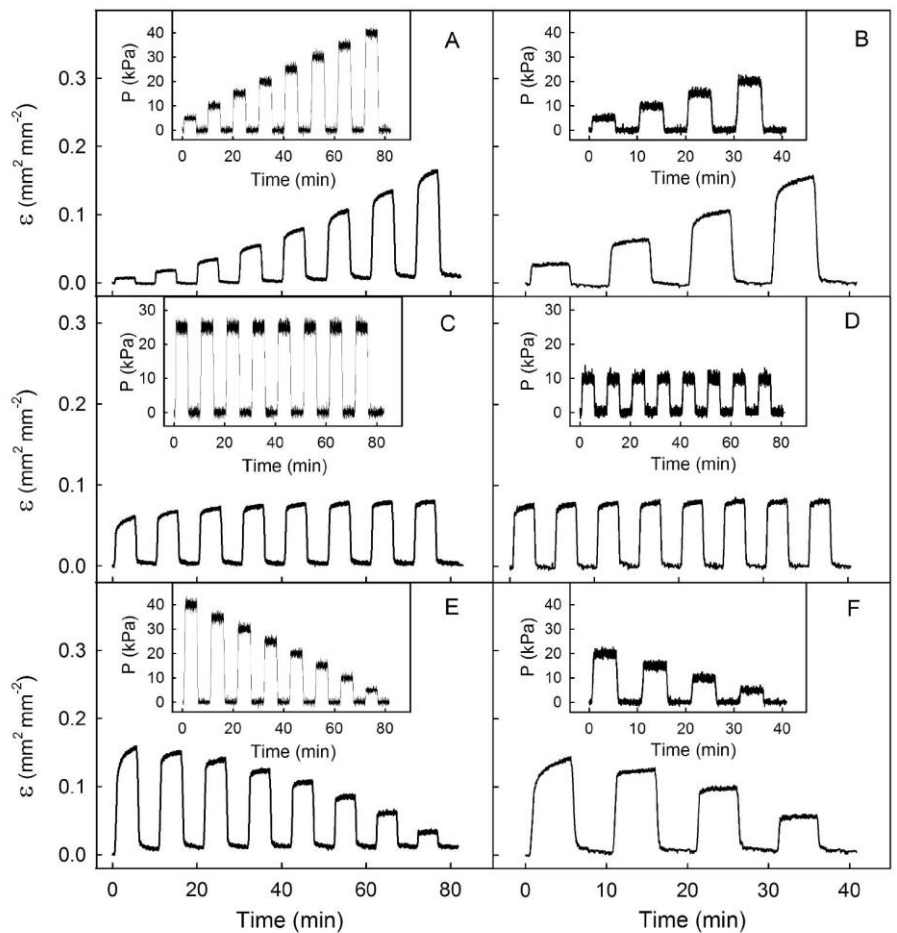


Fig. 2. Time course of change in strain of the fruit skin ( $\varepsilon$ ) of (A, C, E) ‘Regina’ and (B, D, F) ‘Burlat’ sweet cherry when subjected to repeated loading, holding, and unloading cycles. (A, B) Pressures ( $p$ ) during the holding cycles were increased in 5-kPa increments from 0 to 40 kPa for ‘Regina’ and from 0 to 20 kPa for ‘Burlat’. (C, D) Pressures during the holding cycles were held constant at 25 kPa for ‘Regina’ and 10 kPa for ‘Burlat’. (E, F) Pressures during the holding cycles were decreased stepwise in 5-kPa increments from 40 to 0 kPa for ‘Regina’ and from 20 to 0 kPa for ‘Burlat’. Insets (A–F): Time courses of change in pressure.

were markedly higher for ‘Burlat’ than for ‘Regina’ (Table 3).

Destroying the plasma membranes by a single freeze/thaw cycle decreased the values of both  $E$  and  $p_{\text{fracture}}$ . In ‘Burlat’, the value of  $\varepsilon_{\text{fracture}}$  was increased by a single freeze/thaw cycle, but in ‘Regina’ there was no effect (Table 4). The  $E$  and  $p_{\text{fracture}}$  values of ‘Regina’ always exceeded those of ‘Burlat’.

Cell sizes in both ‘Regina’ and ‘Burlat’ skins increased with increasing distance below the surface, to a depth of  $\approx 200 \mu\text{m}$  but remained constant thereafter (Fig. 4A and B). Cell sizes were similar in the two cultivars. Dry mass of cell walls per unit fresh weight, however, was higher in ‘Regina’ ( $21.5 \pm 0.6 \text{ mg}\cdot\text{g}^{-1}$  fresh weight) than in ‘Burlat’ ( $15.8 \pm 0.6 \text{ mg}\cdot\text{g}^{-1}$  fresh weight). The shape of the cells as indexed by the anticlinical aspect ratio (i.e., tangential diameter/radial diameter) decreased with increasing distance from the surface. Cells at the surface had a lower aspect ratio in ‘Regina’ ( $1.86 \pm 0.12$ ,  $r^2 = 0.124^{**}$ ,  $n = 85$ , estimated as the  $y$ -axis intercept of a linear regression line of a plot of aspect ratio vs. distance from the surface) than in ‘Burlat’ ( $2.59 \pm 0.15$ ,  $r^2 = 0.231^{***}$ ,  $n = 90$ ). As distance

from the cuticle increased, cells became more closely isodiametric (aspect ratio  $\approx 1$ ).

## Discussion

Our data establish that ‘Regina’ and ‘Burlat’ differ in the mechanical properties in biaxial tensile tests of their fruit skins. The tensile tests show that 1) the skin of the less cracking-susceptible ‘Regina’ was stiffer and had a higher fracture pressure than that of the more cracking-susceptible ‘Burlat’, 2) the repeated loading and unloading cycles did not cause the skin to fatigue in either cultivar, and 3) the greater stiffness of ‘Regina’ is likely to result from differences in the physical and chemical properties of the cell walls of ‘Regina’ skin, compared with those of ‘Burlat’.

‘REGINA’ AND ‘BURLAT’ DIFFER IN MECHANICAL PROPERTIES OF THEIR FRUIT SKINS. The higher cracking susceptibility of ‘Burlat’ than of ‘Regina’ is consistent with published ratings (Christensen, 1999) and correlates with a weaker mechanical architecture of the fruit’s skin. First, the rates of water uptake

did not differ, but cracking was faster (lower  $T_{50}$ ) in ‘Burlat’ than in ‘Regina’. This resulted in a lower  $WU_{50}$  in ‘Burlat’. Thus, cracking in ‘Burlat’ required only one-third the amount of water uptake as in ‘Regina’. Second, direct evidence for a weaker skin of ‘Burlat’ than ‘Regina’ comes from the biaxial tensile tests. The cultivar comparison established a lower value of  $E$ , and hence a low resistance to extension for ‘Burlat’ than for ‘Regina’ (Table 1). Also, the value  $p_{\text{fracture}}$  for ‘Burlat’ was less than half that for ‘Regina’ (Table 1). These two cultivars fell one at the upper end and the other at the lower end of the range of mechanical properties of the seven cultivars investigated here. The number of loading/holding/unloading cycles that could be applied without fracture in ‘Regina’ was twice that in ‘Burlat’ (M. Brüggewirth, unpublished data). Finally, the slopes of the relationships between total strain and the elastic and the creep strain components vs. pressure were larger in ‘Burlat’ than in ‘Regina’. This indicates that a given strain was reached at a lower pressure in ‘Burlat’ than in ‘Regina’ (Fig. 3). While the relationship between the lower stiffness

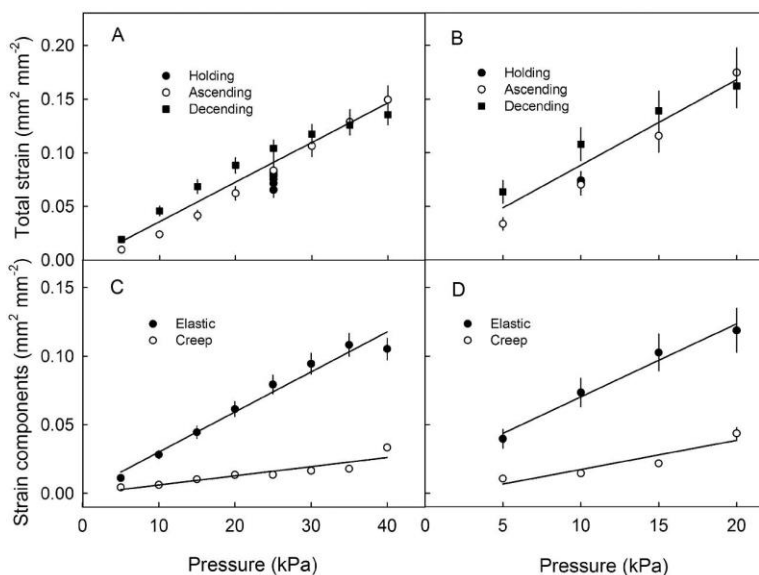


Fig. 3. (A, B) Total strains and (C, D) elastic and creep strains of the skin of (A, C) ‘Regina’ and (B, D) ‘Burlat’ sweet cherry as affected by the pressure applied in the elastometer. (A, B) Data from experiments with cyclic application of increasing, constant, or decreasing pressures.

Table 3. Parameter estimates and ses of linear regression equations describing the relationships between the pressure (kilopascals) applied in the elastometer and total strain, elastic strain, and creep strain (all strains millimeter square per millimeter square) of ‘Regina’ and ‘Burlat’ sweet cherry fruit skin.

Cultivar	Strain component	Parameter estimates		Coefficient of determination $r^2$
		$[\times 10^3 \text{ (slope } \pm \text{ SE)}]$	$[\times 10^3 \text{ (intercept } \pm \text{ SE)}]$	
Regina	Total	$4.2 \pm 0.2$	$-1.5 \pm 5.2$	0.99***
	Elastic	$2.9 \pm 0.2$	$0.9 \pm 1.1$	0.98*
	Creep	$0.7 \pm 0.1$	$-0.6 \pm 2.9$	0.91
Burlat	Total	$7.7 \pm 0.7$	$9.1 \pm 9.3$	0.99***
	Elastic	$5.3 \pm 0.6$	$17.1 \pm 7.8$	0.98**
	Creep	$2.1 \pm 0.6$	$-3.9 \pm 8.1$	0.93

<sup>z</sup>Significance of coefficient of determination at  $P < 0.05$ , 0.01, and 0.001 indicated by \*, \*\*, and \*\*\*, respectively.

Table 4. Effect of destroying plasma membranes of exocarp segments excised from the cheeks of mature ‘Burlat’ and ‘Regina’ sweet cherry fruit by a freeze/thaw cycle. The effects on the modulus of elasticity ( $E$ ), pressure at fracture ( $p_{\text{fracture}}$ ), and strain at fracture ( $\epsilon_{\text{fracture}}$ ) were investigated ( $n = 20$ ).

Cultivar	Treatment	$E$	$p_{\text{fracture}}$	$\epsilon_{\text{fracture}}$
		[mean $\pm$ SE (MPa)]	[mean $\pm$ SE (kPa)]	[mean $\pm$ SE (mm <sup>2</sup> ·mm <sup>-2</sup> )]
Burlat	Control	15.5 $\pm$ 2.0 <sup>c</sup>	26.7 $\pm$ 1.6 <sup>c</sup>	0.16 $\pm$ 0.01 <sup>b</sup>
	Freeze/thaw	5.3 $\pm$ 0.4 <sup>d</sup>	12.5 $\pm$ 0.8 <sup>d</sup>	0.20 $\pm$ 0.01 <sup>a</sup>
Regina	Control	33.9 $\pm$ 1.9 <sup>a</sup>	64.5 $\pm$ 2.2 <sup>a</sup>	0.17 $\pm$ 0.01 <sup>b</sup>
	Freeze/thaw	25.7 $\pm$ 2.3 <sup>b</sup>	45.5 $\pm$ 2.5 <sup>b</sup>	0.16 $\pm$ 0.01 <sup>b</sup>

<sup>a</sup>Mean separation by Tukey’s studentized range test at  $P < 0.05$ .

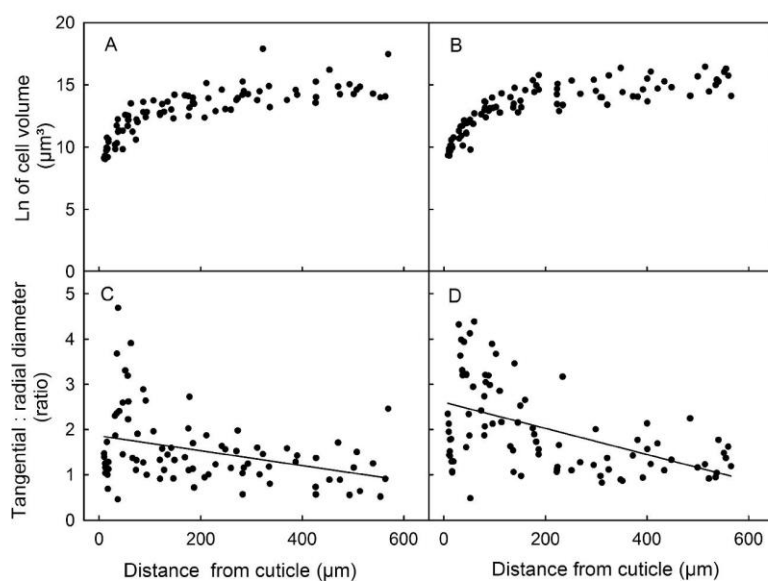


Fig. 4. Properties of cells of cross-sections through the skin of (A, C) ‘Regina’ and (B, D) ‘Burlat’ sweet cherry fruit. (A, B) Relationship between the logarithm of cell volume and the distance of cell centers from the cuticle. (C, D) Relationship between the ratio of tangential to radial diameters of cells and the distance of cell centers from cuticle.

and lower fracture pressure of the cracking-susceptible ‘Burlat’ vs. the higher values of these of the less cracking-susceptible ‘Regina’ are merely correlative (i.e., they are not necessarily causal), nevertheless they are consistent with the general concept in material science that for a pressurized hollow vessel, a weaker shell increases the likelihood of failure.

**MECHANICAL BEHAVIOR OF FRUIT SKIN IN LOADING/UNLOADING CYCLES.** Increasing the number of loading/unloading cycles did not change skin stiffness or fracture threshold (Fig. 3). Also, it made little difference whether the loads increased, decreased, or were maintained constant. Unlike tomato (*Solanum lycopersicum* L.) skin (Matas et al., 2004), there was no strain hardening in sweet cherry. In both cherry cultivars, elastic strain accounted for most of the deformation, whereas creep strain during the holding phases was low. These findings suggest diurnal oscillations in the diameter of a developing fruit (Measham et al., 2014) are unlikely to weaken the fruit skin.

**GREATER STIFFNESS OF ‘REGINA’ SKIN IS THE RESULT OF DIFFERENT PHYSICAL AND CHEMICAL PROPERTIES OF THE CELL WALLS.** The tissue’s water relation affects its mechanical

properties. For example, the shape of a turgid cell resists change as a result of the tangential tension in the cell wall. However, when we destroyed the plasma membrane by imposing a freeze:thaw cycle, the value of  $E$  remained five times higher and that of  $p_{\text{fracture}}$  three times higher in ‘Regina’ than in ‘Burlat’. Hence, because the difference persists in spite of turgor loss, the different  $E$  and  $p_{\text{fracture}}$  values of these two cultivars must be related

to differences in the cell walls themselves—not to cell turgor differences. The reason for the different cell wall mechanical properties of ‘Burlat’ and ‘Regina’ is unknown, but a number of factors may be involved:

First, mass of cell walls per unit fruit mass was higher in ‘Regina’ than in ‘Burlat’. Also, microscopy indicates that the epidermis of ‘Regina’ has thicker anticlinal cell walls ( $2.6 \pm 0.1 \mu\text{m}$ ) than ‘Burlat’ ( $2.2 \pm 0.1 \mu\text{m}$ ) (C. Schumann, unpublished data). Cell wall thickness will affect the mechanical properties. Second, the epidermal cells of ‘Burlat’ had a higher mean anticlinal aspect ratio than those of ‘Regina’. This is consistent with greater strain during growth and/or with less strain relaxation upon preparation of skin sections for microscopy. Third, cell walls could differ in their compositions—differences in cell wall composition can result in differential mechanical behaviors (Chanliaud et al., 2002). For example, the mechanical properties, such as firmness, of a range of sweet cherry cultivars were related to the chemistry of their cell walls, in particular to the composition and solubility of pectin (Basanta et al., 2013; Batisse et al., 1996; Salato et al., 2013). At this stage we do not know which of these factors is the most critical. Based on earlier data from our laboratory a role of the cuticle in mechanical properties of the sweet cherry fruit skin can be excluded (Brüggenwirth et al., 2014).

## Conclusions

Biaxial tensile tests establish that the less cracking-susceptible fruit skin of ‘Regina’ was stiffer and fractured at a higher pressure than the more cracking-susceptible ‘Burlat’. These differences in mechanical properties probably result from different physical and/or chemical properties of the cell walls. Further studies are required to establish relationships between the physical and chemical properties of the cell walls and their mechanical characteristics.

As in earlier studies, the pressures at fracture were of a similar order of magnitude to those reported previously for both cell and fruit turgor (Brüggenwirth and Knoche, 2016; Knoche et al., 2014; Schumann et al., 2014). However, the strains at fracture, resulting from surface area increase following water uptake (0.3% to 1.1%), were markedly lower in the

cracking assay than in the biaxial tensile tests. The reason for this striking discrepancy is unknown and deserves further study. A possible explanation is that cracking at the whole-fruit level is a “local” phenomenon, where failure is triggered by a weak point somewhere in the skin of the whole fruit, whereas the much smaller area of skin employed in the biaxial tensile test will reduce the chances of including such a weak spot in the sample, so its result is proportionately more likely to be representative of a “perfect” fruit skin (Brüggenwirth and Knoche, 2016).

#### Literature Cited

- Bargel, H., H.C. Spatz, T. Speck, and C. Neinhuis. 2004. Two-dimensional tension tests in plant biomechanics: Sweet cherry fruit skin as a model system. *Plant Biol.* 6:432–439.
- Basanta, F.M., M.F. de Escalada Plai, C.A. Stortz, and A.M. Rojas. 2013. Chemical and functional properties of cell wall polymers from two cherry varieties at two developmental stages. *Carbohydr. Polym.* 92:830–841.
- Batisse, C., M. Buret, and P.J. Coulomb. 1996. Biochemical differences in cell wall of cherry fruit between soft and crisp fruit. *J. Agr. Food Chem.* 44:453–457.
- Beyer, M., S. Lau, and M. Knoche. 2005. Studies on water transport through the sweet cherry fruit surface: IX. Comparing permeability in water uptake and transpiration. *Planta* 220:474–485.
- Brüggenwirth, M., H. Fricke, and M. Knoche. 2014. Biaxial tensile tests identify epidermis and hypodermis as the main structural elements of sweet cherry skin. *Ann. Bot. Plants* 6:plu019.
- Brüggenwirth, M. and M. Knoche. 2015. Xylem conductance of sweet cherry pedicels. *Trees (Berl.)* 29:1851–1860.
- Brüggenwirth, M. and M. Knoche. 2016. Factors affecting mechanical properties of the skin of sweet cherry fruit. *J. Amer. Soc. Hort. Sci.* 141:45–53.
- Chanliaud, E., K.M. Burrows, G. Jeronomidis, and M.J. Gidley. 2002. Mechanical properties of primary plant cell wall analogues. *Planta* 215:989–996.
- Christensen, J.V. 1995. Evaluation of fruit characteristics of 20 sweet cherry cultivars. *Fruit Var. J.* 49:113–117.
- Christensen, J.V. 1996. Rain-induced cracking of sweet cherries. Its causes and prevention, p. 297–327. In: A.D. Webster and N.E. Looney (eds.), *Cherries*. CAB Intl., Wallingford, UK.
- Christensen, J.V. 1999. An evaluation of sweet cherry cultivars. Danish Institute of Agricultural Sciences, Årsløv, Denmark.
- Christensen, J.V. 2000. Performance in Denmark of 16 European varieties of sweet cherry. *J. Amer. Pomol. Soc.* 54:172–176.
- Grimm, E., S. Peschel, T. Becker, and M. Knoche. 2012. Stress and strain in the sweet cherry fruit skin. *J. Amer. Soc. Hort. Sci.* 137:383–390.
- Hovland, K.L. and L. Sekse. 2004a. Water uptake through sweet cherry (*Prunus avium* L.) fruit pedicels: Influence of fruit surface water status and intact fruit skin. *Acta Agr. Scand. Sect. B Soil Plant Sci.* 54:91–96.
- Hovland, K.L. and L. Sekse. 2004b. Water uptake through sweet cherry (*Prunus avium* L.) fruit pedicels in relation to fruit development. *Acta Agr. Scand. Sect. B Soil Plant Sci.* 54:264–266.
- Karnovsky, M.J. 1965. A formaldehyde-glutaraldehyde fixative of high osmolality for use in electron microscopy. *J. Cell Biol.* 27:137A–138A.
- Knoche, M. and S. Peschel. 2006. Water on the surface aggravates microscopic cracking of the sweet cherry fruit cuticle. *J. Amer. Soc. Hort. Sci.* 131:192–200.
- Knoche, M., S. Peschel, M. Hinz, and M. Bukovac. 2000. Studies on water transport through the sweet cherry fruit surface: Characterizing conductance of the cuticular membrane using pericarp segments. *Planta* 212:127–135.
- Knoche, M., E. Grimm, and H.J. Schlegel. 2014. Mature sweet cherries have low turgor. *J. Amer. Soc. Hort. Sci.* 139:3–12.
- Lang, A. 1990. Xylem, phloem and transpiration flows in developing apple fruits. *J. Expt. Bot.* 41:645–651.
- Matas, A.J., E.D. Cobb, J.A. Bartsch, D.J. Paolillo, and K.J. Niklas. 2004. Biommechanics and anatomy of *Lycopersicon esculentum* fruit peels and enzyme-treated samples. *Amer. J. Bot.* 91:352–360.
- Measham, P.F., S.A. Bound, A.J. Gracie, and S.J. Wilson. 2009. Incidence and type of cracking in sweet cherry (*Prunus avium* L.) are affected by genotype and season. *Crop Pasture Sci.* 60:1002–1008.
- Measham, P.F., S.A. Bound, A.J. Gracie, and S.J. Wilson. 2010. Vascular flow of water induces side cracking in sweet cherry (*Prunus avium* L.). *Adv. Hort. Sci.* 24:243–248.
- Measham, P.F., S.J. Wilson, A.J. Gracie, and S.A. Bound. 2014. Tree water relations: Flow and fruit. *Agr. Water Mgt.* 137:59–67.
- Montanaro, G., B. Dichio, C. Xiloyannis, and A. Lang. 2012. Fruit transpiration in kiwifruit: Environmental drivers and predictive model. *Ann. Bot. Plants* 6:pls036.
- Ohta, K., T. Hosoki, K. Matsumoto, M. Ohya, N. Ito, and K. Inaba. 1997. Relationships between fruit cracking and changes of fruit diameter associated with solute flow to fruit in cherry tomatoes. *J. Jpn. Soc. Hort. Sci.* 65:753–759.
- Peschel, S. and M. Knoche. 2012. Studies on water transport through the sweet cherry fruit surface: XII. Variation in cuticle properties among cultivars. *J. Amer. Soc. Hort. Sci.* 137:367–375.
- Salato, G.S., N.M.A. Ponce, M.D. Raffò, A.R. Vicente, and C.A. Stortz. 2013. Developmental changes in cell wall polysaccharide from sweet cherry (*Prunus avium* L.) cultivars with contrasting firmness. *Postharvest Biol. Technol.* 84:66–73.
- Schumann, C., H.J. Schlegel, E. Grimm, M. Knoche, and A. Lang. 2014. Water potential and its components in developing sweet cherry. *J. Amer. Soc. Hort. Sci.* 139:349–355.
- Simon, E.W. 1977. Leakage from fruit cells in water. *J. Expt. Bot.* 28:1147–1152.
- Weichert, H. and M. Knoche. 2006. Studies on water transport through the sweet cherry fruit surface: 10. Evidence for polar pathways across the exocarp. *J. Agr. Food Chem.* 54:3951–3958.
- Winkler, A., M. Ossenbrink, and M. Knoche. 2015. Malic acid promotes cracking of sweet cherry fruit. *J. Amer. Soc. Hort. Sci.* 140:280–287.

## **7. Time to fracture and fracture strain are negatively related in sweet cherry fruit skin**

Dieser Artikel wurde im Original 2016 in der Zeitschrift „Journal of the American Society for Horticultural Science“ veröffentlicht:

Brüggenwirth, M. und Knoche, M. (2016c) Time to fracture and fracture strain are negatively related in sweet cherry fruit skin. *Journal of the American Society for Horticultural Science* 141, 485-489.



## Time to Fracture and Fracture Strain are Negatively Related in Sweet Cherry Fruit Skin

Martin Brüggewirth and Moritz Knoche<sup>1</sup>

Fruit Science Section, Institute for Biological Production Systems, Leibniz University Hannover, Herrenhäuser Strasse 2, Hannover 30419, Germany

ADDITIONAL INDEX WORDS. biomechanics, mechanical properties, skin, *Prunus avium*, rheology, cracking

**ABSTRACT.** Rain cracking of sweet cherry fruit (*Prunus avium* L.) is said to occur when the volume increase associated with water uptake, extends the fruit skin beyond its upper mechanical limits. Biaxial tensile tests recorded fracture strains ( $\epsilon_{\text{fracture}}$ ) in the range 0.17 to 0.22  $\text{mm}^2 \cdot \text{mm}^{-2}$  (equivalent to 17% to 22%). In these tests, an excised skin segment is pressurized from its inner surface and the resulting two-dimensional strain is quantified. In contrast, the skins of fruit incubated in water in classical immersion assays are fractured at  $\epsilon_{\text{fracture}}$  values in the range 0.003 to 0.01  $\text{mm}^2 \cdot \text{mm}^{-2}$  (equivalent to 0.3% to 1%)—these values are one to two orders of magnitude lower than those recorded in the biaxial tensile tests. The markedly lower time to fracture ( $t_{\text{fracture}}$ ) in the biaxial tensile test may account for this discrepancy. The objective of our study was to quantify the effect of  $t_{\text{fracture}}$  on the mechanical properties of excised fruit skins. The  $t_{\text{fracture}}$  was varied by changing the rate of increase in pressure ( $p_{\text{rate}}$ ) and hence, the rate of strain ( $\epsilon_{\text{rate}}$ ) in biaxial tensile tests. A longer  $t_{\text{fracture}}$  resulted in a lower pressure at fracture ( $p_{\text{fracture}}$ ) and a lower  $\epsilon_{\text{fracture}}$  indicating weaker skins. However, a 5-fold difference in  $\epsilon_{\text{fracture}}$  remained between the biaxial tensile test of excised fruit skin and an immersion assay with intact fruit. Also, the percentage of epidermal cells fracturing along their anticlinal cell walls differed. It was highest in the immersion assay (94.1%  $\pm$  0.6%) followed by the long  $t_{\text{fracture}}$  (75.3%  $\pm$  4.7%) and the short  $t_{\text{fracture}}$  (57.3%  $\pm$  5.5%) in the biaxial tensile test. This indicates that the effect of water uptake on cracking extends beyond a mere increase in fruit skin strain resulting from a fruit volume increase. Instead, the much lower  $\epsilon_{\text{fracture}}$  in the immersion assay indicates a much weaker skin—some other unidentified factor(s) are at work.

Rain cracking limits the production of sweet cherries in all areas of the world when rainfall occurs during the harvest season (Christensen, 1996). Fruit cracking is thought to be related to water uptake into the fruit. When the volume of the fruit increases, the skin is strained, and this must eventually lead to mechanical failure. On the basis of this concept, water uptake into the fruit and the mechanical properties of the skin are the most critical factors in cracking.

Only a few studies have addressed the mechanical properties of the skin (Bargel et al., 2004; Brüggewirth and Knoche 2016a, 2016b; Brüggewirth et al., 2014). Because of the high Poisson's ratio of the sweet cherry fruit skin, realistic experiments require biaxial tensile tests such as were first described by Bargel et al. (2004). In this test, an excised segment of the fruit surface is pressurized from its inner side. As a result, the segment bulges and its surface area increases thereby mimicking the increase in area associated with water uptake into the fruit (Brüggewirth et al., 2014). Compared with the original protocol, the test procedure has been refined by maintaining the in vivo strain of the fruit skin and by pressurizing the exocarp segments (ES; synonym fruit skin segments) with silicone oil (AK10; Wacker Chemie, Munich, Germany) rather than with water (Brüggewirth and Knoche, 2016a, 2016b; Brüggewirth et al., 2014). Using this protocol, the  $p_{\text{fracture}}$  were of similar

magnitude to the turgor pressures reported for individual cells or those determined at the whole-fruit level (Knoche et al., 2014; Schumann et al., 2014). However, the  $\epsilon_{\text{fracture}}$  (range 0.17 to 0.22  $\text{mm}^2 \cdot \text{mm}^{-2}$ ) was consistently higher in the biaxial tensile tests than in immersion assays where fruit was immersed in water to determine its cracking susceptibility (Brüggewirth and Knoche, 2016a). In these assays, a strain may be calculated from the water uptake required for 50% of the immersed fruit to crack. Typical (area) strain values in such immersion assays are in the order of 0.003 to 0.01  $\text{mm}^2 \cdot \text{mm}^{-2}$  (Brüggewirth and Knoche, 2016a). The mechanistic basis for this difference in strain between the biaxial tensile tests and the immersions assays is unknown. One possible explanation would be the difference in the  $t_{\text{fracture}}$ . In the immersions assays, fruit required on average at least 3 h to fracture, whereas in a biaxial tensile test, the ES fractured within  $\approx$  2 min. To our knowledge, the effect of  $t_{\text{fracture}}$  on the mechanical properties of fruit skins is unknown.

The objective of this study was to quantify the effect of  $t_{\text{fracture}}$  on the measured mechanical properties of excised sweet cherry fruit skins. We varied the  $t_{\text{fracture}}$  by changing the  $p_{\text{rate}}$  in the biaxial tensile tests.

### Materials and Methods

**PLANT MATERIAL.** Off-season 'Sweetheart' sweet cherry fruit from New Zealand were purchased locally and the fruit were selected for freedom from visual defects. The rootstock and cultivation system were unknown. Fruit was in excellent fully mature condition with turgescence green pedicels. There were no signs of pitting or alligator skin or any symptoms of shriveling. Mature 'Regina' sweet cherry fruit was obtained from the horticultural research station of the Leibniz University at Ruthe

Received for publication 29 Apr. 2016. Accepted for publication 6 July 2016. This research was funded in part by grants from the Deutsche Forschungsgemeinschaft.

We thank Dieter Reese and Christoph Knake for constructing, engineering, and programming the elastometer; Simon Sitzenstock for technical support; and Bishnu P. Khanal and Sandy Lang for helpful discussion and useful comments on an earlier version of this manuscript.

<sup>1</sup>Corresponding author. E-mail: moritz.knoche@obst.uni-hannover.de.

(lat. 52°14'N, long. 9°49'E). Trees were grafted on 'Gisela 5' rootstocks (*Prunus cerasus* L. × *Prunus canescens* Bois) and grown in a green house. Fruit were harvested at commercial maturity based on color and taste. Because the elastometer experiment was conducted during a 5-d period, fruit were placed in cold storage at 2 °C for up to 5 d. Fruit processed in a given experiment all originated from the same batch.

**THE ELASTOMETER.** Biaxial tensile tests were carried out using an elastometer (Brüggenwirth et al., 2014). In this system, a skin segment is pressurized from its inner side causing the segment to bulge and to increase in surface area. A brass washer (12-mm inner diameter) was glued on one of the two shoulders of a sweet cherry fruit using a cyanoacrylate adhesive (Loctite 406; Henkel/Loctite Deutschland, Munich, Germany). An ES with a maximum thickness of  $2.4 \pm 0.02$  mm was excised by cutting underneath the washer. Using this procedure, the in vivo strain of the skin was maintained until it was desired to increase it (Knoche and Peschel, 2006). The ES obtained in the washer comprised cuticle, epidermis, hypodermis, and adhering flesh cells (Brüggenwirth et al., 2014). The washer with the ES was mounted on the elastometer. The cuticle faced outward and the cut flesh surface was in contact with the silicone oil in the chamber. The ES was strained by pressurizing the silicone oil. This was achieved by driving a motorized piston into the chamber of the elastometer causing the ES in the washer to bulge outward. The pressure inside the chamber was recorded using a pressure transducer (type 40PC100G; Honeywell Intl., Morristown, NY) and the extent of bulging of the ES was recorded using a displacement transducer (KAP-S/5N; AST Angewandte System Technik, Wolnzach, Germany). The effect of  $t_{\text{fracture}}$  was studied by varying the  $p_{\text{rate}}$ . The  $p_{\text{rate}}$  was set at 0.001, 0.006, 0.04, 0.2, or 1 kPa·s<sup>-1</sup> and maintained to the point of ES failure. The low  $p_{\text{rate}}$  required testing times up to 18 h for an individual ES and minor modifications of the sealing procedure to ensure the absence of even small leaks. The pressure at failure is referred to as the  $p_{\text{fracture}}$  (kilopascals) the strain at  $p_{\text{fracture}}$  as the  $\epsilon_{\text{fracture}}$  (square millimeters per square millimeter). The strain ( $\epsilon$ ) was estimated from the change in surface area [ $\Delta A$  (square millimeters)] relative to the initial surface area of the ES [ $A_0$  (square millimeters)] and is given in Eq. [1].

$$\epsilon = \frac{\Delta A}{A_0} \quad [1]$$

Varying  $p_{\text{rate}}$  caused corresponding variation in the rate of strain that is the increase in strain per unit time ( $\epsilon_{\text{rate}}$ ). The modulus of elasticity [ $E$  (megapascals)] was calculated from the height of the ES [ $h$  (millimeters)], the radius of the washer orifice [ $r$  (millimeters)], the pressure [ $p$  (kilopascals)], and the thickness of the load-bearing layer [ $t$  (millimeters)] in Eq. [2] (Brüggenwirth et al., 2014).

$$E = \frac{p \times r^2 \times (r^2 + h^2)}{h^3 \times t \times 2} \quad [2]$$

Thickness of the load-bearing layer was assumed to be 0.1 mm (Brüggenwirth and Knoche, 2016b). The experiment was conducted at 22 °C. The number of replicates was 10.

**WATER UPTAKE AND CRACKING ASSAY.** Water uptake and cracking were quantified on fruit taken from the same batch used for the biaxial tensile tests. Uptake was restricted to the fruit surface by cutting the pedicel flush with the receptacle and

by sealing the stem/fruit junction (the receptacle and the cut end of the pedicel) using epoxy glue (UHU plus schnellfest; UHU, Bühl/Baden, Germany). Water uptake was determined gravimetrically by immersing fruit in deionized water and weighing them 0, 0.75, and 1.5 h after immersion ( $n = 15$ ). Before each weighing, a fruit was blotted dry using soft tissue paper. Cracking was quantified using a modified cracking assay as described by Verner and Blodgett (1931) and Christensen (1996). Two samples of 25 fruit each were immersed in deionized water, removed from solution at 2, 4, 6, 10, and 24 h after incubation and inspected for macroscopically visible cracks. For cracked fruit incubation was discontinued, non-cracked fruit was reincubated.

**MICROSCOPY.** The mode of fracture was investigated in 'Regina' only. Fruit was subjected to a biaxial tensile test in the elastometer and to the immersion assay as described above. The  $p_{\text{rate}}$  were set at 0.001 and 1 kPa·s<sup>-1</sup>. Following fracture, skin sections were prepared by excising tissue from one side of a crack using a razor blade. The sections were transferred to microscope slides and were viewed in incident light at  $\times 250$  (Axioplan; Carl Zeiss Microscopy, Jena, Germany). The fracture mode was quantified by counting the number of epidermal cells where fracture occurred along the anticlinal cell walls and expressing this number as a percentage of the total number of epidermal cells adjacent to the crack. For each treatment one crack per fruit on a total of 10 fruit per treatment were examined.

**DATA ANALYSIS.** Occasionally, ES fractured at the edge of the orifice during biaxial tensile tests. Because of possible artifacts during mounting these ES were excluded from the analyses (Brüggenwirth et al., 2014). The data were subjected to analysis of variance. Percentage data were arcsine transformed before. Means were compared using Tukey's studentized range test [ $P < 0.05$  (packet multcomp 1.2–12, procedure glht, R 2.13.1; R Foundation for Statistical Computing, Vienna, Austria)]. Significance of the coefficient of determination ( $r^2$ ) at the 0.05, 0.01, and 0.001  $P$  levels is indicated by \*, \*\*, and \*\*\*, respectively. Except for Fig. 1A where representative traces are shown, data are presented as means  $\pm$  SE.

## Results

Varying  $p_{\text{rate}}$  in the elastometer yielded linear pressure/time relationships similar to the example in Fig. 1A, where in each, the slope of the line equals the  $p_{\text{rate}}$ . The arrows indicate the pressure and time of fracture. The  $t_{\text{fracture}}$  was inversely related to  $p_{\text{rate}}$  as indicated by the linear relationship of a log-log plot of time vs. rate [ $\log \text{time (h)} = -0.92 (\pm 0.014) \times \log \text{rate (kPa} \cdot \text{s}^{-1}) - 1.57 (\pm 0.025)$ ;  $r^2 = 0.99^{***}$  (Fig. 1A, inset)].

The stiffness of the ES as indexed by the  $E$  increased as  $t_{\text{fracture}}$  increased (Fig. 1B). In contrast, the  $p_{\text{fracture}}$  and  $\epsilon_{\text{fracture}}$  decreased at longer values of  $t_{\text{fracture}}$  indicating that failures occurred at lower pressures and lower strains when tests were carried out over more extended periods of  $t_{\text{fracture}}$  and, hence, over lower values of  $p_{\text{rate}}$  (Fig. 1C and D). Relationships of mechanical properties with  $t_{\text{fracture}}$  were log linear (Fig. 1B–D, insets). Hence, most changes in  $E$ ,  $p_{\text{fracture}}$ , and  $\epsilon_{\text{fracture}}$  occurred for values of  $t_{\text{fracture}}$  less than 3 h, with little change in these parameters thereafter.

The time course of water uptake by submerged fruit was linear, at a constant rate of uptake of 29.7 mg·h<sup>-1</sup> (Fig. 2, inset). For an average fruit of mass 13.1 g, assuming a spherical shape

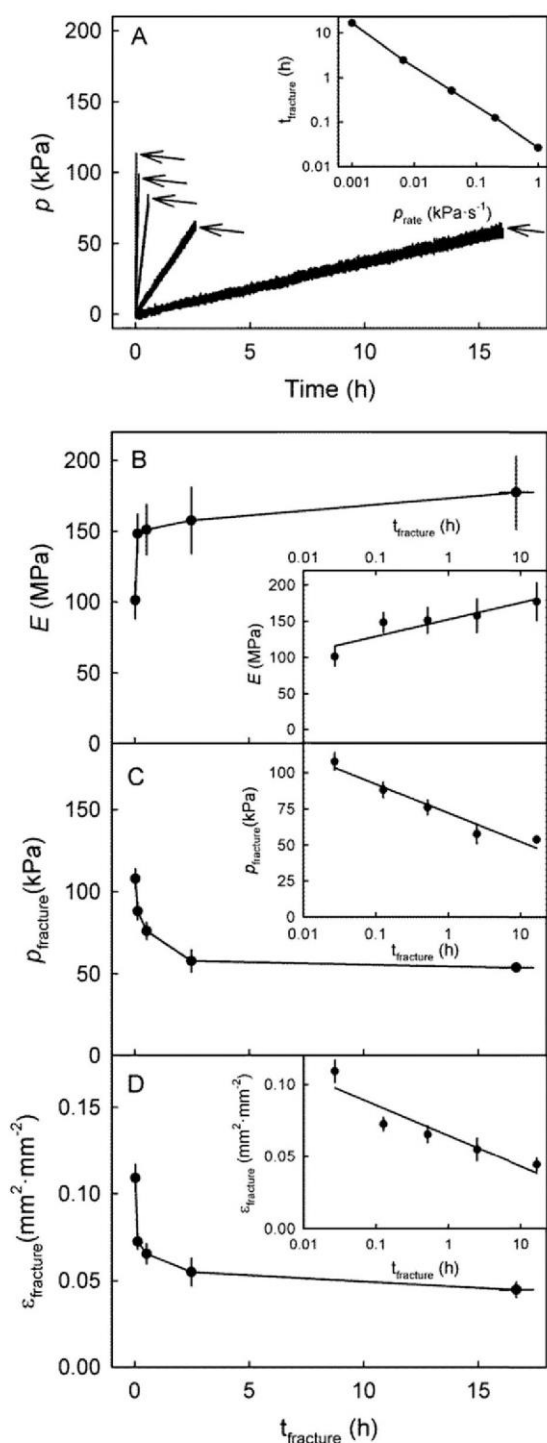


Fig. 1. Effect of time to fracture ( $t_{\text{fracture}}$ ) of the 'Sweetheart' sweet cherry fruit skin on the mechanical properties. The fruit skin was strained by pressurizing the segments from the inner side. (A) Representative traces of pressure vs. time relationships for different rates of increase in pressure ( $p_{\text{rate}}$ ). Arrows indicate the point of fracture. Inset: relationship between  $t_{\text{fracture}}$  and  $p_{\text{rate}}$ . (B–D) Effect of  $t_{\text{fracture}}$  on the (B) modulus of elasticity ( $E$ ), (C) pressure at fracture  $p_{\text{fracture}}$ , and the (D) strain at fracture  $\epsilon_{\text{fracture}}$ . Insets B to D: relationships between  $E$ ,  $p_{\text{fracture}}$ , or  $\epsilon_{\text{fracture}}$  and  $t_{\text{fracture}}$  redrawn on a log scale. Data in B to D represent means  $\pm$  SE ( $n = 10$ ).

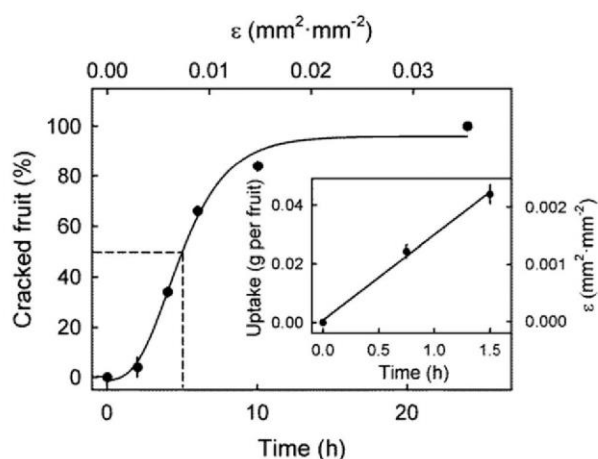


Fig. 2. Time course of cracking (main graph) and of water uptake (inset) in 'Sweetheart' sweet cherry fruit immersed in water. Dashed lines indicate times and cracking levels when 50% of the fruit were cracked. The second x axis gives the corresponding strain ( $\epsilon$ ) of the fruit skin, calculated from cumulative water uptake and fruit mass assuming the fruit to be a sphere and having a density of  $1 \text{ kg}\cdot\text{L}^{-1}$ .

and a density of  $1 \text{ kg}\cdot\text{dm}^{-3}$ , the cumulative water uptake of  $44.6 \pm 2.2 \text{ mg}$  after 1.5 h corresponds to a strain of  $0.002 \text{ mm}^2\cdot\text{mm}^{-2}$ . The percentage of cracked fruit increased in a sigmoidal pattern with time and with strain. The  $t_{\text{fracture}}$  for 50% cracking was calculated at 5.17 h and the corresponding  $\epsilon_{\text{fracture}}$  was calculated at  $0.008 \text{ mm}^2\cdot\text{mm}^{-2}$  (Table 1). Compared with biaxial tensile tests carried out at a similar  $\epsilon_{\text{rate}}$  of the ES, the  $t_{\text{fracture}}$  as measured by water uptake was only about one-third of that in the biaxial tensile tests, and the  $\epsilon_{\text{fracture}}$  was only about one-fifth of it (Table 1).

Comparing low ( $0.001 \text{ kPa}\cdot\text{s}^{-1}$ ) and high  $p_{\text{rate}}$  ( $1 \text{ kPa}\cdot\text{s}^{-1}$ ) in the elastometer and data from the classical immersion assay in 'Regina' revealed that the mode of fracture differed between treatments. The percentage of epidermal cells that fractured along their anticlinal cell walls was highest in the immersion assay ( $94.1\% \pm 0.6\%$ ) followed by the low ( $75.3\% \pm 4.7\%$ ) and the high  $p_{\text{rate}}$  ( $57.3\% \pm 5.5\%$ ). These differences were statistically significant.

## Discussion

Our study produced two new and important findings: 1) A longer  $t_{\text{fracture}}$  results in a higher value of  $E$  (stiffer) but in lower values of  $p_{\text{fracture}}$  and  $\epsilon_{\text{fracture}}$  (weaker) and a higher percentage of epidermal cells fracturing along rather than across their anticlinal cell walls and 2) the  $\epsilon_{\text{fracture}}$  in a biaxial tensile test carried out at comparable values of  $\epsilon_{\text{rate}}$  remains markedly higher than that estimated from an immersion assay.

**EFFECT OF TIME TO FRACTURE IN BIAxIAL TENSILE TESTS.** The mechanical properties of the ES were clearly affected by the  $t_{\text{fracture}}$ . Several explanations may be offered. First, most biological materials exhibit viscoelastic properties in their stress/strain relationships (Niklas, 1992). This includes fruit skins (Brüggenwirth et al., 2014; Hankinson et al., 1977) and fruit cuticles (Lopez-Casado et al., 2010; Matas et al., 2004; Petracek and Bukovac, 1995). In polymer science, viscoelasticity

Table 1. Comparison of mechanical properties of ‘Sweetheart’ sweet cherry fruit skin established in biaxial tensile tests at two different rates of increase in pressure and hence of strain vs. immersion assays of whole fruit. Mechanical properties were indexed by the time to fracture ( $t_{\text{fracture}}$ ) and the strain at fracture ( $\epsilon_{\text{fracture}}$ ). For the immersion assay, strain rates ( $\epsilon_{\text{rate}}$ ) were calculated from water uptake rates into the fruit. The  $\epsilon_{\text{rate}}$  in biaxial tensile tests was measured from the increase in surface area associated with the rate of increase in pressure ( $p_{\text{rate}}$ ).

Treatment	$p_{\text{rate}}$ (kPa·s <sup>-1</sup> )	$\epsilon_{\text{rate}}$ (mm <sup>2</sup> ·mm <sup>-2</sup> ·h <sup>-1</sup> )	Mean ± SE	
			$t_{\text{fracture}}$ (h)	$\epsilon_{\text{fracture}}$ (mm <sup>2</sup> ·mm <sup>-2</sup> )
Biaxial tensile test	1	4.0875 ± 0.0000 a <sup>z</sup>	0.027 ± 0.002 c <sup>z</sup>	0.109 ± 0.008 a <sup>z</sup>
Biaxial tensile test	0.001	0.0025 ± 0.0006 b	16.68 ± 0.743 a	0.041 ± 0.004 b
Immersion assay	–	0.0015 ± 0.0004 b	5.17 ± 0.385 b	0.008 ± 0.001 c

<sup>z</sup>Mean separation by Tukey’s studentized range test at  $P < 0.05$ .

is described in analogical terms using rheological models comprising springs and dash pots arranged in series (Maxwell model), in parallel (Voigt–Kelvin model) or in combinations of both arrangements [Burgers model (Schmiedel, 1992)]. When subjected to a tensile force, stress/strain relationships are obtained that depend on the rate at which the force is applied. In sweet cherry fruit, epidermal and hypodermal cell layers, and not the cuticle, represent the load-bearing structure (Brüggenwirth et al., 2014). Furthermore, the plasma membrane restricts the movement of water as indicated by a decrease in skin stiffness after eliminating cell turgor (Brüggenwirth and Knoche, 2016b). Thus, mechanical properties of the fruit skin reflect those of the cell walls both from a material (composition) and a structural (cells with restricted water movement) point of view (Brüggenwirth and Knoche, 2016b). Therefore, applying the above analogy to cell walls of the sweet cherry skin, it may be speculated that the cellulose represents the spring, whereas the viscous pectins of the middle lamellae and the cellular structure (due to the restricted water movement) represent the dash pot (Vincent, 1990). Consequently, at a high  $\epsilon_{\text{rate}}$  we would expect the cellulose to be stressed and strained, whereas at low  $\epsilon_{\text{rate}}$  the middle lamella is strained and water movement from symplast into the apoplast is induced. This hypothesis would explain why varying  $t_{\text{fracture}}$  resulted in different stiffness,  $p_{\text{fracture}}$  and  $\epsilon_{\text{fracture}}$ . In addition, this explanation would also account for the observed differences in failure mode where a higher percentage of epidermal cells failed along their anticlinal cell walls at the lower  $p_{\text{rate}}$ . That the mode of failure of tissue may be affected by other factors such as turgor is not unusual as De Belie et al. (2000) demonstrated for mechanical properties of pear parenchyma.

Second, formation of cracks may depend on time. For a short  $t_{\text{fracture}}$  a crack may initiate rapidly at low pressure but crack extension and complete failure may require more time and thus, occurs later when the pressure is already higher. This argument would account for the effect of  $t_{\text{fracture}}$  in the biaxial tests; i.e., the linear relationship on the log scale between mechanical properties and  $t_{\text{fracture}}$ . Also, the difference between the biaxial tensile test and the immersion assay may be accounted for by the above argument.

**TENSILE TEST VS. IMMERSION ASSAY.** The calculated  $\epsilon_{\text{fracture}}$  and  $t_{\text{fracture}}$  (Table 1) in the immersion assay are of the same order of magnitude as those of earlier studies (Christensen, 1996; Winkler et al., 2015). However, comparison of biaxial tensile tests for long  $t_{\text{fracture}}$  with the immersion assay, reveals that the  $\epsilon_{\text{fracture}}$  still remains higher in the tensile test. This effect was not unique for off-season ‘Sweetheart’, but could be reproduced with freshly harvested ‘Regina’. The difference in

$\epsilon_{\text{fracture}}$  may be explained by one or several of the following factors. First, the effect of water uptake somehow extends beyond its effect on the strain of the skin that is caused by the volume increase of the fruit. For this to happen, the water taken up directly or indirectly must somehow affect the cell walls causing the mode of fracture to change. For example, an indirect effect could be the bursting of individual epidermal cells that would result in leakage of malic acid into the cell-wall space. Malic acid, in turn,

has been shown to increase the permeability of the plasma membrane and to further weaken cell walls (Winkler et al., 2015). This could result in the spreading of a defect similar to a “zipper” or to a “ladder” in a piece of knitted fabric. Second, spatial heterogeneity of water uptake may lead to localized strains that exceed the average strain calculated on the basis of whole-fruit water uptake. This could result in local  $\epsilon_{\text{fracture}}$  values, comparable to those of the biaxial tensile tests, whereas the mean values calculated on a whole-fruit basis would be much lower. However, there is no indication that preferential sites of water uptake are involved. In the immersion assays, water uptake was restricted to the fruit surface by sealing the pedicel junction with silicone rubber (Beyer et al., 2002). Third, fruit in the immersion assay usually cracked in the styler scar region, whereas the ES in the biaxial tensile test was excised from the shoulders of the fruit. However, there was no difference in the mechanical properties between the shoulder and the styler scar in earlier studies making the above argument less likely (Brüggenwirth and Knoche, 2016b). Fourth, an artifact caused by silicone oil permeating the tissue and weakening the cell wall in the elastometer is unlikely. When establishing the biaxial tensile test, we pressurized cell walls using water and silicone oil and found no significant difference between the two at the standard  $p_{\text{rate}}$ . However, to avoid artefacts due to cell bursting in water during longer exposure times, silicone oil was used as a standard. Finally, it may be visualized that water uptake into epidermal cells increased cell turgor in fruit in the immersion assay. To our knowledge, there is no supporting evidence for this hypothesis in the literature. Cell pressure probe (CPP) techniques are too coarse to puncture the small epidermal cells and obtain direct measurements of turgor. In our earlier study, we found no effect of water uptake on cell turgor of mesocarp cells as determined by CPP (Knoche et al., 2014). At present, the mechanistic basis for the difference in mechanical properties is not known.

## Conclusions

The data demonstrate that  $t_{\text{fracture}}$  affects the mechanical properties and the mode of fracture recorded for the ES. Part of the difference in  $\epsilon_{\text{fracture}}$  between the biaxial tensile tests and the immersions assays is accounted for by the difference in  $t_{\text{fracture}}$ . However, some discrepancies remain, indicating that the volume increase caused by water uptake is not the only factor involved. Apparently, water uptake affects the ES in other ways, which lead to failure at lower  $\epsilon_{\text{fracture}}$  than predicted based on biaxial tensile tests. In addition, a higher percentage of fracture of epidermal cells along their anticlinal cell walls is

observed in the immersion assay. The mechanistic basis of both effects is unknown. Because the mechanical properties of the ES are determined primarily by the cell walls (Brüggenwirth and Knoche, 2016b), further studies should focus on the interaction between water uptake and the mechanical behavior of the cell wall.

#### Literature Cited

- Bargel, H., H.C. Spatz, T. Speck, and C. Neinhuis. 2004. Two-dimensional tension tests in plant biomechanics: Sweet cherry fruit skin as a model system. *Plant Biol.* 6:432–439.
- Beyer, M., S. Peschel, M. Knoche, and M. Knörger. 2002. Studies on water transport through the sweet cherry fruit surface: IV. Regions of preferential uptake. *HortScience* 37:637–641.
- Brüggenwirth, M., H. Fricke, and M. Knoche. 2014. Biaxial tensile tests identify epidermis and hypodermis as the main structural elements of sweet cherry skin. *Ann. Bot. Plants* 6:plu019.
- Brüggenwirth, M. and M. Knoche. 2016a. Factors affecting mechanical properties of the skin of sweet cherry fruit. *J. Amer. Soc. Hort. Sci.* 141:45–53.
- Brüggenwirth, M. and M. Knoche. 2016b. Mechanical properties of skin of sweet cherry fruit of differing susceptibilities to cracking. *J. Amer. Soc. Hort. Sci.* 141:162–168.
- Christensen, J.V. 1996. Rain-induced cracking of sweet cherries. Its causes and prevention, p. 297–327. In: A.D. Webster and N.E. Looney (eds.). *Cherries*. CAB Intl., Wallingford, UK.
- De Belie, N., I.C. Hallett, F.R. Harker, and J. De Baerdemaeker. 2000. Influence of ripening and turgor on the tensile properties of pears: A microscopic study of cellular and tissue changes. *J. Amer. Soc. Hort. Sci.* 125:350–356.
- Hankinson, B., V.N.M. Rao, and C.J.B. Smit. 1977. Viscoelastic and histological properties of grape skins. *J. Food Sci.* 42:632–635.
- Knoche, M., E. Grimm, and H.J. Schlegel. 2014. Mature sweet cherries have low turgor. *J. Amer. Soc. Hort. Sci.* 139:3–12.
- Knoche, M. and S. Peschel. 2006. Water on the surface aggravates microscopic cracking of the sweet cherry fruit cuticle. *J. Amer. Soc. Hort. Sci.* 131:192–200.
- Lopez-Casado, G., A. Salamanca, and A. Heredia. 2010. Viscoelastic nature of isolated tomato (*Solanum lycopersicum*) fruit cuticles: A mathematical model. *Physiol. Plant.* 140:79–88.
- Matas, A.J., E.D. Cobb, J.A. Bartsch, D.J. Paolillo, and K.J. Niklas. 2004. Biomechanics and anatomy of *Lycopersicum esculentum* fruit peels and enzyme-treated samples. *Amer. J. Bot.* 91:352–360.
- Niklas, K.J. 1992. *Plant biomechanics: An engineering approach to plant form and function*. Univ. Chicago Press, Chicago, IL.
- Petracek, P.D. and M.J. Bukovac. 1995. Rheological properties of enzymatically isolated tomato fruit cuticle. *Plant Physiol.* 109:675–679.
- Schmiedel, H. 1992. *Handbuch der Kunststoffprüfung*. Hanser, Munich, Germany.
- Schumann, C., H.J. Schlegel, E. Grimm, M. Knoche, and A. Lang. 2014. Water potential and its components in developing sweet cherry. *J. Amer. Soc. Hort. Sci.* 139:349–355.
- Verner, L. and E.C. Blodgett. 1931. Physiological studies of the cracking of sweet cherries. *Univ. Idaho Agr. Expt Sta. Bul. No.* 184.
- Vincent, J.F.V. 1990. Fracture properties of plants. *Adv. Bot. Res.* 17:235–287.
- Winkler, A., M. Ossenbrink, and M. Knoche. 2015. Malic acid promotes cracking of sweet cherry fruit. *J. Amer. Soc. Hort. Sci.* 140:280–287.

## **8. Cell wall swelling, fracture mode, and mechanical properties of the sweet cherry fruit skin are closely related**

Dieser Artikel wurde im Original 2016 in der Zeitschrift „Journal of the American Society for Horticultural Science“ online veröffentlicht:

Brüggenwirth, M. und Knoche, M. (2016d) Cell wall swelling, fracture mode, and the mechanical properties of cherry skins are closely related. *Planta* doi: 10.1007/s00425-016-2639-7.



# Cell wall swelling, fracture mode, and the mechanical properties of cherry fruit skins are closely related

Martin Brüggewirth<sup>1</sup> · Moritz Knoche<sup>1</sup>Received: 28 September 2016 / Accepted: 9 December 2016  
© Springer-Verlag Berlin Heidelberg 2016

## Abstract

**Main conclusion** Cell wall swelling, fracture mode (along the middle lamellae vs. across cell walls), stiffness, and pressure at fracture of the sweet cherry fruit skin are closely related.

Skin cracking is a common phenomenon in many crops bearing fleshy fruit. The objectives were to investigate relationships between the mode of fracture, the extent of cell wall swelling, and the mechanical properties of the fruit skin using sweet cherry (*Prunus avium*) as a model. Cracking was induced by incubating whole fruit in deionised water or by fracturing exocarp segments (ESs) in biaxial tensile tests. The fracture mode of epidermal cells was investigated by light microscopy. In biaxial tensile tests, the anticlinal cell walls of the ES fractured predominantly *across* the cell walls (rather than *along*) and showed no cell wall swelling. In contrast, fruit incubated in water fractured predominantly *along* the anticlinal epidermal cell walls and the cell walls were swollen. Swelling of cell walls also occurred when ESs were incubated in malic acid, in hypertonic solutions of sucrose, or in water. Compared to the untreated controls, these treatments resulted in more frequent fractures *along* the cell walls, lower pressures at fracture ( $p_{\text{fracture}}$ ), and lower moduli of elasticity ( $E$ , i.e., less stiff). Conversely, compared to the untreated controls, incubating the ES in  $\text{CaCl}_2$  and in high concentrations of ethanol resulted in thinner cell walls, in less frequent fractures *along* the cell walls, higher  $E$  and  $p_{\text{fracture}}$ . Our study demonstrates that fracture mode, stiffness,

and pressure at fracture are closely related to cell wall swelling. A number of other factors, including cultivar, ripening stage, turgor,  $\text{CaCl}_2$ , and malic acid, exert their effects only indirectly, i.e., by affecting cell wall swelling.

**Keywords** Biaxial tensile test · Cracking · Epidermis · Modulus of elasticity · *Prunus avium*

## Abbreviation

ES	Exocarp segments
$E$	Modulus of elasticity
$p_{\text{fracture}}$	Pressure at fracture
$\varepsilon_{\text{fracture}}$	Strain at fracture

## Introduction

Rain cracking is a common phenomenon in a large number of fruit crops—especially of species that bear soft, fleshy fruit. Sweet cherry (*Prunus avium*) is a prominent example of this, where cracking limits the production in all areas which experience rainfall during the fruit-ripening season (Christensen 1996). The close relationship between rainfall and fruit cracking has long been recognised (von Wetzausen 1819). This correlation led to the plausible hypothesis that cracking is caused by excessive water uptake by the fruit. The most popular explanation of rain cracking is based on the simple idea that rainwater is taken up into the fruit by osmosis. This causes the fruit's volume to increase and thus its skin to be stretched (Considine and Kriedemann 1972; Considine and Brown 1981). Then, so the explanation goes, when the skin is stretched beyond some upper limit of extensibility, it tears open.

Today, some 30 or 40 years later, surprisingly little further information is available on the mechanism of fruit

✉ Moritz Knoche  
moritz.knoche@obst.uni-hannover.de

<sup>1</sup> Institute for Horticultural Production Systems, Leibniz-University Hannover, Herrenhäuser Straße 2, 30419 Hannover, Germany

skin failure. This is despite the enormous economic importance of rain cracking to the cherry industry and also to a large number of other fruit-growing industries producing rain cracking susceptible fruits, including grapes (*Vitis vinifera*) and tomatoes (*Solanum lycopersicum*).

In sweet cherry, the epidermis and underlying hypodermal cell layers represent the load-bearing structure of the skin (Brüggenwirth et al. 2014; Brüggenwirth and Knoche 2016a, b, c). In principle, fracture of these layers may occur in one or the other of two distinct modes: (1) separation of adjacent cells *along* the middle lamellae (fracture is *along* cell walls, fracture mode *along*) or (2) by rupture of cells walls (fracture is *across* the cell walls, fracture mode *across*; Niklas 1992). The first of these fractures *along* cell walls is likely indicative of pectin degradation in the middle lamellae, possibly as a result of softening during ripening, while the cellulose and matrix glucans of the cell walls are not necessarily affected (Brummell 2006). In the second mode, if the strength of cell to cell adhesion exceeds the strength of the cell walls themselves, then fracture will likely occur *across* the cell walls.

Softening is a characteristic of the fruit-ripening process, and increased activity of pectinases has been reported in sweet cherry fruit as early as 30 days after full bloom (Barrett and Gonzalez 1994; Kondo and Danjo 2001). Also, fruit cell walls often swell during ripening, and swelling is accompanied by fruit softening (Redgwell et al. 1997a). Swelling of cell walls also occurs in sweet cherry fruit when epidermal cells plasmolyse and turgor decreases (Grimm and Knoche 2015). Furthermore, swelling of cell walls (isolated) and cracking susceptibility have both been reported to increase during the course of fruit development (Christensen 1996; Redgwell et al. 1997a). However, to our knowledge, relationships between cell wall swelling, fracture mode and the mechanical properties of the fruit skin have not been investigated. That fracture mode and fruit firmness of parenchyma tissue may be related has been demonstrated in pear (De Belie et al. 2000). Thus, when firmness is high, cells rupture *across* cell walls, but when firmness is low they rupture *along* the middle lamellae (De Belie et al. 2000). Also, strong cell to cell adhesion results in fracture *across* cell walls in apple flesh, whereas the cells separate *along* the middle lamellae when cell to cell adhesion is weak (Ng et al. 2013).

Using sweet cherry as a model, the objectives of this study were to investigate whether there are relations between: (1) the mode of fracture of the fruit skin, (2) the swelling of the cell walls, and (3) the mechanical properties of the fruit skin. We employ a biaxial tensile test first described by Bargel et al. (2004) to quantify the mechanical properties of the fruit skin.

## Materials and methods

### Plant material

Fruit of seven cultivars of sweet cherry ‘Adriana’, ‘Burlat’, ‘Early Korvic’, ‘Hedelfinger’, ‘Merchant’, ‘Regina’, ‘Sam’, and ‘Samba’ and one cultivar of sour cherry (*Prunus cerasus*) ‘Morellenfeuer’ were obtained from field-grown or glasshouse-grown trees at the Horticultural Research Station of the Leibniz University in Ruthe (lat. 52°14’N, long. 9°49’E). Sweet cherry cultivars were grafted on Gisela 5 rootstocks (*Prunus cerasus* × *P. canescens*), the sour cherry on ‘Maxma Delbard’ rootstock (*P. avium* × *P. mahaleb*). Fruit used in the experiments were free from visual defects, uniform in size, and processed on the day of sampling. Unless otherwise stated, fruit were used at commercial maturity based on size and colour.

### Immersion assay

Fruit was induced to crack by incubation in deionised water (Christensen 1996). Two samples of 25 fruit each were prepared as follows. The receptacle, stem/fruit junction and the cut pedicel end were sealed with silicone rubber (3140 RTV Coating; Dow Corning, Midland, MI, USA). After curing for at least 2 h, fruit were incubated in deionised water. At regular intervals, fruits were removed from the water and individually inspected for macroscopic cracks.

### Elastometer

Biaxial tensile tests were carried out on exocarp segments (ESs) using an elastometer and the procedure described by Brüggenwirth et al. (2014). Briefly, a brass washer (12 mm i.d.) was mounted on one of the two shoulders of the fruit using a cyanoacrylate adhesive (Loctite 406; Henkel/Loctite Deutschland, Munich, Germany). After curing, an ES was excised by cutting underneath the washer using a razor blade. This technique produced an ES with a maximum thickness of  $2.4 \pm 0.02$  mm where the *in vivo* strain of the skin was maintained (Knoche and Peschel 2006; Brüggenwirth et al. 2014). The ES comprised cuticle, epidermis, hypodermis, and some adhering mesocarp (flesh) tissue. The ES was then mounted on the elastometer with the cuticle facing outwards. The inner (cut) surface was in contact with silicone oil (Wacker AK10, Wacker Chemie, Munich, Germany). Pressure was applied to the inner side of the ES by displacing the silicone oil using a motorised piston. This caused the ES to bulge outwards. The oil pressure and the extent of bulging were measured using a pressure transducer (Type 40PC100G, Honeywell International, Morristown, NY, USA) and a displacement



transducer (KAP-S/5N; AST Angewandte System Technik, Wolnzach, Germany). Pressure was increased up to the point of  $p_{\text{fracture}}$  (kPa). The strain ( $\varepsilon$ ) was calculated from the change in surface area ( $\Delta A$  in  $\text{mm}^2$ ) relative to the initial surface area of the bulging ES ( $A_0$  in  $\text{mm}^2$ ) and is given in Eq. 1.

$$\varepsilon = \frac{\Delta A}{A_0} \quad (1)$$

The strain at  $p_{\text{fracture}}$  is referred to as the fracture strain ( $\varepsilon_{\text{fracture}}$ ;  $\text{mm}^2 \text{mm}^{-2}$ ). The  $E$  (MPa) was estimated from the height of the bulging ES ( $h$ ; mm), the radius of the orifice ( $r$ ; mm), the pressure ( $p$ ; MPa), and the thickness of the load-bearing layer ( $t = 0.1$  mm) in Eq. 2 (Brüggenwirth et al. 2014).

$$E = \frac{p \times r^2 \times (r^2 + h^2)}{h^3 \times t \times 2} \quad (2)$$

Experiments were conducted at 22 °C.

### Determining fracture mode and cell wall thickness

Fracture modes were quantified in cracked fruit following immersion assays and also in fractured skins following biaxial tensile tests. Skin samples were prepared for microscopy by removing tissue from one side of a crack using a sharp razor blade. Because of the uniform curvature, skin was excised from one of the two shoulders of the fruit. The skin segments were mounted on a microscope slide using silicone oil (Wacker AK10; Wacker Chemie). Immersion in oil prevented water uptake and bursting of cells and also evaporative water loss and shrinkage. Samples were viewed at 200 $\times$  or 250 $\times$  using a fluorescence microscope (BX-60; Olympus, Hamburg, Germany; Axioplan; Carl Zeiss Microscopy, Jena, Germany). Calibrated digital images were taken (camera: DP73; Olympus). The fracture mode was quantified by counting the number of epidermal cells that fractured *along* their anticlinal cell walls and expressing this as a percentage of the total number of epidermal cells adjacent to the crack (i.e. those fracturing *along* the cell walls + those fracturing *across* the cell walls). For each treatment, one crack per fruit on a total of ten fruit was investigated. This procedure meant that a total of 250–350 epidermal cells were inspected for fracture mode per treatment.

Cell wall thickness was quantified on a separate set of images taken from the same samples at 400 $\times$  (BX-60; Olympus) or 500 $\times$  (Axioplan; Carl Zeiss Microscopy). Cell wall thickness was measured at the thinnest point of the cell wall between two adjacent cells using image analysis software (Cell-P; Olympus Soft Imaging Solution,

Münster, Germany). Thus, our thickness data represent the thickness of the two primary cell walls including the middle lamellae between two neighbouring cells.

### Experiments

Fracture mode, cell wall thickness and mechanical properties were investigated for all sweet cherry cultivars except ‘Early Korvic’ and for one sour cherry cultivar (see above).

Relationships between the final stage of development, fracture mode, cell wall thickness, and mechanical properties of the skin were studied in ‘Regina’. The stage of development was indexed by the change in colour from an immature, inedible pale red ( $27.7 \pm 0.6^\circ$  Hue, mass  $10.2 \pm 0.4$  g) to an edible, dark-red fruit ( $11.9 \pm 0.9^\circ$  Hue, mass  $10.5 \pm 0.3$  g). Colour is a good indicator of ripening sweet cherry (Hansen 2011; Brüggenwirth and Knoche 2016a). It is closely related to sugar content, whereas changes in mass or firmness or relationships with time after full bloom are often variable. For the fruit used in our experiments, the relationship between osmolarity and colour was:  $\text{osmolarity (mmol kg}^{-1}\text{)} = -18.37 (\pm 2.0) \times \text{hue angle (}^\circ\text{)} + 1478 (\pm 39.5)$ ;  $r^2 = 0.80^{***}$ . Colour was quantified using the CIE 1976  $L^*$ ,  $a^*$ ,  $b^*$  scale (CR-200 chromameter; Minolta, Osaka, Japan), and the hue angle was calculated (McGuire 1992). The fruit skin was induced to crack either by incubating whole fruit in water or by straining the ES samples in the elastometer. Fracture mode and cell wall thickness were quantified as described above.

The effect of turgor on the mechanical properties in biaxial tensile tests, the fracture mode, and the cell wall thickness of ES was studied in ‘Regina’ and ‘Early Korvic’. Turgor was varied by incubating the ES for 14 h in a series of sucrose solutions of increasing osmolarity (0, 1, 2.5, 4, and 5 MPa equivalent to 0, 0.4, 0.8, 1.1, and 1.3 M) and in aqueous ethanol at concentrations of 0, 25, 50, 75, and 100% (v/v). After incubation mechanical properties, fracture mode and cell wall thickness were determined.

The effects of malic acid and  $\text{CaCl}_2$  on the mechanical properties, fracture mode, and cell wall thickness were studied in ‘Regina’. The ESs were incubated for 14 h in 70 mM malic acid or 100 mM  $\text{CaCl}_2$ , removed from the solution, blotted, and then tested in the elastometer. The malic acid concentration is equivalent to that found in sweet cherry (Herrmann 2001). Untreated ES served as controls. Fracture mode and cell wall thickness were determined.

Cell wall thickness was also investigated along cracks induced by incubation of whole fruit in deionised water. Digital images were prepared and cell wall thickness quantified using image analysis in the three zones: ahead of

the crack (zone I), in the zone of the crack tip (zone II), and in the older zone of a crack (zone III).

### Data analyses

Data analyses were restricted to those ES that fractured at the centre of the orifice of the elastometer. Any ESs that fractured at the edge were excluded because of possible artefacts caused by the mounting procedure (Brüggenwirth et al. 2014). The data were subjected to analysis of variance (AOV). Percentage data were arcsine transformed before AOV. Mean comparisons were made using Tukey's Studentized range test ( $P < 0.05$ , packet multcomp 1.2–12, procedure glht, R 2.13.1; R Foundation for Statistical Computing, Vienna, Austria). Regression analyses were carried out with Sigma Plot (version 12.5; Systat Software, San Jose, CA, USA). Significance of the coefficients of determination ( $r^2$ ) at the 0.05, 0.01, and 0.001 probability levels is indicated by \*, \*\*, and \*\*\*, respectively. The data are presented as means  $\pm$  standard errors of means (SE). The number of replicates was ten.

### Results

Fruit subjected to the biaxial tensile tests cracked mostly *across* epidermal cell walls. Cell walls were thinner, and only the fractured cells were colourless (Fig. 1a). In contrast, fruits immersed in water cracked predominantly by fracturing *along* their anticlinal cell walls causing two adjacent cells to separate along the intervening middle lamellae. Cell walls were thick, and all cells were colourless, indicating plasma membranes had ruptured and anthocyanin leakage had occurred (Fig. 1b). Averaged across cultivars, the frequency of fracture *along* epidermal cell walls was 2.1-fold higher in the immersion assays (mean 75.0%, range 47.7–89.6%) than in the biaxial tensile tests (mean 35.4%, range 15.5–59.7%; Table 1).

Plotting frequencies of fracture *along* epidermal cell walls of the same species and cultivar but from two consecutive seasons, one against the other, yielded a highly significant 1:1, linear relationship (slope of  $1.00 \pm 0.01$ ;  $r^2 = 0.99^{***}$ ). This indicates differences in fracture mode among cultivars, and species were highly reproducible between seasons (Fig. 2a). This consistency also held for differences between incubation assays and biaxial tensile tests ( $r^2 = 0.77^{**}$ ; Fig. 2b). Interestingly, the effect of cultivar and that of technique were accounted for by their effects on the thickness of the anticlinal epidermal cell walls. The thicker these cell walls, the more frequently did fracture occur *along* cell walls. This relationship could be

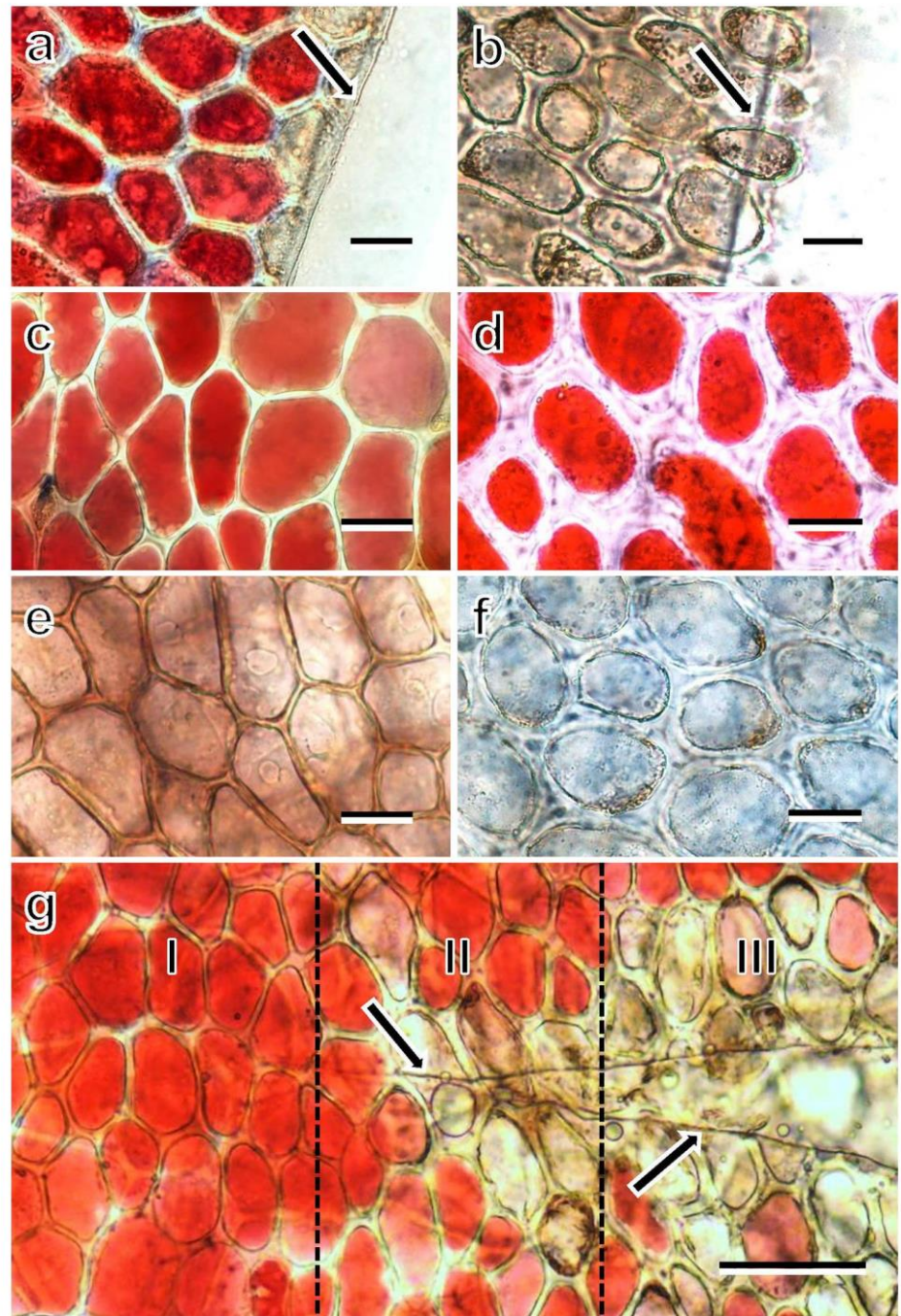
described by the linear regression equation:  $\text{Fracture}_{\text{along}} (\%) = 24.9 (\pm 2.1) \times \text{Thickness} (\mu\text{m}) - 51.2 (\pm 9.8)$ ,  $r^2 = 0.95^{***}$  (Fig. 2c). The sour cherry cultivar 'Morellenfeuer' followed the same relationships as the sweet cherry cultivars (Fig. 2b, c).

Thickness of epidermal cell walls increased during the early stages of ripening (as indexed by the lower hue angle, i.e., darker colour) but then remained constant (Fig. 3a). The fracture mode of the epidermis was again a linear function of cell wall thickness ( $r^2 = 0.97^{**}$ ). Furthermore, during ripening, the stiffness of the fruit skin as indexed by the elastic modulus  $E$  ( $r^2 = 0.80^*$ ) and the strength as indexed by the value of  $p_{\text{fracture}}$  ( $r^2 = 0.99^{***}$ ) both decreased, as cell wall thickness increased (Fig. 3b–d). There was no relationship between the value of  $\varepsilon_{\text{fracture}}$  and the thickness of the cell wall (Fig. 3d, inset).

Immediately after excision, the cell walls of epidermal cells were thin (Fig. 1c). The cell walls thickened when the cells plasmolysed upon incubation in hypertonic sucrose solution (Fig. 1d). The presence of red anthocyanins in the vacuoles indicated that the plasma membranes remained intact. In contrast, ES incubated in aqueous ethanol had thinner cell walls than those in water (Fig. 1e, f). In both treatments, the ESs were discoloured indicating that plasma membranes were damaged and anthocyanins had leaked out (Fig. 1e, f).

In the biaxial tensile tests with ES from the sucrose treatments, increasing osmolarity of the sucrose solutions increased the percentage of cells that fractured *along* cell walls to 90% in the fully plasmolysed stage (Fig. 4a). The only exception to this was in the water control (0 MPa sucrose), where the cells died and the majority of cells separated *along* their cell walls. In the *in vivo* condition, in about 57% of cases, the epidermal cells fractured *along* the cell walls. This is similar to the effects of nearly isotonic sucrose ( $2.8 \pm 0.1$  MPa; Fig. 4a). Increasing the concentration of ethanol in the incubation solution decreased the percentage of epidermal cells fracturing *along* their cell walls. The relationship was linear and described by the equation:  $\text{Fracture}_{\text{along}} (\%) = -0.82 (\pm 0.06) \times \text{ethanol} (\%) + 93.5 (\pm 3.2)$ ,  $r = 0.95^{***}$  (Fig. 4b). Plotting fracture modes determined after incubation in sucrose and ethanol vs cell wall thickness revealed a common, linear and highly significant relationship despite the quite unrelated treatments (Fig. 4c). There was a weak negative relationship between the modulus  $E$  and cell wall thickness which was mostly due to the high and variable  $E$  at low cell wall thickness (Fig. 4d). The value of  $p_{\text{fracture}}$  decreased consistently as cell wall thickness increased (Fig. 4e). However, the value of  $\varepsilon_{\text{fracture}}$  did not depend on cell wall thickness (Fig. 4f).

**Fig. 1** **a, b** Light microscope view of crack in the fruit skin subjected to a biaxial tensile test in the elastometer (**a**) or induced by immersing fruit in deionized water (**b, g**). **c–f** Changes in thickness of anticlinal epidermal cell walls of sweet cherry immediately after excision (**c**, control), after incubating in hypertonic sucrose solution (**d**), in 75% aqueous ethanol (**e**), and in deionized water (**f**). Cell walls are non-swollen in **a, c, e**, but swollen in **b, d, f**. Fruit was incubated for 14 h. **g** Detailed view of crack in fruit skin. Zone I represents an intact area of skin ahead of a crack. Zone II shows the crack tip as indexed by the ruptured cuticle. Zone III demonstrates older region along a crack. Along the crack, cell wall swelling increased and the fraction of dead cells increased. *Arrows in a, b, and g indicate edge of crack in cuticle. Bars 25  $\mu\text{m}$  (a–f) and 100  $\mu\text{m}$  (g)*



Incubation in malic acid caused cell walls to swell and resulted in more fractures *along* the cell wall, higher values of  $\epsilon_{\text{fracture}}$ , and lower values of  $E$  and of  $p_{\text{fracture}}$  compared to the control. In contrast, incubating ES in  $\text{CaCl}_2$  resulted in thinner cell walls, less frequent fracture *along* cell walls, and lower value for  $\epsilon_{\text{fracture}}$ . Also, the values of both  $E$  and  $p_{\text{fracture}}$  were higher than in the untreated control (Table 2).

Pooling data from all experiments confirmed the linear and highly significant relationships for the epidermal cells between: fracture mode, cell wall thickness, and the mechanical properties  $E$  and  $p_{\text{fracture}}$  (Fig. 5a–c). From the regression equations describing these relationships, the following predictions may be made. For an extrapolated cell wall thickness of about 8  $\mu\text{m}$ , fracture is expected to

**Table 1** Fracture mode of anticlinal epidermal cell walls of sweet cherry fruit in immersion and tensile tests as affected by cultivar

Cultivar	Fracture <sub>along</sub> (%)			
	Immersion <sub>test</sub>	Biaxial tensile <sub>test</sub>	Mean <sub>test</sub>	Ratio
Adriana	47.7 ± 4.4	15.5 ± 2.9	31.6 ± 3.65 c <sup>a</sup>	3.1
Burlat	88.5 ± 3.8	38.3 ± 4.6	63.4 ± 4.2 ab	2.3
Hedelfinger	75.1 ± 5.7	32.0 ± 7.3	53.6 ± 6.5 abc	2.3
Merchant	79.2 ± 4.2	51.2 ± 4.8	65.2 ± 4.5 ab	1.5
Regina	89.6 ± 5.7	59.7 ± 4.2	74.7 ± 5.0 a	1.5
Sam	64.3 ± 4.8	22.7 ± 4.3	43.5 ± 4.6 bc	2.8
Samba	80.4 ± 2.9	28.6 ± 3.2	54.5 ± 3.1 abc	2.8
Mean <sub>cultivar</sub>	75.0 ± 4.5 a	35.4 ± 4.5 b		2.1

Fracture was induced by immersing whole fruit in water ('immersion') or by a biaxial tensile test of the fruit skin using an elastometer. The fracture mode was quantified by expressing the number of epidermal cells that fractured *along* their anticlinal cell walls as a percentage of the total number of epidermal cells fractured (i.e. *along* + *across*;  $n = 10$ )

<sup>a</sup> Significant main effects for test and cultivars by two factorial analysis of variance, mean separation by Tukey's Studentized range test at  $P < 0.05$

occur exclusively *along* the cell walls. At this point, the values of  $E$  and  $p_{\text{fracture}}$  would be close to zero (Table 3). There was only a weak positive relationship between the value of  $\varepsilon_{\text{fracture}}$  and cell wall thickness (Fig. 5d).

When fruit cracked during water immersion, the cell walls in the zone ahead of the crack (zone I) were thin, like those in the surrounding epidermis away from the crack. Epidermal cells in zone I were intact as indexed by the presence of large vacuoles containing anthocyanin (Table 4; Fig. 1g). In the zone at the tip of a crack (zone II), the cuticle had ruptured. Immediately below the crack tip, the cell walls began to swell and to separate one from another. Individual epidermal cells also showed discolouration indicating death. In the older zone of a crack (zone III), the crack had split the skin. Cell walls of epidermal cells on either side of crack were very swollen, and nearly all the cells along the crack were dead (Table 4; Fig. 1g).

## Discussion

Our study establishes several new findings:

1. The mode of fracture of sweet cherry fruit skin is related to the thickness of the epidermal cell walls which reflects swelling of cell wall and middle lamella in our system;
2. The mechanical properties of the fruit skin depend on cell wall thickness. The closest relationships are obtained for  $p_{\text{fracture}}$ , followed by  $E$  which is markedly more variable. The value of  $\varepsilon_{\text{fracture}}$  is little affected by cell wall thickness. The effects of cultivar, ripening stage, sucrose, ethanol,  $\text{CaCl}_2$ , and malic acid are

largely accounted for by their effects on cell wall thickness.

3. Fruit that crack in water had thicker cell walls and more often showed fracture *along* the cell walls, compared to ES fractured in the biaxial tensile test.

## Fracture mode, cell wall swelling, and mechanical properties

The mode of fracture clearly depended on the thickness of the epidermal cell walls. Thicker cell walls fractured more frequently *along* the cell wall, and thinner walls more frequently fractured *across* the cell wall. This observation was consistent across all cultivars, ripening stages, and treatments (sucrose, ethanol,  $\text{CaCl}_2$ , or malic acid). Variation in cell wall thickness was caused by different degrees of cell wall swelling (Redgwell et al. 1997a; Grimm and Knoche 2015). Cell wall swelling is a characteristic of the ripening process in soft, fleshy fruits (Hallett et al. 1992; Redgwell et al. 1997a; Brummell 2006) including sweet cherry (Kondo and Danjo 2001; Grimm and Knoche 2015). It is preceded by biochemical modifications of the cell wall during maturation and ripening. Swelling occurs within hours after removal of turgor when the slight pressure of the symplast on the cell wall is released, for example, by plasmolysis or by destroying plasma membrane integrity using ethanol (Figs. 4, 5). This behaviour is indicative of a low swelling pressure relative to cell turgor (Saladié et al. 2007; Schumann et al. 2014; Grimm and Knoche 2015).

The  $p_{\text{fracture}}$  and—to a lesser extent—the  $E$  of the ES are closely related to the thickness of the anticlinal epidermal cell walls (Figs. 4, 5). This is in agreement with our earlier

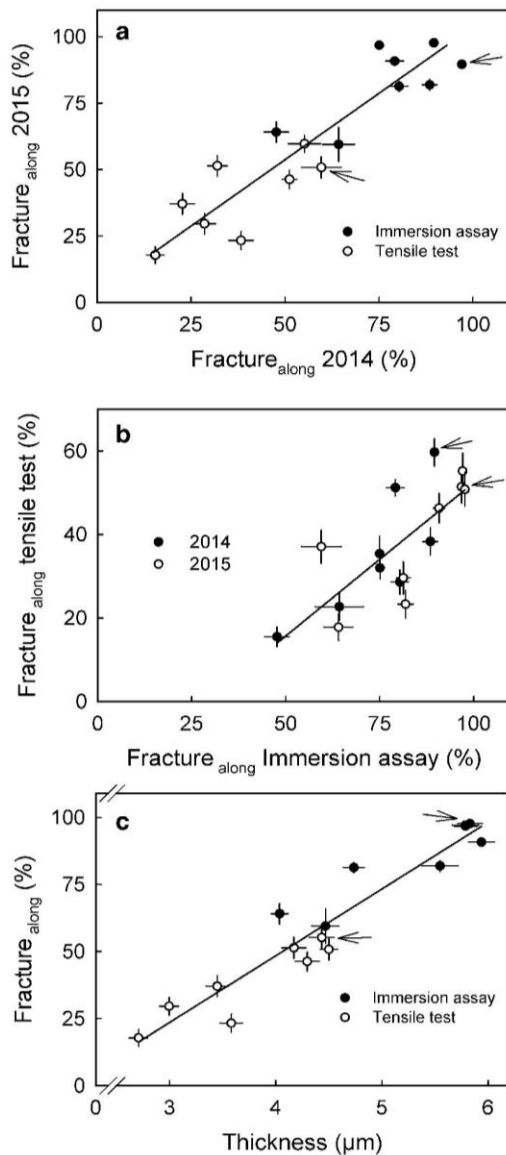


**Fig. 2** Effect of cultivar and season on the mode of fracture and thickness of anticlinal epidermal cell walls of sweet and sour cherry fruit. Cracks were induced in immersion assays or in biaxial tensile tests using the elastometer. **a** Reproducibility of fracture mode across cultivars and assays (immersion of whole fruit or biaxial tensile skin test) in two successive seasons. **b** Relationship between fracture mode in biaxial tensile tests and immersion assays. **c** Relationship between the fracture mode and cell wall thickness (data from 2015 only). Data symbols represent mean  $\pm$  SE for seven sweet cherry and one sour cherry cultivars (indicated by arrow). The fracture mode was quantified by expressing the number of epidermal cells that fractured *along* their anticlinal cell walls as a percentage of the total number of epidermal cells fractured (i.e. *along* + *across*). Values are mean  $\pm$  SE ( $n = 10$ )

finding that the epidermis and hypodermis together represent the structural backbone of the sweet cherry skin (Brüggenwirth et al. 2014; Brüggenwirth and Knoche 2016a, b).

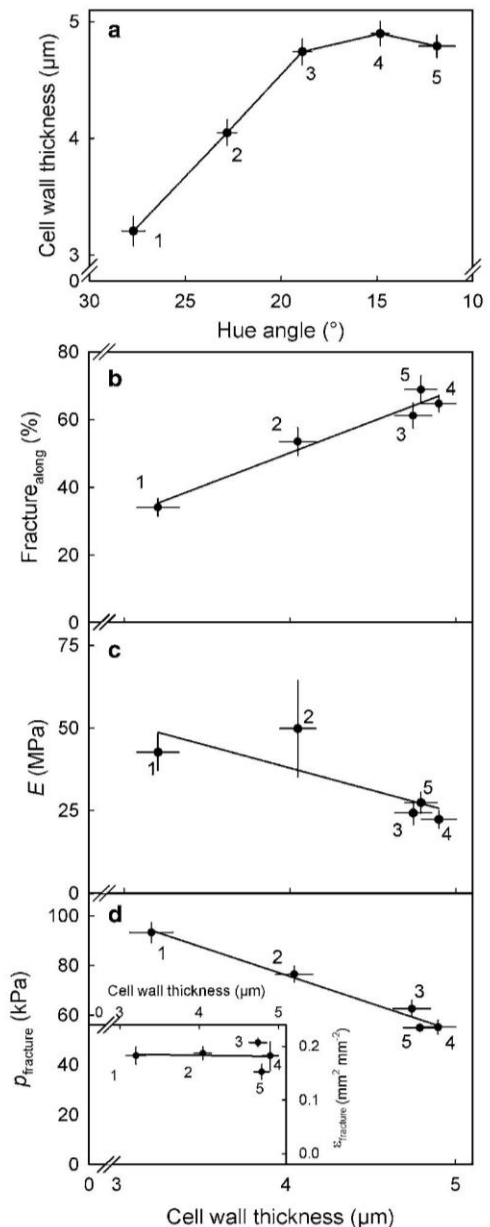


**Fig. 3** Relationship between the thickness of anticlinal epidermal cell walls of ‘Regina’ sweet cherry and the mechanical properties of the skin tested in biaxial tensile tests. Fruits were sampled during the final stage of maturation and ripening. **a** Relationship between cell wall thickness and maturity as indexed by the change in colour. The colour is expressed as the hue angle. High hue angles imply less mature, pale red fruit; low hue angles imply more mature, darker fruit. **b–d** Relationship between the mechanical properties of the fruit skin and cell wall thickness. **b** Fracture mode, **c** modulus of elasticity ( $E$ ), **d** pressure at fracture ( $p_{\text{fracture}}$ ) and *Inset* strain at fracture ( $\epsilon_{\text{fracture}}$ ). Numbers next to data symbols refer to the stages of maturation ranging from less mature (‘1’) to fully mature fruit (‘5’). The fracture mode was quantified by expressing the number of epidermal cells that fractured *along* their anticlinal cell walls as a percentage of the total number of epidermal cells fractured (i.e. *along* + *across*). Values are mean  $\pm$  SE ( $n = 10$ )

**Fig. 4 a, b** Effects of the concentrations of ethanol or sucrose solutions on the mode of fracture of the skin of sweet cherry fruit. **c** Same data as in **a, b**, but fracture mode redrawn as a function of the thickness of anticlinal epidermal cell walls. The fracture mode was determined on fruit skin segments subjected to a biaxial tensile test. The fracture mode was quantified by expressing the number of epidermal cells that fractured *along* their anticlinal cell walls as a percentage of the total number of epidermal cells fractured (i.e. *along* + *across*). Values are mean  $\pm$  SE ( $n = 10$ )

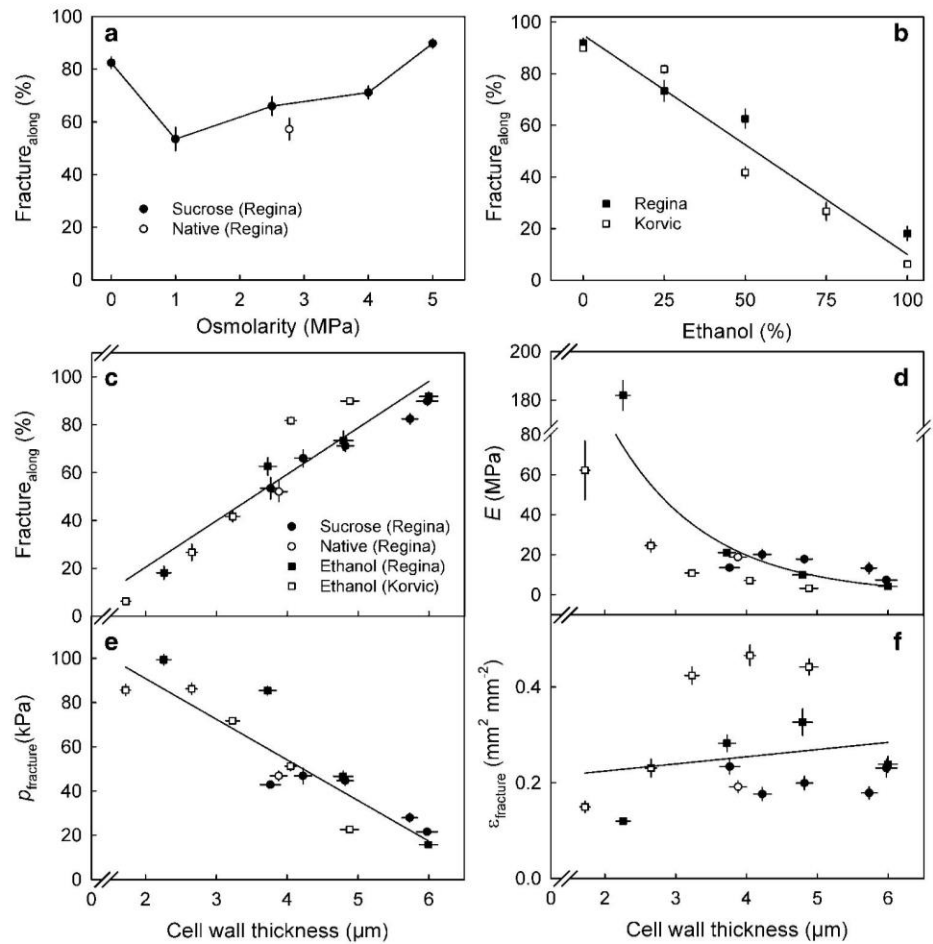


**Table 2** Effect of malic acid (70 mM) and CaCl<sub>2</sub> (100 mM) on the thickness of anticlinal epidermal cell walls, the fracture mode, the modulus of elasticity (*E*), the pressure at fracture (*p*<sub>fracture</sub>), and the strain at fracture (*ε*<sub>fracture</sub>) of the sweet cherry fruit skin

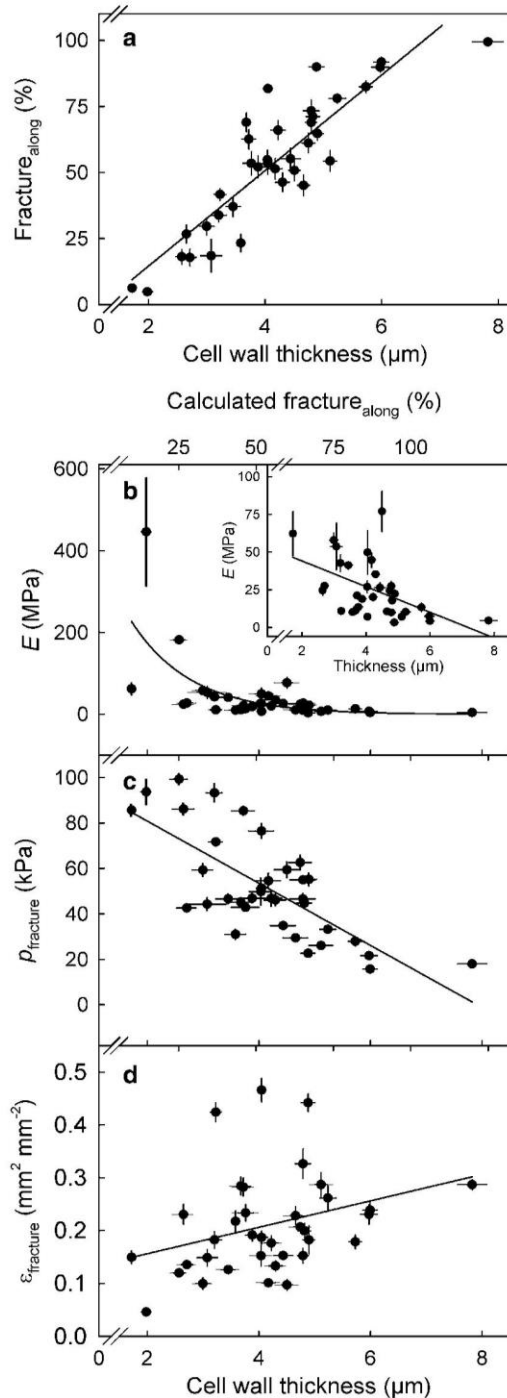
Treatment	Thickness (μm)	Fracture <sub>along</sub> (%)	<i>E</i> (MPa)	<i>p</i> <sub>fracture</sub> (kPa)	<i>ε</i> <sub>fracture</sub> (mm <sup>2</sup> mm <sup>-2</sup> )
Control	5.2 $\pm$ 0.1 b <sup>a</sup>	78.0 $\pm$ 1.8 b	10.3 $\pm$ 1.1 b	33.2 $\pm$ 1.8 b	0.26 $\pm$ 0.02 a
Malic acid	7.8 $\pm$ 0.3 a	99.4 $\pm$ 0.4 a	4.5 $\pm$ 0.5 c	18.0 $\pm$ 1.2 c	0.29 $\pm$ 0.01 a
CaCl <sub>2</sub>	4.0 $\pm$ 0.1 c	54.7 $\pm$ 3.7 c	27.0 $\pm$ 3.9 a	49.8 $\pm$ 6.0 a	0.15 $\pm$ 0.02 b

The fracture mode was quantified by expressing the number of epidermal cells that fractured *along* their anticlinal cell walls as a percentage of the total number of epidermal cells fractured (i.e. *along* + *across*;  $n = 10$ ). The control represents the cell wall in the *in vivo* state

<sup>a</sup> Mean separation within columns by Tukey’s Studentized range test,  $P < 0.05$

It may be argued that the decrease in *p*<sub>fracture</sub> of the fruit skin upon plasmolysis and cell death was due to the removal of turgor rather than to the swelling of cell walls. These effects are difficult to separate in our system because removal of turgor is accompanied by swelling of the cell wall in this and earlier studies (McClendon 1981; Grimm and Knoche 2015). Also, effects of turgor on mechanical properties have often been reported in the literature (Niklas 1992; De Belie et al. 2000; Oey et al. 2007; Knoche et al.

2014; Brüggewirth and Knoche 2016a). However, when skin sections were incubated in ethanol, the turgor was destroyed, but cell walls remained thin due to a slight dehydration by the ethanol (Fig. 4). The mechanical properties of these skins did not differ from turgescient skins of comparable cell wall thickness indicating that cell wall swelling and not the lack of turgor was the dominating factor. Also, cell turgor in the outer mesocarp of mature sweet cherry is very low (17–64 kPa; Knoche et al. 2014)



relative to the osmotic potential of the fruit ( $-2500$  to  $-4000$  kPa), and the turgor of the epidermis is most likely even lower (Grimm and Knoche 2015). This too makes an effect of turgor unlikely.

The stiffness of the fruit skin as indexed by  $E$  was also related to cell wall thickness. Compared to  $p_{\text{fracture}}$ ,

**Fig. 5** **a** Relationship between the fracture mode and the thickness of anticlinal epidermal cell walls of the skin of sweet cherry. Data points represent pooled data from all experiments conducted. **b–d** Mechanical properties of the skin as affected by the thickness of epidermal cell walls. **b** Modulus of elasticity ( $E$ ). *Inset*  $E$  redrawn on a different scale (outlier for 100% ethanol treatment omitted). **c** Pressure at fracture ( $p_{\text{fracture}}$ ) and **d** strain at fracture ( $\epsilon_{\text{fracture}}$ ). Because fracture mode and cell wall thickness were linearly related, a fracture mode calculated using the regression equation and line depicted in **a** was included as a second x-axis in **b–d**. The fracture mode was quantified by expressing the number of epidermal cells that fractured *along* their anticlinal cell walls as a percentage of the total number of epidermal cells fractured (i.e. *along* + *across*). Values are mean  $\pm$  SE ( $n = 10$ )

however, variability in  $E$  was considerably higher, particularly for thinner cell walls (Fig. 5; Table 3). When cell walls are thin (at low water content), the intrinsic properties of the non-swollen polymer dominate and cause significant variability. Variability decreases as swelling progresses, and the effect of cell wall swelling becomes more and more dominant over that of any compositional and/or structural differences in the cell wall under the various treatments.

The above discussion demonstrates that the effects observed in our experiments (i.e. those of cultivar, ripening stage, sucrose, ethanol,  $\text{CaCl}_2$  and malic acid on the  $p_{\text{fracture}}$  and on  $E$ ) were largely accounted for by their effects on cell wall swelling. Clearly, some specific effects of individual treatments must have remained as indicated by the larger scatter and decreased  $r^2$  when comparing the relationships depicted in Figs. 4 and 5. However, these treatment-specific effects were minor.

From the regression equations fitted through plots of  $p_{\text{fracture}}$  vs. mode of fracture as indexed by the frequency of fracture *along cell* walls, some further interesting conclusions may be drawn (Fig. 5; Table 3). The pressure required for 100% failure *along* cell walls is about 20 kPa, whereas that required for 100% fracture *across* cell walls is about four times higher, about 81 kPa. Furthermore, only non-swollen cell walls will fracture *across* cell walls. In swollen walls, it would appear that the pressure required to overcome cell to cell adhesion (i.e. the middle lamella) must fall below the pressure required for fracture *across* cell walls.

Our findings on the striking effect of cell wall swelling on the mechanical properties are consistent with those observed in hydrated onion epidermal cell walls (Ha et al. 1997; Zamil et al. 2015). In onion (*Allium cepa*), as in sweet cherry, increased hydration decreased the modulus of elasticity (Zamil et al. 2015). This effect was related to the hydration and swelling of pectins (Ha et al. 1997; Zamil et al. 2015). The same argument applies with sweet cherry, where fracture mode and cell wall thickness are closely related.

**Table 3** Parameter estimates and standard errors (SE) of linear regression equations describing the relationships between the modulus of elasticity ( $E$ ), pressure at fracture ( $p_{\text{fracture}}$ ) and strain at fracture ( $\epsilon_{\text{fracture}}$ ) and the mode of fracture of the sweet cherry fruit skin (Fig. 5b–d)

Dependent variable	Independent variable	Parameter estimates		Coefficient of determination
		Slope	Intercept	
$E$ (MPa)	Cell wall thickness ( $\mu\text{m}$ )	$-8.5 \pm 2.5$	$61.1 \pm 10.9$	$0.52^{***a}$
	Fracture <sub>along</sub> (%)	$-1.6 \pm 0.4$	$127.5 \pm 26.4$	$0.52^{***}$
$p_{\text{fracture}}$ (kPa)	Cell wall thickness ( $\mu\text{m}$ )	$13.7 \pm 2.2$	$108.2 \pm 9.5$	$0.73^{***}$
	Fracture <sub>along</sub> (%)	$-0.6 \pm 0.1$	$81.9 \pm 7.2$	$0.62^{***}$
$\epsilon_{\text{fracture}}$ ( $\text{mm}^2 \text{mm}^{-2}$ )	Cell wall thickness ( $\mu\text{m}$ )	$0.025 \pm 0.013$	$0.11 \pm 0.06$	0.32
	Fracture <sub>along</sub> (%)	$0.002 \pm 0.001$	$0.10 \pm 0.03$	$0.54^{**}$

The fracture mode was quantified by expressing the number of epidermal cells that fractured *along* their anticlinal cell walls as a percentage of the total number of epidermal cells fractured (i.e. *along* + *across*;  $n = 28$ )

<sup>a</sup> Significance of coefficient of determination at  $P < 0.05$ ,  $0.01$ , and  $0.001$  indicated by \*, \*\*, and \*\*\*, respectively

**Table 4** Cell wall thickness of different zones of a crack (see Fig. 1g) in the fruit skin induced by immersing fruit in deionized water ( $n = 10$ )

Position	Zone	Cell wall thickness ( $\mu\text{m}$ )
Ahead of crack (intact)	I	$3.6 \pm 0.1 \text{ c}^a$
Crack tip with cuticle rupture	II	$5.3 \pm 0.2 \text{ b}$
Cell wall rupture with separation of cells	III	$6.1 \pm 0.1 \text{ a}$

<sup>a</sup> Mean separation by Tukey's Studentized range test,  $P < 0.05$

### Hypothetical mechanism of failure

The physicochemical process of the absorption of water in the cell wall and/or middle lamellae that led to swelling must have been preceded by biochemical changes in the wall and/or the middle lamellae. The consequence of these changes is a higher frequency of cells fracturing along cell walls at reduced pressure. Separation along cell walls is indicative for reduced cell to cell adhesion. Mechanistically, cell to cell adhesion is realised by (1) calcium ion crosslinking of low-esterified homogalacturonan (HG), (2) alkali-labile covalent ester bonds, and (3) alkali-resistant covalent or intermolecular linkage (Jarvis et al. 2003; Zamil et al. 2014).

It is well established that marked changes occur in the pectin fraction of ripening sweet cherry fruit (Batisse et al. 1996; Basanta et al. 2013; Salato et al. 2013). Cell adhesion decreases during ripening due to enzymatic and non-enzymatic processes, resulting in the disassembly of the middle lamella and the solubilisation of pectins (Hallett et al. 1992; Redgwell et al. 1997a; Brummell 2006). Enzymatic processes contributing to the solubilisation of pectins include the cleavage of homogalacturonans by polygalacturonases (Jarvis et al. 2003), the demethylesterification of homogalacturonans by polygalacturonases and pectin methylesterases (Roy et al. 1992; Tieman and Handa 1994), and the removal of neutral side chains that anchor pectins to matrix glycans and cellulose in the primary cell

wall (Paniagua et al. 2014; Redgwell et al. 1997b). The effect of malic acid on decreasing cell adhesion may be accounted for by increased activity of polygalacturonases caused by a decrease in the extracellular pH (Chun and Huber 1998). Non-enzymatic mechanisms of pectin degradation stimulated by acids include breakdown due to reactive oxygen species (ROS), produced by acids such as ascorbate, causing the cleavage of neutral galactose residues (Dumville and Fry 2003) and removal and complexation of cell wall bound  $\text{Ca}^{2+}$ , resulting in the loosening of the crosslinks (Glenn and Poovaiah 1989; Tibbits et al. 1998; Brummell 2006). Accordingly, the effect of  $\text{Ca}^{2+}$  would be attributable to increased crosslinking, resulting in stronger cell walls (Jarvis 1984; Roy et al. 1994).

Swelling may occur due to (1) a deesterification of pectins in the primary cell wall and the middle lamella which increases the charge density, causing electric repulsion and hydration (Jarvis 1991) and/or (2) the filling of intermicrofibrillar spaces in the primary cell wall that were previously filled with pectins (Redgwell et al. 1997a). In addition, osmotic processes due to increased osmolarity in the apoplast (Wada et al. 2008, 2009) may be visualised that cause water to partition into the cell wall. Pectin gels are capable of large changes in hydration and stiffness. This alters the mechanical behaviour of tissues which would also be consistent with our observations on the sweet cherry skin (Levesque-Tremblay et al. 2015). Clearly, the above arguments are speculative and alternate



mechanisms cannot be excluded. However, at present the interrelationship of cell wall swelling, fracture pressure, and mode of fracture makes failure of a middle lamella, which is weakened by ripening processes and cell wall swelling, the most likely explanation. Further investigations are needed on the interaction of cell wall constituents, i.e., the pectins in the middle lamellae, and water.

### Implications for fruit cracking

Fracture surfaces of fruit that cracked in an immersion assay due to water uptake differed from those that cracked from strain in the biaxial tensile test. First, cell walls were thinner in the biaxial tensile tests, compared to in the immersion assays (Fig. 1). Second, in the tensile test, fracture occurred more frequently *across*, rather than *along* the cell walls. Third, cell walls below the surface of an intact fruit skin were thinner immediately after excision than cell walls located along cracks induced by incubating fruit in water (Fig. 1g). In addition, cracking occurs at lower strain values in immersion assays where fruit is incubated in water compared to in biaxial tensile tests (Brüggenwirth and Knoche 2016b). These observations suggest that (1) the two fracture processes differ between fruit cracking in an immersion assay and skin rupture in tensile tests and (2) cell wall swelling in fruit incubated in water is an early, critical, and essential step in a chain reaction of events that ultimately leads to cracking.

Based on these observations and literature data, the following scenario may be hypothesized. First, microcracks in the cuticle result from a lack of synchronisation of fruit growth and cuticle deposition (Knoche et al. 2004; Peschel and Knoche 2005), coupled with exposure of the strained cuticle to surface wetness (Knoche and Peschel 2006). Microcracks impair the cuticle's barrier function (Kerstiens 1996) and so focus water uptake in the region immediately underlying the microcrack. This causes individual cells just below a microcrack to burst, thereby releasing cell contents into the apoplast (Simon 1977; Glenn and Poovaiah 1989). Besides glucose, fructose, and anthocyanins, a number of acids including malic, citric, and ascorbic acid are also released (Herrmann 2001; Demir 2013). Plasma membranes of adjacent cells are damaged by these acids (Winkler et al. 2015), leading to a chain reaction of further bursting of cells in the vicinity. Exposure of the cell walls to acids leads to pectin solubilisation and removal of  $\text{Ca}^{2+}$  crosslinks (Dumville and Fry 2003; Brummell 2006). The lack of turgor, the pectin solubilisation, and the extraction of  $\text{Ca}^{2+}$  increases swelling (Grimm and Knoche 2015), resulting in decreased cell wall stiffness, decreased pressure at fracture, and decreased cell to cell adhesion (Figs. 4, 5). The weaker cell walls cannot any longer withstand the strain of the fruit skin (Grimm et al. 2012).

The low turgor pressure at the whole fruit level is sufficient to result in the formation of macrocracks by rupture *along* cell walls (Knoche et al. 2014). The continuation of this process at the crack tip and the phenomenon of stress concentration at a crack tip will result in crack elongation in much the same way as a 'zipper' or a 'ladder' is propagated in a piece of knitted fabric (Fig. 1g). The swelling of cell walls and, in consequence, the decrease in stiffness and lower pressure at fracture allow a microcrack in a strained cuticle to extend into a macrocrack through the load-bearing fruit skin that subsequently causes the entire fruit to crack deep into the flesh.

The data presented here demonstrate that swelling of cell walls precedes failure of the fruit skin in water-induced cracking, but not necessarily when inducing fracture in a biaxial tensile test. Cell wall swelling favours fracture of epidermal cell walls *along* cell walls, decreases stiffness of the cell wall, and decreases the pressure at fracture. Factors affecting fracture modes and mechanical properties—such as cultivar, ripening stage, and turgor as manipulated by incubation in sucrose or aqueous ethanol,  $\text{CaCl}_2$  or malic acid—do so primarily by altering cell wall swelling. Future studies are required to identify the cell wall constituent(s) responsible for swelling and the mechanism of swelling in sweet cherry. Based on the arguments presented above, the pectins are the most likely candidate. Of particular interest is the mechanism responsible for the weakening of cell to cell adhesion and the subsequent separation of adjacent cells. A better understanding of these processes is a prerequisite to the development of suitable countermeasures and possibly and ultimately to mitigate the rain cracking of fruit. Cultural means include the application of foliar sprays of Ca-salts that, as we have shown, prevent the swelling of cell walls in the load-bearing skin. Also, approaches that modify the processes of pectin solubilisation are well documented for apple (*Malus × domestica*; Atkinson et al. 2012), tomato (Brummell and Harpster 2001; Wen et al. 2013), and strawberry (*Fragaria × ananassa*; Quesada et al. 2009; for recent review see Sénéchal et al. 2014). Such strategies could be useful in modifying cracking susceptibility of the sweet cherry in the long term in breeding programs.

**Author contribution statement** MK obtained the funds to support the study. MK and MB planned the experiments. MB conducted the experiments. MB and MK analysed the data and wrote, revised, and edited the manuscript.

**Acknowledgements** We thank Dieter Reese and Christoph Knake for constructing, engineering, and programming the elastometer; Simon Sitzenstock for technical support; Sandy Lang and Andreas Winkler for helpful discussion and useful comments on an earlier version of this manuscript. This study was funded in part by a grant from the German Science Foundation (DFG).

**Compliance with ethical standards**

**Conflict of interest** The authors declare that they have no conflict of interest.

**References**

- Atkinson RG, Sutherl PW, Johnston SL, Gunaseelan K, Hallett IC, Mitra D, Brummell DA, Schroder R, Johnston JW, Schaffer RJ (2012) Down-regulation of *POLYGALACTURONASE1* alters firmness, tensile strength and water loss in apple (*Malus × domestica*) fruit. *BMC Plant Biol* 12:129. doi:10.1186/1471-2229-12-129
- Bargel H, Spatz HC, Speck T, Neinhuis C (2004) Two-dimensional tension tests in plant biomechanics—sweet cherry fruit skin as a model system. *Plant Biol* 6:432–439
- Barrett DM, Gonzalez C (1994) Activity of softening enzymes during cherry maturation. *J Food Sci* 59:574–577
- Basanta FM, de Escalada Plá MF, Stortz CA, Rojas AM (2013) Chemical and functional properties of cell wall polymers from two cherry varieties at two developmental stages. *Carbohydr Polym* 92:830–841
- Batisse C, Buret M, Coulomb PJ (1996) Biochemical differences in cell wall of cherry fruit between soft and crisp fruit. *J Agric Food Chem* 44:453–457
- Brüggenwirth M, Knoche M (2016a) Factors affecting mechanical properties of the skin of sweet cherry fruit. *J Am Soc Hort Sci* 141:45–53
- Brüggenwirth M, Knoche M (2016b) Mechanical properties of skin of sweet cherry fruit of differing susceptibilities to cracking. *J Am Soc Hort Sci* 141:162–168
- Brüggenwirth M, Knoche M (2016c) Time to fracture and fracture strain are negatively related in sweet cherry fruit skin. *J Am Soc Hort Sci* 141:1–5
- Brüggenwirth M, Fricke H, Knoche M (2014) Biaxial tensile tests identify epidermis and hypodermis as the main structural elements of sweet cherry skin. *Ann Bot Plants* 6:plu019. doi:10.1093/aobpla/plu019
- Brummell DA (2006) Cell wall disassembly in ripening fruit. *Funct Plant Biol* 33:103–119
- Brummell DA, Harpster MH (2001) Cell wall metabolism in fruit softening and quality and its manipulation in transgenic plants. *Plant Mol Biol* 47:311–340
- Christensen JV (1996) Rain-induced cracking of sweet cherries. Its causes and prevention. In: Webster AD, Looney NE (eds) cherries. CAB International, Wallingford, pp 297–327
- Chun JP, Huber DJ (1998) Polygalacturonase-mediated solubilization and depolymerization of pectic polymers in tomato fruit cell walls. *Plant Physiol* 117:1293–1299
- Considine J, Brown K (1981) Physical aspects of fruit growth: theoretical analysis of distribution of surface growth forces in fruit in relation to cracking and splitting. *Plant Physiol* 68:371–376
- Considine JA, Kriedemann PE (1972) Fruit splitting in grapes. Determination of the critical turgor pressure. *Aust J Agr Res* 23:17–24
- De Belie N, Hallett IC, Harker FR, De Baerdemaeker J (2000) Influence of ripening and turgor on the tensile properties of pears: a microscopic study of cellular and tissue changes. *J Am Soc Hort Sci* 125:350–356
- Demir T (2013) Determination of carotenoid, organic acid and sugar content in some sweet cherry cultivars grown in Sakarya, Turkey. *J Food Agric Environ* 11:73–75
- Dumville JC, Fry SC (2003) Solubilisation of tomato fruit pectins by ascorbate: a possible non-enzymic mechanism of fruit softening. *Planta* 217:951–961
- Glenn GM, Poovaiah BW (1989) Cuticular properties and postharvest calcium applications influence cracking of sweet cherries. *J Am Soc Hort Sci* 114:781–788
- Grimm E, Knoche M (2015) Sweet cherry skin has a less negative osmotic potential than the flesh. *J Am Soc Hort Sci* 140:472–479
- Grimm E, Peschel S, Becker T, Knoche M (2012) Stress and strain in the sweet cherry skin. *J Am Soc Hort Sci* 137:383–390
- Ha M, Apperley DC, Jarvis MC (1997) Molecular rigidity in dry and hydrated onion cell walls. *Plant Physiol* 115:593–598
- Hallett IC, MacRae EA, Wegrzyn TF (1992) Changes in kiwifruit cell wall ultrastructure and cell packing during postharvest ripening. *Int J Plant Sci* 153:49–60
- Hansen M (2011) When is the best time to pick? Good Fruit Grower. <http://www.goodfruit.com/when-is-the-best-time-to-pick/>. Accessed 27 Sept 2016
- Herrmann K (2001) Inhaltsstoffe von Obst und Gemüse. Ulmer, Stuttgart
- Jarvis MC (1984) Structure and properties of pectin gels in plant cell walls. *Plant Cell Environ* 7:153–164
- Jarvis MC (1991) Control of thickness of collenchyma cell walls by pectins. *Planta* 187:218–220
- Jarvis MC, Briggs SPH, Knox JP (2003) Intercellular adhesion and cell separation in plants. *Plant Cell Environ* 26:977–989
- Kerstiens G (1996) Barrier properties of the cuticle to water, solutes and pest and pathogen penetration in leaves of plants grown in polluted atmospheres. In: Yunus M, Iqbal M (eds) Plant response to air pollution. Wiley, Chichester, pp 167–178
- Knoche M, Peschel S (2006) Water on the surface aggravates microscopic cracking of the sweet cherry fruit cuticle. *J Am Soc Hort Sci* 131:192–200
- Knoche M, Beyer M, Peschel S, Oparlakov B, Bukovac MJ (2004) Changes in strain and deposition of cuticle in developing sweet cherry fruit. *Physiol Plant* 120:667–677
- Knoche M, Grimm E, Schlegel HJ (2014) Mature sweet cherries have low turgor. *J Am Soc Hort Sci* 139:3–12
- Kondo S, Danjo C (2001) Cell wall polysaccharide metabolism during fruit development in sweet cherry ‘Satohnishiki’ as affected by gibberellic acid. *J Jpn Soc Hortic Sci* 70:178–184
- Levesque-Tremblay G, Pelloux J, Braybrook SA, Müller K (2015) Tuning of pectin methylesterification: consequences for cell wall biomechanics and development. *Planta* 242:791–811
- McClendon JH (1981) The balance of forces generated by the water potential in the cell-wall-matrix: a model. *Am J Bot* 68:1263–1268
- McGuire RG (1992) Reporting of objective color measurements. *HortScience* 27:1254–1255
- Ng JKT, Schröder R, Sutherland PW, Hallett IC, Hall MI, Prakash R, Smith BG, Melton LD, Johnston JW (2013) Cell wall structures leading to cultivar differences in softening rates develop early during apple (*Malus x domestica*) fruit growth. *BMC Plant Biol* 13:183. doi:10.1186/1471-2229-13-183
- Niklas KJ (1992) Plant biomechanics—an engineering approach to plant form and function. University of Chicago Press, Chicago
- Oey ML, Vanstreels E, De Baerdemaeker J, Tijskens E, Ramon H, Hertog MLATM, Nicolai B (2007) Effect of turgor on micromechanical and structural properties of apple tissue: a quantitative analysis. *Postharvest Biol Technol* 44:240–247
- Paniagua C, Pose S, Morris VJ, Kirby AR, Quesada MA, Mercado JA (2014) Fruit softening and pectin disassembly: an overview of nanostructural pectin modifications assessed by atomic force microscopy. *Ann Bot* 114:1375–1383

- Peschel S, Knoche M (2005) Characterization of microcracks in the cuticle of developing sweet cherry fruit. *J Am Soc Hort Sci* 130:487–495
- Quesada MA, Blanco-Portales R, Pose S, Garcia-Gago JA, Jimenez-Bermudez S, Munoz-Serrano A, Caballero JL, Pliego-Alfaro F, Mercado JA, Munoz-Blanco J (2009) Antisense downregulation of the *FaPGI* gene reveals an unexpected central role for polygalacturonase in strawberry fruit softening. *Plant Physiol* 150:1022–1032
- Redgwell RJ, MacRae E, Hallett I, Fischer M, Perry J, Harker R (1997a) In vivo and in vitro swelling of the cell walls during fruit ripening. *Planta* 203:162–173
- Redgwell RJ, Fischer M, Kendal E, MacRae EA (1997b) Galactose loss and fruit ripening: high-molecular-weight arabinogalactans in the pectic polysaccharides of fruit cell walls. *Planta* 203:174–181
- Roy S, Vian B, Roland J-C (1992) Immunocytochemical study of the deesterification patterns during cell wall autolysis in the ripening of cherry tomato. *Plant Physiol Biochem* 30:139–146
- Roy S, Conway WS, Watada AE, Sams CE, Pooley CD, Wergin WP (1994) Distribution of the anionic sites in the cell wall of the apple fruit after calcium treatment. *Protoplasma* 178:156–167
- Saladié M, Matas AJ, Isaacson T, Jenks MA, Goodwin SM, Niklas KJ, Xiaolin R, Labavitch JM, Shackel KA, Fernie AR, Lytovchenko A, O'Neill MA, Watkins CB, Rose JKC (2007) A reevaluation of the key factors that influence tomato fruit softening and integrity. *Plant Physiol* 144:1012–1028
- Salato GS, Ponce NMA, Raffo MD, Vicente AR, Stortz CA (2013) Developmental changes in cell wall polysaccharide from sweet cherry (*Prunus avium* L.) cultivars with contrasting firmness. *Postharvest Biol Technol* 84:66–73
- Schumann C, Schlegel HJ, Grimm E, Knoche M, Lang A (2014) Water potential and its components in developing sweet cherry. *J Am Soc Hort Sci* 139:349–355
- Sénéchal F, Wattier C, Rusterucci C, Pelloux J (2014) Homogalacturonan-modifying enzymes: structure, expression, and roles in plants. *J Exp Bot* 65:5125–5160
- Simon EW (1977) Leakage from fruit cells in water. *J Exp Bot* 28:1147–1152
- Tibbits CW, MacDougall AJ, Ring SG (1998) Calcium binding and swelling behavior of a high methoxyl pectin gel. *Carbohydr Res* 310:101–107
- Tieman DM, Handa AK (1994) Reduction in pectin methylesterase activity modifies tissue integrity and cation levels in ripening tomato (*Lycopersicon esculentum* Mill.) fruits. *Plant Physiol* 106:429–436
- von Wetzhausen C (1819) Systematische Classification und Beschreibung der Kirschenarten. Friedrich Timotheus Heim (ed) Cottische Buchhandlung, Stuttgart
- Wada H, Shackel KA, Matthews MA (2008) Fruit ripening in *Vitis vinifera*: apoplastic solute accumulation accounts for pre-ripening turgor loss in berries. *Planta* 227:1351–1361
- Wada H, Matthews MA, Shackel KA (2009) Seasonal pattern of apoplastic solute accumulation and loss of cell turgor during ripening of *Vitis vinifera* fruit under field conditions. *J Exp Bot* 60:1773–1781
- Wen B, Ström A, Tasker A, West G, Tucker GA (2013) Effect of silencing the two major tomato fruit pectin methylesterase isoforms on cell wall pectin metabolism. *Plant Biol* 15:1025–1032
- Winkler A, Ossenbrink M, Knoche M (2015) Malic acid promotes cracking of sweet cherry fruit. *J Am Soc Hort Sci* 140:280–287
- Zamil MS, Hojae Y, Puri VM (2014) Mechanical characterization of outer epidermal middle lamella of onion under tensile loading. *Am J Bot* 101:778–787
- Zamil MS, Hojae Y, Puri VM (2015) The mechanical properties of plant cell walls soft material at the subcellular scale: the implications of water and of the intercellular boundaries. *J Mater Sci* 50:6608–6623

## 9. Generelle Diskussion

Aus den Ergebnissen dieser Arbeit geht hervor, dass

1. die Kirschhaut isotrop in der tangentialen Ebene ist und elastisches und viskoelastisches Verhalten aufweist, sich aber wenig plastisch verformt (Kapitel 4).
2. die Epidermis und Hypodermis das mechanische Rückgrat der Kirschfruchthaut sind, nicht jedoch die Kutikula. (Kapitel 4 und 5).
3. die größere Platzanfälligkeit der Sorte ‚Burlat‘ im Gegensatz zu ‚Regina‘ auf physikalische und möglicherweise auch chemische Eigenschaften der Zellwand zurückzuführen ist (Kapitel 6).
4. eine längere Bruchzeit ( $t_{\text{fracture}}$ ) zu höherem E-Modul ( $E$ ) aber zu niedrigerem Bruchdruck ( $p_{\text{fracture}}$ ) und Bruchdehnung ( $\epsilon_{\text{fracture}}$ ) führt. Die  $\epsilon_{\text{fracture}}$  im biaxialen Zugtest ist jedoch immer noch höher als die berechnete  $\epsilon_{\text{fracture}}$  im Platztest (Kapitel 7).
5. der Rissmodus der Epidermis, die Quellung antiklinaler Zellwände der Epidermis und die mechanischen Eigenschaften der Kirschfruchthaut eng miteinander korreliert sind. Dabei zeigt sich, dass im klassischen Platztest die Epidermiszellen öfter entlang der Zellwand reißen und gequollene Zellwände haben, im Gegensatz zu „durchgerissenen“ Zellen im biaxialen Zugtest. Alle Behandlungseffekte, wie Turgor, Wasseraufnahme,  $\text{CaCl}_2$  und Äpfelsäure sind ursächlich auf eine veränderte Zellwandquellung zurückzuführen (Kapitel 9).

Die genannten Schlüsselergebnisse werden in den jeweiligen Veröffentlichungen ausführlich zusammen mit der Literatur diskutiert. Die nachfolgende übergreifende Diskussion konzentriert sich daher auf (1) den Vergleich des biaxialen Zugtests mit dem klassischen Platztest und (2) den hypothetischen Mechanismus des Versagens der Fruchthaut beim Platzen der Kirsche.

### Vergleich biaxialer Zugtest mit Platztest

Der biaxiale Zugtest bietet die Möglichkeit, mit einem standardisierten *in-vitro* Prüfverfahren die mechanischen Eigenschaften der Fruchthaut zu untersuchen und dadurch Rückschlüsse auf das Platzverhalten von Kirschen unter *Ceteris-paribus*-Bedingungen zu ziehen. Üblicherweise wird das Platzen von Kirschen in einem Immersionstest oder Platztest nach Christensen (1996) *in-vitro* untersucht. In diesem Test wird das Platzen der Früchte in Abhängigkeit der Zeit ermittelt. Wird zusätzlich die Wasseraufnahme der Früchte quantifiziert, so kann die intrinsische Platzfestigkeit ( $WU_{50}$ ) ermittelt werden (Weichert et al., 2004; Winkler et al., 2015). In Analogie zu einem  $LD_{50}$  (lethal dose) beschreibt der  $WU_{50}$  (water uptake) die Wasseraufnahme, bei der 50% der Früchte platzen. Damit kann das Platzen mit der Wasseraufnahme der Früchte in Beziehung gesetzt werden. Um Rückschlüsse zu erhalten, inwieweit der biaxiale Zugtest die natürliche Situation des Platzens realitätsnah abbildet, werden im Folgenden der biaxiale Zugtest mit dem Platztest verglichen.

Wie im biaxialen Zugtest, kann  $\epsilon_{\text{fracture}}$  aus einem Platztest berechnet werden. Dazu müssen die Höhe der Wasseraufnahme und die durchschnittliche Zeit bis zum Platzen der Kirschen bekannt sein. Unter den Annahmen, dass die Kirsche eine Kugel ist und die Dichte der Kirsche  $1 \text{ g cm}^{-3}$  beträgt, ist es möglich, die Volumenzunahme der Frucht bis zum Platzen zu bestimmen. Aus der Volumenzunahme lassen sich die Oberflächenzunahme und damit die Dehnung der Fruchthaut berechnen. Die so ermittelten  $\epsilon_{\text{fracture}}$  aus dem Platztest betragen 0,8 - 5,0% (Kapitel 7) und sind mit Werten aus der Literatur vergleichbar, die von 0,3% (Christensen, 1972) über 4,0% (Knoche & Peschel, 2006) bis zu 7.8% (Kertesz & Nebel, 1935) reichen. Die mittleren  $\epsilon_{\text{fracture}}$  von sieben Sorten im biaxialen Zugtest hatten dagegen eine Spannweite von 17,0 - 22,0% (Kapitel 6) und waren damit etwa um eine Zehnerpotenz höher als die berechneten  $\epsilon_{\text{fracture}}$  aus dem Platztest.

Die  $p_{\text{fracture}}$  lassen sich dagegen nicht im Platztest bestimmen, da es keine Möglichkeiten gibt den Druck einer intakten Kirsche beim Platzen zu bestimmen. Es ist jedoch möglich, Turgordrücke mit einer Druckmesssonde und in einem Druckplattentests an intakten Kirschen zu messen (Knoche et al., 2014). Die gemessenen Drücke mit der Druckmesssonde lagen bei 9 - 12 kPa

und mit dem Druckplattentest bei 18 - 36 kPa. Der biaxiale Zugtest im Elastometer lieferte über sieben Sorten mittlere  $p_{\text{fracture}}$  von 24 - 67 kPa (Kapitel 6). Die  $p_{\text{fracture}}$  waren damit etwa in der gleichen Größenordnung wie die gemessenen Turgordrücke. Die Turgordrücke wurden allerdings nur an intakten Kirschen gemessen. Grundsätzlich ist anzunehmen, dass die Wasseraufnahme vor dem Platzen den Turgor weiter erhöhen sollte und somit die gemessenen Turgordrücke nur als konservative Schätzer der  $p_{\text{fracture}}$  in intakten Kirschen zu betrachten sind.

Für die größeren  $\epsilon_{\text{fracture}}$  und möglicherweise auch größeren  $p_{\text{fracture}}$  im biaxialen Zugtest im Vergleich zum Platztest gibt es mehrere Gründe. (1) Die Dehnungsraten im normalen biaxialen Zugtest sind deutlich größer als im Platztest (Kapitel 3 und 5). In der Tat führte die Senkung der Dehnungsrate im Zugtest zu einer Halbierung der  $\epsilon_{\text{fracture}}$  und  $p_{\text{fracture}}$  (Kapitel 5). (2) Risse im Platztest weisen einen höheren Anteil an gerissenen Zellwänden entlang der Zellwand sowie eine höhere Zellwandquellung als im biaxialen Zugtest auf (Kapitel 8). Wurde die Quellung der Zellwand vorher an der Fruchthaut induziert, so halbierte sich der  $p_{\text{fracture}}$  im biaxialen Zugtest, wodurch sich der Unterschied zwischen dem biaxialen Zugtest und dem Platztest verringerte (Kapitel 8). (3) Im biaxialen Zugtest wird nur ein Segment der Fruchthaut getestet, während im Platztest die 17fach größere Oberfläche der gesamten Fruchthaut gedehnt wird. Aufgrund der größeren Oberfläche erhöht sich die Wahrscheinlichkeit von Fehlstellen, die zu schwächeren mechanischen Eigenschaften der Fruchthaut führen. So konnte in Kapitel 2 gezeigt werden, dass  $p_{\text{fracture}}$  und  $\epsilon_{\text{fracture}}$  mit zunehmender Größe der ES im Halter abnehmen und sich damit den mechanischen Eigenschaften des Platztests annäherten.

Zwei wesentliche Punkte lassen sich aus dem Vergleich mit dem biaxialen Zugtest und dem Platztest ableiten. (1) Der biaxiale Zugtest liefert bei entsprechender Modifikation der Testweise (d.h. kleinere Dehnungsraten, Induktion von Zellwandquellung und größere ES)  $\epsilon_{\text{fracture}}$  und  $p_{\text{fracture}}$  in der gleichen Größenordnung wie der Platztest. Es ist somit möglich mit dem biaxialen Zugtest bei entsprechender (Vor)Behandlung der isolierten Fruchthaut das Platzen ganzer Früchte zu simulieren. (2) Der biaxiale Zugtest im Elastometer bietet als *in-vitro* Test die Möglichkeit nur eine Einflussgröße zu

verändern und alle anderen Faktoren konstant zu halten. Diese *Ceteris-paribus*-Bedingungen ermöglichen erstmals die Trennung der Wasseraufnahme von den mechanischen Eigenschaften der Fruchthaut. Im Platztest ist die Trennung dieser beiden Faktoren nicht möglich (sog. Confounding). Diese Besonderheiten des Elastometers ermöglichten den Nachweis, dass die Wasseraufnahme offenbar weitere, über die einfache Volumenzunahme der Frucht hinausgehende Einflüsse auf das Platzen der Kirschen hat (Kapitel 7). Der biaxiale Zugtest war damit die Voraussetzung die Zellwandquellung als eine zentrale Rolle für das Platzen von Kirschen zu identifizieren.

### Mechanismus des Platzens

Die Ergebnisse dieser Arbeit erlauben eine Reihe wichtiger Rückschlüsse auf den Mechanismus des Platzens. Das Platzen von Früchten wurde bislang mit dem Ballon-Modell erklärt (Considine & Brown, 1981). In dieser Theorie wird die Fruchthaut mit einer Außenhaut eines Wassergefüllten Ballons verglichen, die bei Wasseraufnahme immer weiter gedehnt wird und schließlich beim Überschreiten eines kritischen Turgordruckes die Fruchthaut dem Druck nicht mehr standhält und reißt (Considine und Kriedemann, 1972). Basierend auf dieser Hypothese wird in zahlreichen Publikationen der kritische Turgordruck von Kirschen berechnet und als Argument für das Platzen der Früchte verwendet (Sekse et al., 2005; Meashem et al., 2009).

Allerdings sprechen eine Reihe von Argumenten gegen das Ballon-Modell: (1) Reife Kirschen haben einen geringen Zellturgor und der Turgor der gesamten Frucht steigt beim Platzen der Kirschen nicht an (Knoche et al., 2014). (2) Die Wasseraufnahme ist nicht mit dem Platzen der Früchte korreliert (A. Winkler unveröffentlichte Daten). (3) Das Platzen von Früchten kann lokal durch Wasser induziert werden, während der Rest der Frucht trocken bleibt und transpiert, wodurch die Frucht sogar netto Wasser verliert (Knoche & Peschel, 2006). (4) Die Zellwände an Rissen im Platztest sind gequollen im Gegensatz zu Zellwänden von intakten Fruchthäuten (Kapitel 8). (5) Im Vergleich zum klassischen Platztest nimmt eine Kirsche etwa das Zehnfache an Wasser auf bevor sie platzt, wenn das Wasser direkt mittels eines Perfusors über eine Spritzenkanüle in die Kirsche gedrückt wird (M. Knoche unveröffentlichte

Daten). Dies entspricht  $\epsilon_{\text{fracture}}$ , die deutlich größer sind als die aus einem Platztest berechneten  $\epsilon_{\text{fracture}}$ . Aus diesen Gründen scheint die Wasseraufnahme offenbar weitere, über die Volumenzunahme der Fruchthaut hinausgehende Einflüsse auf das Platzen zu haben (Kapitel 7). Das Platzen ist vermutlich eher ein „lokales“ Phänomen in der Fruchthaut und damit nicht mit dem Ballon-Modell erklärbar.

Die Kette von Ereignissen, die zum Platzen der Kirschen führt, kann sich aufgrund der Ergebnisse und der Literatur folgendermaßen vorgestellt werden. Durch die Benetzung der gespannten Kutikula mit Wasser entstehen Mikrorisse (Knoche & Peschel, 2006). Bei Regen findet über diese Mikrorisse eine verstärkte Wasseraufnahme in die Frucht statt. Das Wasser bringt einzelne Zellen zum Platzen (Simon, 1977; Glenn & Poovaiah, 1989) und die Zellwände quellen (Grimm und Knoche, 2015). Als weitere Folge gelangt der Zellinhalt unter anderem Anthocyane, Glucose, Fructose und Äpfelsäure in den Apoplasten. Schon geringe Konzentrationen von Äpfelsäure (1 mM) im Apoplasten erhöhen die Durchlässigkeit von Plasmamembranen und führen zur Zellwandquellung (Winkler et al., 2015; Kapitel 8). Es kommt zu einer Kettenreaktion, bei der immer mehr Zellen platzen, Äpfelsäure freigesetzt wird und Zellwände quellen. Die gequollenen Zellwände können irgendwann der internen Spannung in der Fruchthaut (Grimm et al., 2012) nicht mehr widerstehen und reißen entlang der Zellwände (Kapitel 8). Dieser Riss in der Fruchthaut setzt sich, wie ein Reißverschluss, immer weiter fort. Es entsteht ein sichtbarer Makroriss. Die bevorzugten Orte an denen die Frucht reißt (Stielgrube und Griffelansatz) lassen sich mit einer höheren Dichte an Mikrorissen an dieser Stelle (Peschel & Knoche, 2005) und/oder mit einer größeren *in-vivo* Spannung (Knoche et al., 2002) erklären.

Zusammenfassend ermöglichte der biaxiale Zugtest im Elastometer die Zellwandquellung als eine entscheidende Ursache für das Platzen von Kirschen zu identifizieren. Weiterhin ist anzunehmen, dass der Mechanismus des Platzens bei anderen Früchten ähnlich abläuft. So bilden sich bei reifen Pflaumen und Weinbeeren ebenfalls Mikrorisse in der Kutikula (Knoche und Peschel, 2007; Becker und Knoche, 2012). Auch ist Zellwandquellung bei vielen weichen Früchten zur Reife hin zu beobachten (Redgwell et al., 1997).



Zukünftige Arbeiten sollten untersuchen, welche Zellwandbestandteile für die Zellwandquellung verantwortlich sind. Aus diesen Erkenntnissen lassen sich dann mögliche Maßnahmen zur Verhinderung des Platzens unter Feldbedingungen ableiten. Bei diesen Untersuchungen kann das Elastometer eine zentrale Rolle spielen, wie die Ergebnisse dieser Arbeit am Beispiel der Kirschen belegen.

## 10. Literaturverzeichnis

- Bargel, H., Spatz, H.C., Speck, T. und Neinhuis, C. (2004) Two-dimensional tension test in plant biomechanics—sweet cherry fruit skin as a model system. *Plant Biology* 6, 432-439.
- Becker, T., Grimm, E. und Knoche, M. (2012) Substantial water uptake into detached grape berries occurs through the stem surface. *Australian Journal of Grape and Wine Research* 18, 109-114.
- Becker, T. und Knoche, M. (2012) Deposition, strain, and microcracking of the cuticle in developing 'Riesling' grape berries. *Vitis* 51, 1-6.
- Beyer, M. und Knoche, M. (2003) Ausgewählte Strategien zur Verminderung des Platzrisikos von Süßkirschen (*Prunus avium* L.): Eine Bewertung auf Basis von Literaturdaten und Simulationsrechnungen. *Erwerbsobstbau* 45, 169-180.
- Beyer, M., Peschel, S., Knoche, M. und Knörger, M. (2002) Studies on water transport through the sweet cherry fruit surface: IV. Regions of preferential uptake. *HortScience* 37, 637-641.
- Børve, J., Sekse, L. und Stensvand, A. (2000) Cuticular fractures promote postharvest fruit rot in sweet cherries. *Plant Disease* 84, 1180-1184.
- Brüggenwirth, M., Winkler, A. und Knoche, M. (2016) Xylem, phloem, and transpiration flows in developing sweet cherry fruit. *Trees* doi: 10.1007/s00468-016-1415-4.
- Christensen, J.V. (1972) Cracking in cherries I. Fluctuation and rate of water absorption in relation to cracking susceptibility. *Danish Journal of Plant and Soil Science* 76, 1-5.
- Christensen, J.V. (1996) Rain-induced cracking of sweet cherries: Its causes and prevention. In: Webster, A.D. and Looney, N.E. (eds.). *Cherries: Crop physiology, production and uses*. CAB International, Wallingford, UK, pp.297-327.

Considine, J. und Brown, K. (1981) Physical aspects of fruit growth. Theoretical analysis of distribution of surface growth forces in fruit in relation to fruit cracking and splitting. *Plant Physiology* 68, 371-376.

Considine, J.A. und Kriedemann, P.E. (1972) Fruit splitting in grapes. Determination of the critical turgor pressure. *Australian Journal of Agricultural Research* 23, 17-24.

Glenn, G.M. und Poovaiah, B.W. (1989) Cuticular properties and postharvest calcium applications influence cracking of sweet cherries. *Journal of the American Society for Horticultural Science* 114, 781-788.

Grimm, E. und Knoche, M. (2015) Sweet cherry skin has a less negative osmotic potential than the flesh. *Journal of the American Society for Horticultural Science* 140, 472-479.

Grimm, E., Peschel, S., Becker, T. und Knoche, M. (2012) Stress and strain in the sweet cherry skin. *Journal of the American Society for Horticultural Science* 137, 383-390.

Lichter, A., Dvir, O., Fallik, E., Cohen, S., Golan, R., Shemer Z. und Sagi, M. (2002) Cracking of cherry tomatoes in solution. *Postharvest Biology and Technology* 26, 305-312.

Looney, N.E. (1985) Benefits of calcium sprays below expectations in B.C. tests. *Goodfruit Grower* 36, 7-8.

Kertesz, Z.I. und Nebel, B.R. (1935) Observations on the cracking of cherries. *Plant Physiology* 10, 763-772.

Knoche, M., Beyer, M., Peschel, S., Parlakov, B. und Bukovac, M.J. (2004) Changes in strain and deposition of cuticle in developing sweet cherry fruit. *Physiologia Plantarum* 120, 667-677.

Knoche, M., Grimm, E. und Schlegel, H.J. (2014) Mature sweet cherries have low turgor. *Journal of the American Society for Horticultural Science* 139, 3-12.

Knoche, M. und Peschel, S. (2006) Water on the surface aggravates microscopic cracking of the sweet cherry fruit cuticle. *Journal of the American Society for Horticultural Science* 131, 192-200.

Knoche, M. und Peschel, S. (2007) Deposition and strain of the cuticle of developing european plum fruit. *Journal of the American Society for Horticultural Science* 132, 597-602.

Knoche, M., Peschel, S. und Hinz, M. (2002) Studies on water through the sweet cherry fruit surface: III. Conductance of the cuticle in relation to fruit size. *Physiologia Plantarum* 114, 414-421.

Khanal, B.P., Grimm, E. und Knoche, M. (2011) Fruit growth, cuticle deposition, water uptake, and fruit cracking in jostaberry, gosseberry, and black currant. *Scientia Horticulturae* 128, 289-296.

Matas, A.J., Cobb, E.D., Bartsch, J.A., Paolillo, D.J. und Niklas, K.J. (2004) Biommechanics and anatomy of *Lycopersicon esculentum* fruit peels and enzyme-treated samples. *American Journal of Botany* 91, 352-360.

Measham, P.F., Bound, S.A., Gracie, A.J. und Wilson, S.J. (2009) Incidence and type of cracking in sweet cherry (*Prunus avium* L.) are affected by genotype and season. *Crop and Pasture Science* 60, 1002-1008.

Measham, P.F., Wilson, S.J., Gracie, A.J. und Bound, S.A. (2014) Tree water relations: Flow and fruit. *Agricultural Water Management* 137, 59-67.

Mrozek, R.F. und Burkhard, T.H. (1973) Factors causing prune side cracking. *Transaction of the American Society of Agriculture Engineers* 16, 686-692.

Peschel, S., Beyer, M. und Knoche, M. (2003) Surface characteristics of sweet cherry fruit: stomata number, distribution, functionality and surface wetting. *Scientia Horticulturae* 97, 265-278.

Peschel, S. und Knoche, M. (2005) Characterization of microcracks in the cuticle of developing sweet cherry fruit. *Journal of the American Society for Horticultural Science* 130, 487-495.

- Peschel, S. und Knoche, M. (2012) Studies on water transport through the sweet cherry fruit surface: XII. Variation in cuticle properties among cultivars. *Journal of the American Society for Horticultural Science* 137, 367-375.
- Redgwell, R.J., MacRae, E., Hallett, I., Fischer, M., Perry, J. und Harker, R. (1997) In vivo and in vitro swelling of the cell walls during fruit ripening. *Planta* 203, 162-173.
- Sekse, L., Bjerke, K.L. und Vangdal, E. (2005) Fruit cracking in sweet cherries - An integrated approach. *Acta Horticulturae* 667, 471-474.
- Simon, E.W. (1977) Leakage from fruit cells in water. *Journal of Experimental Botany* 28, 1147-1152.
- Weichert, H. und Knoche, M. (2006) Studies on water transport through the sweet cherry fruit surface: 10. Evidence for polar pathways across the exocarp. *Journal of Agricultural and Food Chemistry* 54, 3951-3958.
- Weichert, H., von Jagemann, C., Peschel, S., Knoche, M., Neumann, D. und Erfurth, W. (2004) Studies on water transport through the sweet cherry fruit surface: VIII. Effect of selected cations on water uptake and fruit cracking. *Journal of the American Society for Horticultural Science* 129, 781-788.
- Winkler, A., Brüggewirth, M., Ngo, N.S. und Knoche, M. (2016) Fruit apoplast tension draws xylem water into mature sweet cherries. *Scientia Horticulturae* 209, 270-278.
- Winkler, A., Ossenbrink, M. und Knoche, M. (2015) Malic acid promotes cracking of sweet cherry fruit. *Journal of the American Society for Horticultural Science* 140, 280-287.
- Yamaguchi, M., Sato, I., Takase, K., Watanabe, A. und Ishiguro, M. (2004) Differences and yearly variation in number and size of mesocarp cells in sweet cherry (*Prunus avium* L.) cultivars and related species. *Journal of the Japanese Society for Horticultural Science* 73, 12-18.

## 11. Abkürzungsverzeichnis

A	surface area	Flächeninhalt
$A_0$	initial surface area	Ursprünglicher Flächeninhalt
AOV	analysis of variance	Varianzanalyse
b	length of the arc	Länge des Bogens
c	radius hypothetical sphere	Radius der hypothetischen Kugel
CM	cuticular membrane	Kutikular
D	diameter	Durchmesser
DAFB	days after full bloom	Tage nach Vollblüte
$\Delta A$	change in area	Flächenänderung
$\Delta l$	change in length	Längenänderung
E	east (longitude)	Ost (Länge)
$E$	E-Modul, Modulus of elasticity	E-Modul, Elastizitätsmodul
ES or ESs	exocarp segment (s)	Exokarp Segment (e)
Eq	equation	Gleichung
$\varepsilon$	strain	Dehnung
$\varepsilon_{\text{biaxial}}$	biaxial strain	biaxiale Dehnung
$\varepsilon_{\text{biaxial}}^{\text{calculated}}$	calculated biaxial strain	berechnete biaxiale Dehnung
$\varepsilon_{\text{fracture}}$	strain at fracture	Bruchdehnung
$\varepsilon_{\text{rate}}$	rate of strain	Dehnungsrate
$\varepsilon_{\text{latitudinal}}$	latitudinal strain	Dehnung in die Breite
$\varepsilon_{\text{longitudinal}}$	longitudinal strain	Dehnung in die Länge

---

$\epsilon_{\text{uniaxial}}$	uniaxial strain	Uniaxiale Dehnung
$\epsilon_{\text{uniaxial}}^{\text{axial}}$	axial uniaxial strain	axiale uniaxiale Dehnung
$\epsilon_{\text{uniaxial}}^{\text{transverse}}$	transverse uniaxial strain	transversale uniaxiale Dehnung
Fig	figure	Abbildung
h	height	Höhe
k	distance between dots	Distanz zwischen den Punkten
$l_0$	initial length	Ursprüngliche Länge
N	North (latitude)	Nord (Breite)
n	number of replicates	Anzahl der Wiederholungen
$P$	probability	Wahrscheinlichkeit
$p$	pressure	Druck
$p_{\text{fracture}}$	pressure at fracture	Bruchdruck
R	radius	Radius
r	coefficient of correlation	Korrelationskoeffizient
$r^2$	coefficient of determination	Bestimmtheitsmaß
RH	relative humidity	Relative Luftfeuchte
SE	standard error	Standardfehler
t	thickness	Dicke
Tab	table	Tabelle
$T_{\text{fracture}}$	time to fracture	Bruchzeit
$T_{50}$	time to 50% fruit cracking	Zeit bis 50% der Früchte platzen
v/v	volume by volume	Volumenanteil

## Abkürzungsverzeichnis

---

v	poisson's ratio	Poisson-Verhältnis
w/w	weight by weight	Massenanteil
WU <sub>50</sub>	water uptake for 50% of fruit to crack	Wasseraufnahme bei der 50% der Früchte platzen



## Danksagungen

An dieser Stelle möchte ich mich bei all denjenigen bedanken, die mich in den letzten drei Jahren begleitet und diese Arbeit ermöglicht haben:

Mein besonderer Dank gilt Herrn **Prof. Dr. Moritz Knoche**, dessen Tür für Fragen jeglicher Art immer offen stand. Sein Enthusiasmus, seine Verlässlichkeit und sein hoher Einsatz für die Wissenschaft haben mich geprägt. Ohne seine Hilfe wäre diese Arbeit nicht möglich gewesen.

Vielen Dank an Herrn **Prof. Dr. Hartmut Stützel** für die Übernahme des Ko-Referats dieser Arbeit, **Prof. Dr. Lukas Schreiber** für die Übernahme des externen Prüfers und Frau **Prof. Dr. Jutta Papenbrock** für die Übernahme des Prüfungsvorsitzes bei der Disputation.

Vielen Dank an Herrn **Prof. Dr. Hanns-Christof Spatz** für die Hilfe der Erstellung der Berechnungsformel des E-Moduls und Herrn **Dr. Sandy Lang** für die sprachliche Korrektur und die hilfreichen Kommentare an den Manuskripten.

Vielen Dank an Herrn **Dr. Eckhard Grimm**, Herrn **Dr. Bishnu Khanal**, Herrn **Andreas Winkler**, Frau **Christine Schumann**, Herrn **Simon Sitzenstock**, Frau **Frederike Schröder** und Frau **Sylvia Janning**, die mir immer eine große Hilfe waren und die für ein hervorragendes Arbeitsklima im Institut gesorgt haben. Vielen Dank an Herrn **Peter Grimm-Wetzel**, Herrn **Marcel Pastwa** und dem inzwischen verstorbenen Herrn **Bernward Göbel**, die stets frische Kirschen aus Ruthe geliefert haben.

Vielen Dank an Herrn **Dieter Reese**, Herrn **Christoph Knake** und Herrn **Heiko Fricke**, die das Elastometer maßgeblich gebaut, programmiert und getestet haben. Ohne deren Einsatz wären die mechanischen Tests nicht möglich gewesen.

Vielen Dank an alle **Mitarbeiter** und **Studenten** des Campus Herrenhausen, die mir in vielen kleinen Dingen geholfen haben.

Ein sehr herzlicher Dank gilt meiner **Familie** und meiner **Freundin**, die immer mein Rückhalt waren.

## Publikationsliste

Brüggenwirth, M. und Knoche, M. (2016d) Cell wall swelling, fracture mode, and the mechanical properties of cherry skins are closely related. *Planta* doi: 10.1007/s00425-016-2639-7.

Brüggenwirth, M. und Knoche, M. (2016c) Time to fracture and fracture strain are negatively related in sweet cherry fruit skin. *Journal of the American Society for Horticultural Science* 141, 485-489.

Winkler, A., Brüggenwirth, M., Ngo, N.S. und Knoche, M. (2016) Fruit apoplast tension draws xylem water into mature sweet cherries. *Scientia Horticulturae* 209, 270-278.

Brüggenwirth, M., Winkler, A. und Knoche, M. (2016) Xylem, phloem, and transpiration flows in developing sweet cherry fruit. *Trees* doi: 10.1007/s00468-016-1415-4.

Brüggenwirth, M. und Knoche, M. (2016b) Mechanical properties of skin of sweet cherry fruit of differing susceptibilities to cracking. *Journal of the American Society for Horticultural Science* 141, 162-168.

Brüggenwirth, M. und Knoche, M. (2016a) Factors affecting mechanical properties of the skin of sweet cherry fruit. *Journal of the American Society for Horticultural Science* 141, 45-53.

Brüggenwirth, M. und Knoche, M. (2015) Xylem conductance of sweet cherry pedicels. *Trees* 29:1851-1860.

Knoche, M., Athoo, T.O., Winkler, A. und Brüggenwirth, M. (2015) Postharvest osmotic dehydration of pedicels of sweet cherry fruit. *Postharvest Biology and Technology* 108, 86-90.

Brüggenwirth, M., Fricke, H. und Knoche, M. (2014) Biaxial tensile tests identify epidermis and hypodermis as the main structural elements of sweet cherry skin. *Annals of Botany – Plants* doi: 10.1093/aobpla/plu019.

## Lebenslauf

---

**Name** Brüggenwirth  
**Vorname** Martin  
**Geburtsdatum und Ort** Geboren am 15.01.1988 in  
Bückeberg/Niedersachsen  
**Staatsangehörigkeit** deutsch

## Studium und Schulausbildung

---

**Aug. 2013- heute** Promotion am Institut für gartenbauliche  
Produktionssysteme, Fachbereich Produktqualität  
Obstbau der Leibniz Universität Hannover  
**Okt. 2011- Jun. 2013** Gartenbaustudium (Master) an der Leibniz  
Universität Hannover Thema Masterarbeit:  
Mechanische Eigenschaften des Exokarps von  
Süßkirschen im biaxialen Zugtest  
**Okt. 2008- Aug. 2011** Gartenbaustudium (Bachelor) an der Leibniz  
Universität Hannover Thema Bachelorarbeit: Einfluss  
der Ascorbinsäure auf das Auftreten von  
Schalenflecken bei der Apfelsorte Elstar  
**Aug. 2005- Jun. 2008** Allgemeines Abitur, Ratsgymnasium Stadthagen  
**Aug. 2001- Jun. 2005** Integrierte Gesamtschule Schaumburg  
**Aug. 1999- Jun. 2001** Orientierungsstufe Bad Nenndorf  
**Aug. 1995- Jun. 1999** Grundschule Haste

## Auszeichnungen und Stipendien

---

Stipendium IP@Leibniz „Maßnahmen zur Erhöhung der Doktorandenmobilität“  
Gewinn der Green Challenge 2011 (Wettbewerb der  
Gartenbauwissenschaftlichen Gesellschaft e.V.)  
Stipendium „Preis des Präsidiums“ 2010 (Leibniz Universität Hannover)